

**EXPERIMENTAL ANALYSIS OF OIL
DISPLACEMENT BY HYBRID ENGINEERED WATER
/ CHEMICAL EOR APPROACH IN CARBONATES**

by

MARIAM SHAKEEL

2021

Thesis submitted to the School of Mining and Geosciences of Nazarbayev
University in Partial Fulfillment of the Requirements for the Degree of
Master of Science in Petroleum Engineering

Nazarbayev University

2021

Acknowledgements

First and foremost, I would like to convey a grateful appreciation to my supervisor Dr. Peyman Pourafshary for his invaluable input, continuous guidance, and unwavering support throughout my research work. He continuously and persuasively transferred the real essence to my research potential. I would also express sincere gratitude to my co-supervisor Dr. Muhammad Rehan Hashmet, who incessantly encouraged and guided me throughout this challenging experimental study. Without their research aptitude, leadership, and timely assistance, this thesis would not have been possible.

I dedicate my extended thanks to respected reviewers for their affirmative and expert recommendations to improve the quality of the dissertation. I also thank MDPI for allowing me to include my published research in this thesis.

I would like to express my profound love to my parents for their prayers, my husband Rizwan Muneer for his continuous encouragement, and to my son Muhammad Shaheer whose unconditional love, warmth, and naughty gestures always put a smile on my face even during the difficult times of this task. His presence in my life motivated me to redefine my goals and pursue them for a professional career.

Finally, I am thankful to have the honor of attending the prestigious Nazarbayev University under state and research scholarship programs, and especially the School of Mining and Geosciences for providing all the research facilities and resources to accomplish great success. Best regards to my colleague Aida Samanova and all lab staff members for their prompt assistance to complete this work on schedule. Thank you all!

Originality Statement

I, Mariam Shakeel, hereby declare that this submission is my own work and to the best of my knowledge it contains no materials previously published or written by another person, or substantial proportions of material which have been accepted for the award of any other degree or diploma at Nazarbayev University or any other educational institution, except where due acknowledgement is made in the thesis.

Any contribution made to the research by others, with whom I have worked at NU or elsewhere is explicitly acknowledged in the thesis.

I also declare that the intellectual content of this thesis is the product of my own work, except to the extent that assistance from others in the project's design and conception or in style, presentation and linguistic expression is acknowledged.

Signed on May 04, 2021

Mariam Shakeel.

ABSTRACT

Fast depletion in oil reserves has steered the petroleum industry towards developing novel enhanced oil recovery (EOR) techniques to get the most out of reservoirs. The standalone EOR methods such as engineered water flooding (EWF) and chemical EOR (CEOR) have associated merits and demerits. In this study, hybrid approaches utilizing engineered water (EW) and CEOR methods are investigated and the underlying mechanisms e.g., wettability alteration, interfacial tension (IFT) reduction, and mobility control are evaluated. Finally, the critical parameters influencing the performance of hybrid methods and criteria for selection of a hybrid method are presented.

The hydrolyzed polyacrylamide polymer viscous and viscoelastic properties were analyzed as a function of pH. The effect of crude oil aging and temperature on wettability modification by EW was assessed by measuring contact angles. Various combinations of EW and CEOR were designed, and oil displacement tests were carried out to select the best formulation. Three coreflood tests were conducted to evaluate the effect of initial wettability on EW performance. Next, the hybrid EW/surfactant/polymer flooding (EWSPF) was performed and finally EW / alkali / surfactant/polymer flooding (EWSPF) was evaluated in slug-wise and continuous injection modes. All the coreflood experiments were conducted at 80 °C.

The optimum pH range for the best polymer performance in terms of viscous and viscoelastic behavior was found to be 7-10. The contact angle measurements confirmed that EW was not suitable for water-wet reservoirs. A larger wettability shift towards water-wet condition by EW was observed at high temperature. The overall incremental oil recovery by hybrid EWPF in oil-wet medium was 16-20% higher compared to water-wet medium. Hybrid EWSPF provided additional oil recovery of 29% of original-oil-in-place (OOIP), comparable to hybrid EWPF. The best combination in terms of oil recovery and chemical consumption, was the hybrid EWASP flooding in slug-wise injection mode. This scheme resulted in 36% OOIP incremental recovery, 7% higher than EWPF and EWSPF scenarios and 3% higher than EWASP flooding in continuous injection mode. The overall performance of all hybrid combinations was better compared to their individual counterparts, as investigated by capillary desaturation tendency.

These results are helpful in selection of a hybrid EOR method for a particular carbonate reservoir. The criteria for the implementation of EW based hybrid methods must include the assessment initial wettability of the rock, acid number of the crude oil, reservoir temperature, and compatibility between designed EW and chemicals.

TABLE OF CONTENTS

LIST OF FIGURES.....	VIII
LIST OF TABLES.....	XI
1. INTRODUCTION.....	16
1.1 Background.....	16
1.2 Polymer Flooding	17
1.2.1 Recovery Mechanism	18
1.2.2 Viscoelastic Polymers.....	19
1.2.3 Challenges Associated with Polymer Flooding.....	19
1.2.4 Field Examples	21
1.3 Surfactant Flooding (SF).....	21
1.3.1 Recovery Mechanisms	22
1.3.2 Challenges in Surfactant Flooding	22
1.4 Alkaline Flooding (AF)	23
1.4.1 Recovery Mechanism	23
1.4.2 Challenges Associated with Alkaline Flooding	23
1.5 Engineered Water Flooding (EWF)	24
1.5.1 Recovery Mechanisms	24
1.5.2 Conditions for Engineered Water Flooding	28
1.5.3 Limitations of EWF.....	28
1.5.4 Lab-based Studies.....	29
1.6 Hybrid Engineered Water-Polymer Flooding (EWPF)	31
1.6.1 Enhanced Oil Recovery by Hybrid EWPF in Carbonates	32
1.6.2 Recovery Mechanisms	33
1.6.3 Potential Risks associated with EWPF.....	41
1.6.4 Lab-Scale Studies	42
1.6.5 Numerical Modeling Studies	43
1.7 Hybrid Engineered Water-Surfactant-Polymer Flooding (EWSPF).....	47
1.8 Hybrid Engineered Water-Alkali-Surfactant-Polymer (EWASP) Flooding	48
1.9 Problem Statement	49
1.10 Research Objectives	50
1.10.1 Main objectives.....	51
1.10.2 Thesis structure	51
2. METHODOLOGY	52
2.1 Materials.....	52

2.1.1	Crude Oil	52
2.1.2	Rock Samples	53
2.1.3	Brines	53
2.1.4	Chemicals.....	54
2.2	Procedures	57
2.2.1	Brines and Chemical Solutions Preparation.....	57
2.2.2	Crude Oil Properties	57
2.2.3	Rock Properties	60
2.2.4	Polymer Shear and Viscoelastic Characterization.....	61
2.2.5	Contact Angle Measurements.....	63
2.2.6	Design of Oil Displacement Experiments.....	66
2.2.7	Coreflooding	66
3.	RESULTS	71
3.1	Shear Characterization.....	71
3.1.1	Effect of pH on Viscosity.....	71
3.1.2	Effect of Polymer Concentration and pH on Viscosity	72
3.1.3	Effect of pH on Thermal Stability.....	72
3.2	Viscoelastic Characterization.....	75
3.2.1	Analysis of Amplitude Sweep Test.....	75
3.2.2	Analysis of Frequency Sweep Test.....	76
3.3	Results of Contact Angle Measurements.....	81
3.3.1	Effect of Aging Time on Initial Wettability	81
3.3.2	Effect of Initial Wettability on EW Performance	81
3.3.3	Effect of Temperature on Wettability Alteration by EW.....	83
3.3.4	Effect of Polymer on EW Performance.....	84
3.4	Polymer Concentration Determination for Coreflood Experiments.....	85
3.5	Results of Coreflood Experiments	86
3.5.1	Hybrid EW/Polymer Flooding in Water-wet System (Experiment-1).....	86
3.5.2	Hybrid EW/Polymer Flooding in Intermediate Oil-wet System (Experiment-2). 89	
3.5.3	Hybrid EW/Polymer Flooding in Strongly Oil-Wet Condition (Experiment-3) ...	90
3.5.4	Hybrid EW-Surfactant Polymer Flooding (Experiment-4)	92
3.5.5	Hybrid EW-ASP Flooding - Continuous Injection (Experiment-5)	93
3.5.6	Hybrid EW-ASP Flooding - Slug Injection (Experiment-6)	95
3.6	Effect of Initial Wettability on EWF and Hybrid EWPF Performance.....	97
3.7	Comparative Analysis of Oil Recovery by Different Hybrid Methods	100

3.7.1	Effect of Hybrid EW/CEOR Methods on S_{or} : Capillary Desaturation.....	100
3.7.2	Recovery Efficiency of Different Hybrid Processes	103
3.7.3	Calculation of Mobility Ratio for Hybrid Methods.....	104
3.7.4	Oil Breakthrough during EWF	105
4.	CONCLUSION AND RECOMMENDATIONS	107
5.	REFERENCES.....	110

List of Figures

Figure 1. (a) Chemical structure [38] (reproduced with permission from Liu et al. J. Pet. Sci. Eng.; published by Elsevier, 2020); and (b) physical structure of HPAM polymer.....	18
Figure 2. Schematic illustration of polymer degradation and adsorption in high salinity water.	20
Figure 3. Effect of salinity on different polymers' adsorption [43]. Reproduced with permission from James J. Sheng, Elsevier Books; published by Elsevier, 2011.	20
Figure 4. Schematic of processes involved during surfactant flooding [81].	22
Figure 5. Mechanism of IFT reduction by in situ anionic surfactant generated by NaOH [87].	23
Figure 6. (a) IFT reduction, (b) Wettability change and (c) Incremental oil recovery by LSW injection [144].....	30
Figure 7. Oil recovery by LSWF in (a) Tertiary injection mode and (b) Secondary injection mode; FW: Formation water (204,201 ppm TDS), DSAL: Low salinity water (241 ppm TDS) [123].....	30
Figure 8. Summary of experimental and simulation studies showing incremental oil by EWPF in carbonates [159].....	31
Figure 9. (a) Reduction in Sor after LSPF [5] (reproduced with permission from Lee et al., J. Pet. Sci. Eng.; published by Elsevier, 2019); and (b) additional recovery by EWPF in carbonate reservoir cores [163].....	32
Figure 10. Illustration of governing mechanisms for incremental oil by hybrid LSPF. (a), (b), (c) and (d) depict the functions of LSW [92, 164] (reproduced with permission from Zhang et al., Energy & Fuels; published by American Chemical Society, 2006; and Al Shalabi et al., J. Pet. Sci. Eng.; published by Elsevier, 2016); (e) shows polymer stability in LSW; (f) shows formation of the oil bank [165]; and (g) presents the final outcome of the process i.e. detachment, mobilization, and displacement of the residual oil bank by combined LSPF.....	33
Figure 11. Effect of PDIs and pH of water on (a) oil recovery and (b) wettability alteration by EW [5]. Reproduced with permission from Lee et al., J. Pet. Sci. Eng.; published by Elsevier, 2019.	35
Figure 12. Studies showing reduction in required polymer concentration by LSW.	37
Figure 13. Reduction in HPAM concentration using LSW as the makeup brine [152]. Adapted with permission from Shehadeh et al., published by IPTC, 2014. TDS: Total dissolved solids.	37
Figure 14. The smart water effect on polymer concentration required for target viscosity [176]. Reproduced with permission from Al Sofi et al., J. Pet. Sci. Eng.; published by Elsevier, 2018.	38
Figure 15. Better thermal stability of SAV10 polymer in LSW at 113 °C. LSW, 1/5 brine, and seawater have 2935, 47,869 and 49,878 ppm of TDS, respectively [15].....	38
Figure 16. Polymer retention in the presence of (a) injection water and (b) smart water [176]. Reproduced with permission from Al Sofi et al., J. Pet. Sci. Eng.; published by Elsevier, 2018.	39
Figure 17. Studies showing reduction in required polymer adsorption by LSW.	39
Figure 18. (a) A higher reduction in zeta potential and (b) increased wettability shift to water-wetness in the presence of HPAM polymer in smart water [176]. Reproduced with permission from Al Sofi et al., J. Pet. Sci. Eng.; published by Elsevier, 2018.....	40
Figure 19. Oil recovery and pressure trend for LSPF using reservoir core [152]. Reproduced with permission from Shehadeh et al., published by IPTC, 2014.....	42

Figure 20. Oil recovery as a function of zeta-potential, showing higher recovery by the hybrid method compared to standalone processes; coreflood-1 shows PF and LSPF comparison while coreflood-2 displays LSW and LSPF comparison [163].	43
Figure 21. Comparison of oil recovery, Sor and pressure drop by LSWF followed by LSPF for a Kuwait carbonate oil reservoir composite core [15].	43
Figure 22. Numerical modeling results showing oil recovery as a function of (a) mobility ratio for different flooding scenarios and (b) brine salinity used for PF [156].	44
Figure 23. Analytical solution results showing the effect of LSPF on (a) oil recovery and (b) water cut [155]. Reproduced with permission from Borazjani et al., J. Pet. Sci. Eng.; published by Elsevier, 2016.	45
Figure 24. Effect of different design parameters on LSPF performance in terms of incremental oil recovery [153].	45
Figure 25. Comparison of LSPF with high salinity WF (50,000+ ppm), LSWF (2000 ppm), and HSP flooding after 0.6 PV injection [154].	46
Figure 26. Comparison of EWASP flooding with other flooding scenarios [207].	49
Figure 27. Elemental analysis of crushed rock sample using SEM.	53
Figure 28. Chemical structure of sulphonated polyacrylamide polymer.	55
Figure 29. Temperature dependency of crude oil viscosity and density.	58
Figure 30. Procedure for determination of crude oil AN.	59
Figure 31. Step-by-step procedure for F5115 rheological and viscoelastic characterization.	62
Figure 32. Limestone pellets for CA measurements.	64
Figure 33. Illustration of OCA instrument for CA measurements.	64
Figure 34. Sequence of CA measurements.	65
Figure 35. Schematic of Vinci aging cell apparatus used for oil displacement experiments.	68
Figure 36. Effect of pH on 1500 ppm F5115 viscosity at 25 °C.	71
Figure 37. Effect of polymer concentration and pH on F5115 viscosity at 25 °C.	72
Figure 38. Effect of pH on thermal stability of 1500 ppm F5115. The solutions were kept at 80 °C while the viscosity was measured at 25 °C.	73
Figure 39. 1500 ppm F5115 viscosity loss as a function of pH after one week aging time at 80 °C.	74
Figure 40. AST results for LVER detection for 1500, 3000 and 4500 ppm neutral pH solutions at 25 °C.	75
Figure 41. pH Effect on storage modulus for 1500, 3000 and 4500 ppm neutral pH solutions at 25 °C.	76
Figure 42. FST results for 1500, 3000 and 4500 ppm neutral pH solutions at 25 °C.	77
Figure 43. G' and G'' as a function of pH for 4500 ppm solution at 25 °C.	78
Figure 44. Relaxation time as a function of pH for 1500, 3000, and 4500 ppm solution at 25 °C.	79
Figure 45. Loss factor as a function of pH for 4500 ppm solution at 25 °C.	80
Figure 46. Mechanism for HPAM F5115 performance under acidic and basic conditions.	81

Figure 47. Effect of aging time on wettability change by EW and HSW.	82
Figure 48. Comparison of CA change by HSW and EW at different aging times.	83
Figure 49. Effect of temperature on CA change by EW at different aging times.	84
Figure 50. Effect of polymer F5115 on EW wettability alteration extent.	85
Figure 51. Polymer concentration selection for coreflood experiments.	85
Figure 52. Water production as a function of oil injection for all core samples.	86
Figure 53. Oil recovery and pressure drop profile for hybrid EWPF experiment in a weak oil-wet system.	87
Figure 54. Oil recovery and pressure drop profile for hybrid EWPF test in an intermediate oil-wet system.	89
Figure 55. Oil recovery and pressure drop profile for hybrid EWPF in strong oil-wet medium.	91
Figure 56. Effect of initial wettability on oil recovery by HSWF.	91
Figure 57. Oil recovery and pressure drop profile for hybrid EWSPF experiment.	93
Figure 58. Oil recovery and pressure drop profile for hybrid EWASP experiment in continuous injection mode.	94
Figure 59. Oil recovery and pressure drop profile for hybrid EWASP slug-wise injection mode.	96
Figure 60. Mechanisms involved in incremental oil recovery by hybrid EWASP flooding.	97
Figure 61. EW and EWPF oil recovery comparison for different wettability conditions.	99
Figure 62. Effect of aging time on contact angle and rock wettability.	99
Figure 63. Oil recovery comparison for different hybrid EW/CEOR methods.	101
Figure 64. Comparison of capillary desaturation tendency of hybrid EW/CEOR methods with conventional ones.	102
Figure 65. Recovery efficiency of different hybrid methods as a function of viscosity and IFT.	103
Figure 66. Comparison of displacement efficiency of different hybrid methods.	104
Figure 67. Relationship between mobility and recovery of remaining oil.	105
Figure 68. Oil breakthrough time during EWF stage of different tests.	106

List of Tables

Table 1. Summary of corefloods showing incremental oil recovery by EWF in carbonates.	25
Table 2. Oil/water IFT measurements showing negligible effect of smart water and polymer on IFT.	35
Table 3. Key conditions for polymer, engineered water and engineered water/polymer flooding.	47
Table 4. Composition of crude oil.....	53
Table 5. Salts used in brines preparation.....	54
Table 6. Ionic composition of different brines used in the study.	55
Table 7. Recipe for different brines.....	55
Table 8. Chemical and physical properties of F5115.	55
Table 9. Chemical and physical properties of Soloterra-113H.	56
Table 10. Amount of polymer added for different concentration solutions.	57
Table 11. Crude oil properties as a function of temperature.....	58
Table 12. Core samples porosities.	61
Table 13. Core samples permeabilities.	61
Table 14. Design of oil displacement experiments for EW based hybrid EOR methods.	67
Table 15. Injection rates and chemical concentrations for coreflood experiments.....	69
Table 16. Initial water saturation for core samples.	86
Table 17. Summary of oil recoveries by hybrid EWPF under different initial wettability conditions.	98
Table 18. Summary of oil recoveries by various hybrid EWF/CEOR combinations.	100
Table 19. Mobility during HSWF and chemical flooding stages.	105

LIST OF ABBREVIATIONS

AF	Alkaline flooding
AN	Acid number
AS	Alkali/surfactant
ASP	Alkali/surfactant/polymer
AST	Amplitude sweep test
CA	Contact angle
CBR	Crude oil-brine-rock
CDC	Capillary desaturation curve
CEOR	Chemical EOR
COOH	Carboxylic oil material
CSW	Caspian seawater
EOR	Enhanced oil recovery
EUR	Estimated ultimate recovery
EW	Engineered water
EWASF	Engineered water/alkali/surfactant flooding
EWASP	Engineered water/alkali/surfactant/polymer
EFW	Engineered waterflooding
EWPF	Engineered water/polymer flooding
EWSF	Engineered water/surfactant flooding
EWSPF	Engineered water/surfactant/polymer flooding
F5115	Flopaam 5115 polymer
FST	Frequency sweep test
FW	Formation water
HPAM	Hydrolyzed polyacrylamide
HSP	High salinity polymer
HSW	High salinity water
IFT	Interfacial tension
IOR	Improved oil recovery
IPV	Inaccessible pore volume
IW	Injection water
LSPF	Low salinity polymer flooding
LSSF	Low salinity surfactant flooding
LSSPF	Low salinity/surfactant/polymer flooding
LSW	Low salinity water
LVER	Linear viscoelastic region

MIE	Multi ion exchange
NPV	Net present value
OOIP	Original oil in place
PDI	Potential determining ions
PF	Polymer flooding
ppm	Parts per million
PV	Pore volume
RF	Recovery factor
ROIC	Remaining oil in core
RRF	Residual resistance factor
SEM	Scanning electron microscope
SF	Surfactant flooding
SP	Surfactant/polymer
TDS	Total dissolved solids
WF	Waterflooding
XRD	X-ray diffraction

LIST OF SYMBOLS

A	Cross-sectional area of core sample
C	Concentration of KOH solution
C_p	Polymer concentration, ppm
d	Diameter of core sample
E_d	Displacement efficiency
G'	Elastic or storage modulus, Pa
G''	Viscous or loss modulus, Pa
k	Permeability
k_{abs}	Absolute permeability
k_{eff}	Effective permeability
k_{ro}	Oil relative permeability
k_{rw}	Water relative permeability
L	Length of core sample
M	Mobility ratio
m_{sample}	Mass of sample, g
N_c	Capillary number
q	Flow rate
S_{oi}	Initial oil saturation in core
S_{or}	Residual oil saturation
S_{orw}	Residual oil saturation after waterflooding
S_{wi}	Initial water saturation
$\tan \delta$	Loss factor
V_b	Bulk volume
V_{blank}	Titration volume use for blank, cc
V_{HSW}	Volume of oil produced by HSW
V_{oi}	Initial volume of oil in the core
V_p	Pore volume, cc
V_{sample}	Titration volume in sample, cc
V_w	Volume of water produced
w_{dry}	Dry weight of core sample, g
w_{wet}	Wet weight of core sample, g
Δp	Pressure drop
Δp_{EWF}	Pressure drop during EWF stage
Δp_{EWPf}	Pressure drop during EWPf stage
$\Delta p_{EW-Postflush}$	Pressure drop during EW-postflush stage

γ	Shear strain rate, %
λ_D	Mobility of the displacing fluid
λ_d	Mobility of the displaced fluid
μ_0	Fresh polymer solution viscosity, cp
$\mu_{effluent}$	Effluent polymer solution viscosity, cp
μ_o	Oil viscosity
μ_t	Viscosity of polymer solution after one week at 80°C, cp
μ_w	Water viscosity
ω	Angular frequency, rad/s
ϕ_{He}	Porosity from Helium porosimeter
ϕ_{wt}	Porosity by weight method
ρ_w	Density of water, g/cc
σ	Oil-water IFT, dynes/cm

1. Introduction

1.1 Background

As reported by the World Energy Outlook, about 60% of oil reserves in the world are concentrated in carbonate reservoirs [1]. However, due to the presence of the organic and polar acidic compounds in crude oil, the majority of carbonate reservoirs tend to be oil-wet [2-4]. This results in higher residual oil saturations in carbonates, even after waterflooding. During the primary recovery phase, only 10-15% of oil-originally-in-place (OOIP) is recovered. Secondary recovery using water/gas injection can further extract 10-30% of remaining OIP. However, almost 40-60% oil remains trapped and inaccessible even after the secondary recovery. Various enhanced oil recovery (EOR) practices are in place to recover the trapped oil volume such as polymer flooding (PF), surfactant flooding, miscible gas injection, and steam injection. Each EOR method modifies rock-fluid interaction (crude oil-brine-rock, CBR) properties in a certain manner resulting in an improved recovery. For example, polymer flooding increases the displacing fluid viscosity, resulting in a favorable mobility ratio whereas surfactant EOR causes reduction in the oil/water interfacial tension (IFT) and the residual oil saturation (S_{or}) [5].

Engineered water flooding (EWF) is a relatively new EOR technique which involves injection of a properly designed low salinity water (LSW) disturbing the original equilibrium state of OWR system and resulting in an incremental oil production mainly by wettability modification. Additional oil recovery by EWF in sandstone was first documented in 1967 [6]. In 2004, its first ever field application in sandstone as an EOR technique was published. The idea of EWF as a potential EOR process in carbonates was triggered first in 1980s when exceptionally high oil recoveries were observed due to the seawater injection into fractured chalk formations under the North Sea [7-9]. Engineered water for carbonates is designed by tuning the injected water salinity, ionic strength, and the concentration of potential determining ions (PDIs), Ca^{2+} , Mg^{2+} , and SO_4^{2-} . EWF also has some inherent limitations, such as viscous fingering due to unfavorable mobility ratio, oil trapping, and fines migration [10]. Hence, this method may not qualify as an optimum EOR option under certain conditions, even though it is a low-cost technique.

In the current low crude price scenario, the development and implementation of novel cost effective EOR methods is critical for sustainable growth of the oil industry. Research on various levels is underway to develop economically viable hybrid EOR methods and overcome the limitations of individual methods. Utilizing EWF, novel hybrid methods such as hybrid

engineered water/polymer flooding (EWPF), or hybrid engineered water/surfactant flooding (EWSF) are developed. The idea behind hybrid EWPF is to enhance oil recovery by the combination of oil displacement mechanisms by the optimized injection water composition and polymer flooding. Engineered water modifies the wetting characteristics of the rock surface due to the salinity and composition difference that affects the bonding of the crude oil polar components (carboxylic material, -COOH group) with the carbonate surface and helps in oil detachment [11-13]. Polymer flooding improves macroscopic sweep efficiency by decreasing the mobility ratio [14]. In addition, EW promotes polymer stability and reduces the required polymer concentration, making PF applicable to high salinity, high temperature carbonate formations [15]. Hence, the hybrid method results in the incremental oil recovery greater than that obtained by standalone methods.

Similarly, other EOR chemicals such as alkali and surfactant can also be combined with EW to obtain multiple benefits. This section provides a review of various chemical EOR (CEOR) methods including polymer flooding, alkaline flooding, and surfactant flooding. EWF and hybrid EOR methods are then discussed with focus on hybrid EWPF technique. The purpose here is to identify the gaps in the literature regarding the application of hybrid EW/CEOR methods in carbonate reservoirs.

1.2 Polymer Flooding

Application of polymers in EOR, as mobility control agents, was first investigated in 1964 [16]. Later, various laboratory studies of polymer properties were performed [17-19]. The first field scale applications of polymers to augment oil recovery were carried out during 1960-1970 in the United States. Many researchers have conducted detailed reviews regarding PF projects implemented worldwide [20-23]. A successful PF project was implemented in Marmul sandstone oil field in Oman, where PF reduced the water cut and improved the oil rate [24]. As far as implementation of PF in carbonate reservoirs is concerned, the literature shows a small number of field projects [25, 26]. In a review by Standnes and Skjevrak [27], only 5% of field projects were reported in carbonate formations. Some of these carbonate reservoirs are the Upper Shaunavon Unit of Rapdan field [28], Ember formation of Byron and North Oregon basin fields [29], Eliasville Caddo Limestone Unit [30], and Pettit formation Crane zone of the Northeast Hallsville field [31].

Polymers are high molecular-weight materials with specific properties based on their structures, such as viscosification, toughness, viscoelasticity, etc. In contrast to water, a polymer solution

exhibits behavior of a non-Newtonian fluid, i.e. either shear-thinning or shear-thickening as a function of shear rate [32]. Two fundamental types of polymers used widely in EOR are synthetic and biopolymers [33]. Hydrolyzed polyacrylamide (HPAM) is extensively used as a synthetic polymer due to the low cost and high molecular weight [34]. Standnes and Skjevrak [27] conducted a comprehensive review of implemented polymer flooding projects and reported that HPAM was used in ~79% of the projects studied. HPAM is formed by copolymerization of acrylamide and acrylic acid [35, 36]; its chemical and physical configurations are shown in Figure 1. HPAM consists of long flexible chains with negatively charged carboxylic groups on backbones, which repel each other and keep the polymer chains stretched, resulting in high solution viscosity [37].

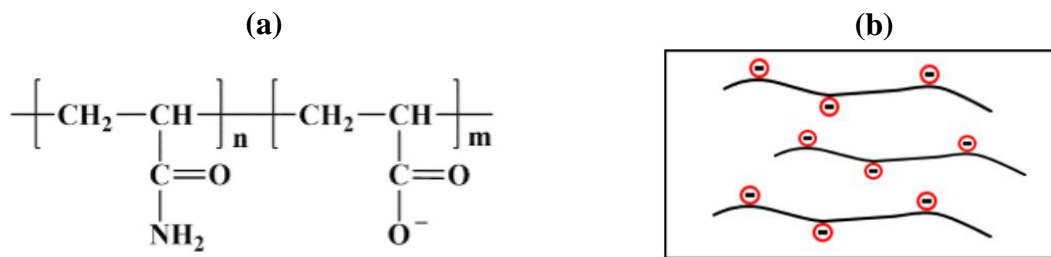


Figure 1. (a) Chemical structure [38] (reproduced with permission from Liu et al. J. Pet. Sci. Eng.; published by Elsevier, 2020); and (b) physical structure of HPAM polymer.

1.2.1 Recovery Mechanism

The main recovery mechanism involved in PF is the viscosification of displacing fluid by the addition of polymer, which is favorable for better hydrocarbon recovery [39]. The polymer addition to the displacing fluid increases its viscosity and, hence, results in a decreased mobility ratio, as per the fundamental relationship, shown below:

$$\text{Mobility ratio, } M = \frac{\text{Mobility of the displacing fluid, } \lambda_D}{\text{Mobility of the displaced fluid, } \lambda_d} = \frac{\mu_o k_{rw}}{\mu_w k_{ro}} \quad (1)$$

where, μ_o , μ_w are oil and water viscosities, respectively, whereas k_{ro} and k_{rw} are oil and water relative permeabilities, correspondingly. For the mobility ratio $M > 1$, water moves faster, causing an unstable front advancement, early breakthrough of water, and lower ultimate oil recovery. The polymer, on the other hand, provides a relatively stable front movement, delayed water breakthrough, and better sweep efficiency. Much research has been performed in the area of PF to improve its applicability and outcomes [40, 41]. Many researchers have studied chemical and physical properties of polymers and their dependency on various subsurface reservoir conditions [42, 43].

1.2.2 Viscoelastic Polymers

In addition to shear deformation, a complicated viscoelastic behavior is exhibited by synthetic HPAM polymers owing to their flexible chain structure [33, 44], resulting in an increased resistance during flow through porous media. Viscoelastic effect of synthetic polymers is characterized specifically by shear-thickening regime during which extensional flow is dominant and apparent polymer viscosity increases with shear rate [45-47]. Polymer chains stretching and intermolecular interactions of the elongated coils lead to shear-thickening behavior [48, 49]. Extensional flow exists in porous media when polymer solution passes through pore throats and constrictions, aligning the molecules and stresses in the direction of flow [50]. Such viscoelastic effects can cause injectivity issues but can also reduce residual oil saturation [51].

Several studies have reported additional oil recovery and reduction in S_{or} beyond waterflooding by viscoelastic polymers [52, 53]. Qi et al. [54] performed coreflood experiments on Bentheimer sandstone cores and observed 5% reduction in S_{or} by viscoelastic HPAM polymer flooding compared to viscous glycerin flood at the constant pressure drop. In another study, 4% reduction in S_{or} was observed by low salinity viscoelastic polymer flooding. The reduction in S_{or} by viscoelastic polymers can be triggered by various mechanisms including but not limited to shear-thickening behavior, oil-thread stabilization, and pulling and stripping of oil from pore walls [55]. There are different parameters and methods in the literature to quantify polymer's viscoelastic effect and resulting residual oil recovery such as Deborah number, strain hardening index (SHI), relaxation time, screen factor, pore-scale studies, and continuum viscoelastic models. Although, the injectivity response of viscoelastic polymers is accepted universally, there is still a debate on their capability to reduce S_{or} . There exist contradictory studies in which no reduction in S_{or} was observed by viscoelastic polymers from different Berea and Bentheimer cores [56-58].

1.2.3 Challenges Associated with Polymer Flooding

The viscosification ability of a polymer (particularly HPAM) is dramatically affected by ionic strength and salinity of the make-up brine, as well as the formation water. This is because the polymer chains undergo severe coiling and distortion in high saline water due to shielding or neutralization of charges present on the backbone. As a result, the polymer solution loses its viscosity. Similarly, hard water also has a deteriorating effect on HPAM viscosity for the same reason that divalent ions (Ca^{2+} and Mg^{2+}) reduce the polymer chain expansion by consuming

the negative backbone charges, resulting in polymer precipitation if the Ca^{2+} concentration is more than 200 ppm. High temperature also poses a challenge for HPAM as it causes hydrolysis of the polymer. Many researchers have studied the effects of these critical parameters on polymer performance [14, 59-63]. Some important challenges for PF, including salinity and hardness, are given below:

- The adsorption of HPAM in carbonate reservoirs is quite high compared to sandstones, possibly due to strong attraction forces between the negatively charged carboxylates on the HPAM backbone and positively charged calcite surface Figure 2.

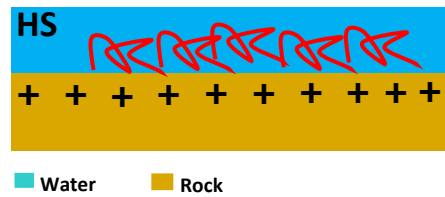


Figure 2. Schematic illustration of polymer degradation and adsorption in high salinity water.

- The degree of polymer adsorption increases with increasing brine salinity (NaCl concentration), as seen in Figure 3 [43].

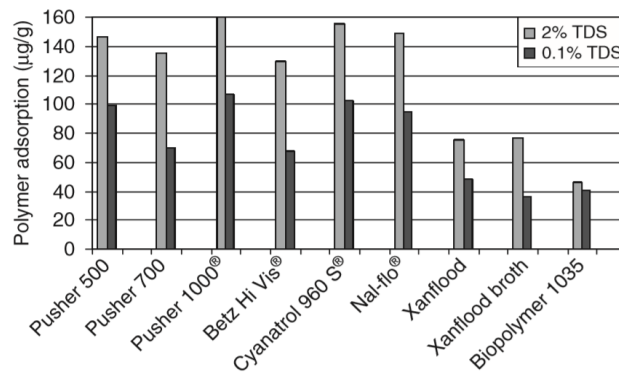


Figure 3. Effect of salinity on different polymers' adsorption [43]. Reproduced with permission from James J. Sheng, Elsevier Books; published by Elsevier, 2011.

- High salinity and high temperature conditions pose a major challenge for conventional PF due to instability and degradation of polymer under such conditions [64].
- Extraction and recycling of polymer from production stream is a major operational challenge and can substantially increase the project cost [65-67].

Scientists and researchers have put forth a great deal of effort, and PF technique has greatly improved over the years. Despite the advancement, there are a few limitations which need to be carefully evaluated to make it an economically viable solution for carbonates. The applicability of polymer flooding in carbonates is primarily limited by the formation water

salinity, make-up water salinity, hardness, formation temperature, and high polymer chemical degradation [21, 68, 69]. These constraints need to be addressed to accomplish oil recovery objectives and, hence, lead us to the idea of a novel hybrid EOR method that includes both PF and EWF.

1.2.4 Field Examples

With the aim to improve the mobility ratio, a major polymer flooding project was carried out in 1996 at Daqing oilfield in China. Around 31 commercial-scale projects were active in 2004, consisting of about 2916 producers and 2427 injectors. Polymer flooding in Daqing and Shengli oilfields collectively contributed about 250,000 bbl/day in 2004 and provided additional oil recovery of 6-12%. By the end of year 2006, total water intake had reduced by 21.8 m³/m³ of produced oil, with 25% reduction in water cut resulting in reduced expenditure for produced water treatment and disposal [39].

In 1990s, another successful polymer flooding project was reported in Courtenay, France, which recovered 5 to 30% extra oil by implementing augmented waterflooding technology during secondary recovery stage.

1.3 Surfactant Flooding (SF)

Surfactant flooding (SF) is one of the established EOR techniques in which surfactants are used to unlock low to medium viscosity crude oil potential from petroleum reservoirs. Co-surfactants are used to improve the properties of the primary surfactant solution such as the viscosity or surface energy of liquids, and aid in the designing process by providing optimum conditions concerning reservoir pressure, temperature, and salinity. Surfactant flooding technology is not new and has been utilized in the petroleum industry for the last 40 years [70-76]. Surfactant injection into the reservoir efficiently changes the phase behavior by producing microemulsions.

Application of surfactant effectively lowers the IFT between crude oil and water phase, diminishing the forces which are responsible for capillary trapping, and hence, decreases the residual oil saturation by altering the wettability [77, 78]. In its structural form, a surfactant molecule has a polar part, also known as a hydrophilic head, and a nonpolar part known as lipophilic hydrocarbon tail [79]. Surfactants are categorized based on the ionic charge of the head group such as anionic, cationic, or nonionic. All these types show specific properties based on their ionization in the aqueous solution. Anionic surfactant has a negatively charged head

group. They are mostly used in EOR processes as they are excellent in lowering the IFT between oil and water, quite stable under harsh reservoir conditions, show low adsorption on the rock surface, and economical to manufacture. Cationic surfactant has a positive charge. Their synthesis process requires a high-pressure hydrogenation reaction which is extremely expensive and makes it impractical to use cationic surfactants for chemical EOR. On the other side, nonionic surfactants have no charge and cannot reduce IFT, therefore, they are mainly used as co-surfactants in surfactant flooding EOR applications [80].

1.3.1 Recovery Mechanisms

Surfactant molecules are called amphiphilic, as they are made of both polar and nonpolar moieties. The hydrophilic-lipophilic property of surfactants makes them useful for immiscible flooding. In surfactant flooding EOR, the lipophilic tail interacts with the remaining crude oil and the hydrophilic head interacts with the water molecules, thus make oil-in-water or water-in-oil emulsions. A detailed schematic has been shown in Figure 4 illustrating the mechanisms of reduction in IFT and wettability alteration, emulsification, and adsorption of surfactant onto sandstone rock surface. M12 is a cationic surfactant while SDS is an anionic surfactant.

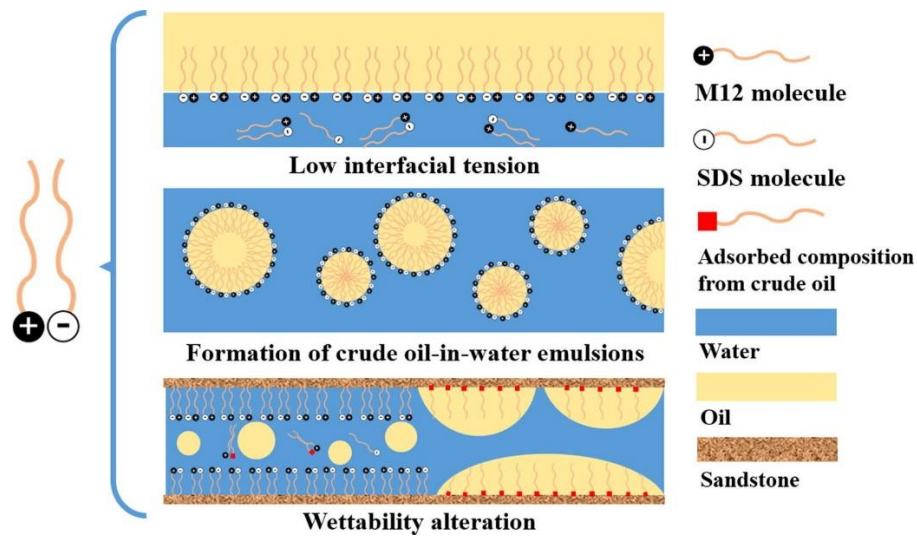


Figure 4. Schematic of processes involved during surfactant flooding [81].

1.3.2 Challenges in Surfactant Flooding

There are some risks associated with surfactant flooding, such as adsorption of surfactants and co-surfactants onto rock surface and their chemical separation and precipitation under reservoir conditions. Therefore, the main objectives of surfactant flooding design are to achieve the lowest possible IFT with low surfactant concentration, and minimum adsorption on the rock

surface [79, 82]. Furthermore, surfactants are also prone to become unstable and inactive in a high salinity and high temperature environment.

1.4 Alkaline Flooding (AF)

Alkaline flooding is one of the economical EOR techniques in which an alkali such as sodium carbonate (Na_2CO_3), sodium hydroxide (NaOH), or sodium orthosilicate ($\text{Na}_4\text{O}_4\text{Si}$) is mixed with water and injected into the reservoir to improve oil production. The alkaline chemicals increase the pH of injection water and help in mobilizing the trapped crude oil. This technique is applied only in reservoirs containing a high viscosity and high-acid number crude oils. This is because heavy oil has higher contents of natural petroleum acids than light oils [83].

1.4.1 Recovery Mechanism

The main mechanism of alkaline flooding is emulsification [84-86]. A water-mixed alkali reacts with the acidic component of crude oil, forming in-situ anionic surfactants which result in the reduction of IFT between oil and aqueous phases and triggers an increase in oil recovery as shown in Figure 5.

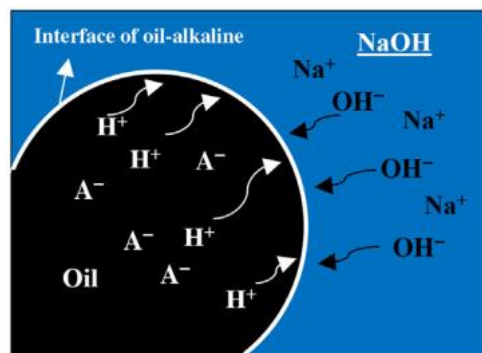


Figure 5. Mechanism of IFT reduction by in situ anionic surfactant generated by NaOH [87].

1.4.2 Challenges Associated with Alkaline Flooding

Alkaline flooding is not popular because of the complications it causes on the field level [88]. Particularly it is not suitable for carbonate formations because high concentration of calcium ions can form hydroxide precipitates (scaling issue) and increase the probability of formation damage. A huge concentration of alkali is used during this process. Moreover, the emulsification process, which is the main mechanism of alkaline flooding, generates extremely stable emulsions that increase the operating expenses required for the separation and treatment of produced fluids with surface facilities. Therefore, alkaline flooding is usually applied as a hybrid technique with polymer and surfactant to improve the oil recovery.

1.5 Engineered Water Flooding (EWF)

At present, research work for the enhancement in oil production with the modification of the injected brine chemistry, is being extended to carbonates, which is apparent from an increasing number of related research publications [89-93]. A number of coreflood studies have shown the incremental oil recovery ranging from 5-30% from different carbonate rocks, including limestone and dolomites, using low salinity or chemically tuned water (Table 1). Despite the variation in additional oil recovery, the EOR effect of EW is supported by all the studies. Different recoveries can be attributed to variations in oil, rock, formation and injection water compositions, temperature, etc. The method gives better performance in strongly oil-wet to intermediate-wet systems and at temperatures greater than 70 °C [94]. Spiking the low salinity water with SO_4^{2-} ions has shown higher incremental recovery in most of the studies [95-97]. Despite the increased interest in EWF EOR in carbonates, there is still a debate on its principal driving mechanisms. In some cases, mineral dissolution acts as a primary mechanism for wettability change [98, 99] and incremental recovery, whereas, in other cases multi-ion-exchange (MIE) reactions and surface charge modification are dominant [100-102].

Hence, characteristics of a reservoir-fluid system have strong influence on success or failure of the EWF process. The research conducted, thus far, indicates that more than one mechanism is responsible, and certain conditions need to be met for EWF EOR effect. Also, the mechanisms in carbonates are different from those reported in sandstones, possibly due to the absence of clays in carbonates [103, 104]. In sandstones, clay presence is considered to be critical for low salinity EOR effect, as the clay particles release from the rock surface due to salinity difference between injected and in-situ brines, detaching organic oil components and altering the sandstone wettability [6, 94, 105]. However, only low salinity may not be enough to recover trapped/adsorbed oil in carbonates due to their positive surface charge. Presence of active ions e.g. Ca^{2+} and SO_4^{2-} in injected water is necessary to aid oil detachment from carbonate surface [106]. Different factors govern incremental oil by EW, and those discussed in the literature are summarized in the next section.

1.5.1 Recovery Mechanisms

In carbonates, the main parameter contributing to a low water-wet nature is the acid number (AN, mg KOH/g of oil, -COOH group) of the crude oil [2, 107, 108]. The rock tends to be more oil-wet if it contains crude oil with a higher AN, due to the high attraction between the negatively charged carboxyl group of oil and positively charged carbonate surface [109, 110].

Table 1. Summary of corefloods showing incremental oil recovery by EWF in carbonates.

Study	Rock Type	Brine TDS (g/L)	Potential Determining Ions (PDIs)	Acid Number (AN) (mg KOH/g)	Temperature (°C)	Injection Mode	Incremental Recovery (%OOIP)	Remarks
Bagci, Kok [111]	Unconsolidated limestone	FW: Nil EW: 20	KCl	-	50	Secondary	18.4	2 wt% KCl case resulted in maximum recovery due to reduction in pH.
Fathi, Austad [95]	Outcrop chalk cores	FW: 62.80 EW: 16.79	4 times SO ₄ ²⁻ and 4 times Ca ²⁺	Oil A: 2.0 and Oil B: 0.5	70 – 120	Secondary	24	The highest recoveries using EW were observed in 90-120°C temperature range with SO ₄ ²⁻ ions. Effect of Ca ²⁺ was observed only at 120 °C indicating that Ca ²⁺ is less active at lower temperatures.
Gupta, Smith [112]	Limestone and dolomite	FW: 181 EW: 33	4 times SO ₄ ²⁻	0.11	70 °C for dolomite and 121 °C for limestone	Tertiary	9% in dolomite and 5.1% in limestone	The lower recovery for limestone core was attributed to anhydrite precipitation at higher temperatures.
Yousef, Al-Saleh [113]	Limestone	FW: 213 EW: 5.7	SO ₄ ²⁻ , Ca ²⁺ and Mg ²⁺ present in seawater	0.25	100	Tertiary	18	Higher tertiary recovery by LSW is attributed to improved connectivity between pore systems due to mineral dissolution by salinity gradient.
Zahid, Shapiro [94]	Reservoir carbonate and Outcrop chalk	FW: 213 EW: 5.7	SO ₄ ²⁻ , Ca ²⁺ and Mg ²⁺ present in seawater	0.96	Ambient and 90°C	Tertiary	90 °C: 18% for carbonate and 0.6% for chalk Ambient: 1.7% for carbonate and 0.6% for chalk	LSW did not result in any incremental oil at ambient temperature because of negligible activity of potential ions. Higher recovery from carbonate at 90 °C was possibly due to dissolution reactions. Poor recovery from chalk was due to water wet nature of cores.
Chandrasekhar and Mohanty [96]	Limestone	FW: 179 EW: 5.7	SO ₄ ²⁻ , Ca ²⁺ and Mg ²⁺	2.45	120	Secondary and Tertiary	32 – 36	LSW with SO ₄ ²⁻ and Mg ²⁺ gave best results in terms of oil recovery and wettability alteration. Ca ²⁺ ions were not effective. Ion-exchange and mineral dissolution were dominant mechanisms. Higher EW recovery can also be due to higher AN oil.
Al-Attar, Mahmoud [97]	Limestone	FW: 197 EW: 5	SO ₄ ²⁻ and Ca ²⁺	-	25	Secondary	24	SO ₄ ²⁻ addition gave the highest recovery. However, addition of Ca ²⁺ had a negative effect on recovery.

Awolayo, Sarma [114]	Limestone	FW: 261 EW: 43.9	4 times SO_4^{2-}	-	110	Tertiary	10	Increasing SO_4^{2-} beyond 4 times did not give any incremental recovery possibly due to CaSO_4 precipitation triggered at higher temperatures.
Alameri, Teklu [115]	Fractured Limestone	FW: 100 EW: 12.8	-	-	90.6	Tertiary	7	LSW can work for low permeability rocks, but the incremental recovery is high in less heterogeneous reservoirs.
Puntervold, Strand [116]	Outcrop chalk cores	FW: 62.83 EW: 20.24	4 times SO_4^{2-}	0.5	90	Secondary	20	LSW spiked with 4 times SO_4^{2-} ions gave maximum incremental oil as compared to original seawater.
Qiao, Li [117] and Fathi, Austad [118]	Chalk	Molarity FW: 2.198 EW: 0.794	4 times SO_4^{2-} and 4 times Ca^{2+}	1.9	110	Secondary	14 – 22	Effective LSW design should include higher amount of SO_4^{2-} and small amount of divalent ions to increase water-wet fraction of rock.
Mohsenzadeh, Pourafshary [119]	Limestone	FW: 136 EW: 4.5	-	-	87	Tertiary	22.5	IFT reduction was observed to be the main LSW recovery mechanism at low reservoir temperature and lower concentration of active ions.
Fani, Al-Hadrami [120]	Limestone	FW: 102.5 EW: 8.7	4 times SO_4^{2-}	-	87	Tertiary	22.2	Smaller tertiary EW slugs can provide comparable recovery as larger slugs if reasonable soaking time is given for EW to interact with the rock.
Nasralla, Mahani [121]	Limestone	FW: 239 EW: 4.4	SO_4^{2-} and Mg^{2+} present in seawater	-	100	Secondary and Tertiary	7	LSW performance varies with rock properties and mineralogy. In low permeable formations, LSW results in accelerated oil production at lower injection rates.
Sarvestani, Ayatollahi [122]	Limestone	FW: 150 EW: 4	SO_4^{2-} , Ca^{2+} and Mg^{2+}	0.14	90	Secondary	12	Mg^{2+} affected the oil recovery more than Ca^{2+} . (SO_4^{2-})/(Mg^{2+}) ratio is the controlling factor for the wettability modification.
Masalmeh, Al-Hammadi [123]	Limestone	FW: 204 EW: 0.24	-	9.25	127	Secondary and Tertiary	6.5 – 12.5	Crude oils with high ANI lead to extra oil recovery by LSW in both secondary and tertiary modes due to formation of micro-dispersions.

Consequently, oil recovery by waterflooding is reduced with increasing AN [124]. The main mechanism governing EOR by chemically tuned or LSW is the change of carbonate rock wettability to more water-wet conditions, subsequently improving the relative permeability and fractional flow of oil [12, 109, 125-127]. However, the extent of this wettability change depends on many factors, including presence of potential active ions in low salinity water, reservoir temperature, type of rock, and composition of crude oil.

Multi-Ion Exchange (MIE)

In carbonate reservoirs, the main factor for wettability modification is the potential determining ions (PDIs; Mg^{2+} , Ca^{2+} , and SO_4^{2-}), particularly SO_4^{2-} , in injected water along with reduced salinity. The decrease in NaCl results in a reduced ionic density in electric double layer, formed on a positively charged carbonate surface, making surface access of the PDIs easier. SO_4^{2-} adsorption makes the carbonate surface less positive, and consequently, the negatively charged carboxylic group of oil is detached, making the rock more water-wet [11, 13, 116, 128-130]. Hence, EWF results in improved microscopic displacement. However, the macroscopic efficiency is generally poor for EWF due to an unfavorable mobility ratio. This can result in early water breakthrough, and target incremental oil recovery may not be achieved [129, 131, 132]. No EW EOR effect may be observed when the system is strongly water-wet under initial equilibrium conditions.

Mineral Dissolution Reactions

Another mechanism for wettability alteration is the enhanced connectivity between micropores and macropores due to mineral dissolution by EW at the micro level [9, 99, 133, 134]. Study conducted by Den et al. [135] showed that more calcite was dissolved with decreasing injected low salinity brine pH. The effluent brine pH was higher in this case, leading to crude-rock surface charge modification and additional oil recovery. Another study also documented similar results that increase in effluent pH and Ca^{2+} concentration was observed by injecting different dilutions of seawater which could lead to incremental oil production by wettability modification or alkali formation [98]. Reduction in IFT, instead of wettability alteration, has also been reported in some cases [119, 136]. Experiments performed by Mohsenzadeh et al. [119] showed around 42% reduction in IFT using 20 times diluted seawater in a low temperature carbonate reservoir.

Fluid-Fluid Interactions (Micro-dispersion)

The interaction between injected EW and crude oil is also critical to observe incremental oil recovery by EWF. When a properly designed EW contacts the adsorbed crude oil, water-in-oil

micro dispersions are formed, resulting in residual oil recovery. In the presence of LSW, a viscoelastic interaction exists at oil-water interface and the crude oil snap-off process is minimized by this mechanism. As a result, a more uniform oil phase is available in the pore spaces during EWF, and oil recovery is increased [137]. Presence of SO_4^{2-} ions in EW also promote fluid-fluid interactions at elevated temperature by forming water-in-oil emulsions [138]. However, not all crude oils provide incremental oil by EWF. It is necessary to consider the oil composition and interaction with injected LSW in the screening criteria for carbonate reservoirs and to assess the suitability of reservoir for EWF. Recently, Masalmeh et al. [123] carried out a comprehensive study of almost 30 offshore and onshore carbonate formations in Abu Dhabi to develop robust screening criteria for low salinity waterflooding (LSWF) based on oil/brine interactions and analysis of resulting micro-dispersions. Some oils formed micro-dispersions with LSW (positive crude oils) and, also, resulted in incremental oil recovery, while others did not form micro-dispersions (negative crude oils) and provided negligible additional recovery upon LSWF. Similar studies have also confirmed the role of fluid-fluid interactions in incremental recovery by LSWF [122, 137, 139].

1.5.2 Conditions for Engineered Water Flooding

Chemically altered water injection results in extra oil production from carbonate rocks if favorable conditions exist. First of all, the injection water salinity should be appreciably less than the formation water salinity to disturb the initial equilibrium of the system [140]. Secondly, the injection water must contain active ions, most importantly SO_4^{2-} , to change the carbonate rock surface charge and release adsorbed oil [106]. Temperature has also a strong influence on EWF performance and most of the studies suggest the temperature to be in the range of 70-120 °C for effective oil production by engineered water [141, 142]. The reservoirs having crude oil with organic acidic components are better candidates for EWF, as these reservoirs tend to be oil-wet and more residual oil saturation is available to be displaced by low salinity engineered water [123].

1.5.3 Limitations of EWF

The results reported in literature show that EWF can be a potential EOR technique for carbonate rocks. The corefloods performed by Ravari et al. [143] showed ~ 28% incremental oil recovery by chemically-tuned water. Experiments performed by Yousef et al. [144] also showed encouraging results using diluted versions of seawater. However, there are unsuccessful cases, where EWF did not provide any incremental oil in both sandstone and carbonate reservoirs

[131, 132, 145-148]. The injection of low salinity water (440 ppm) in North Sea Snorre field single-well pilot test resulted in negligible extra oil, despite 2% OOIP incremental recovery in laboratory corefloods. The main reason was the initial reservoir wettability that was water-wet.

As with conventional waterflooding, the problem of unfavorable mobility ratio also exists with EWF due to the viscosity difference between the displaced and displacing fluid [131]. LSWF in four different fields in Russia resulted in very little to negligible incremental oil. Field tests in Pervomaiskoye field showed three times reduction in water relative permeability and corresponding 3.5% extra oil recovery by LSWF. However, no incremental recovery was obtained by LSW (1.0 mol/L ionic strength) in Bastrykskoye sandstone field pilot test, despite a five-times reduction in relative permeability of water in corefloods. 2.7% additional oil was recovered in Romashkinskoye field pilot tests by diluted seawater, whereas no LSW effect was observed in Arkhangelskoye field [131].

One of the reasons for such discouraging results is the viscosity contrast between oil and injected LSW, leading to unfavorable mobility ratio and poor sweep efficiency. This problem may be even worse in pilot or field-scale applications if high permeability channels/layers exist in the reservoirs [149]. Hence, EWF has the potential to enhance the microscopic displacement efficiency, but it can, on the other hand, result in a poor volumetric sweep efficiency if mobility control treatment is not considered. These limitations can be addressed by adding surfactant to EW, thereby reducing IFT and increasing capillary number which is still low in EWF alone. Similarly, addition of polymer to EW can improve the displacing fluid viscosity, hence increasing the volumetric sweep efficiency.

1.5.4 Lab-based Studies

By using EW, the oil recovery factor can be considerably increased from both carbonate and sandstone reservoirs. The experiments performed by Yousef et al. [144] showed encouraging results by using diluted versions of seawater. IFT reduction and wettability change towards water-wet condition was observed as the injected water salinity was reduced progressively (Figure 6). However, it must be noted that although, the ion-adjusted EW can result in in-situ soap (surfactant) generation if the pH of the system is increased because of mineral dissolution reactions, but the resulting IFT reduction is too low to cause any decrease in residual oil saturation. Nasralla et al. [121] also performed a detailed special core analysis (SCAL) study on limestone reservoir core plugs to demonstrate the low salinity water effect on oil production and to select the optimum salinity and composition of ions for the reservoir under study. The

coreflooding experiments performed on the aged reservoir cores using formation water (239,400 ppm TDS), seawater (43,700 ppm TDS) and different diluted samples of seawater showed ~ 7% increased oil recovery by LSW in comparison of formation water injection.

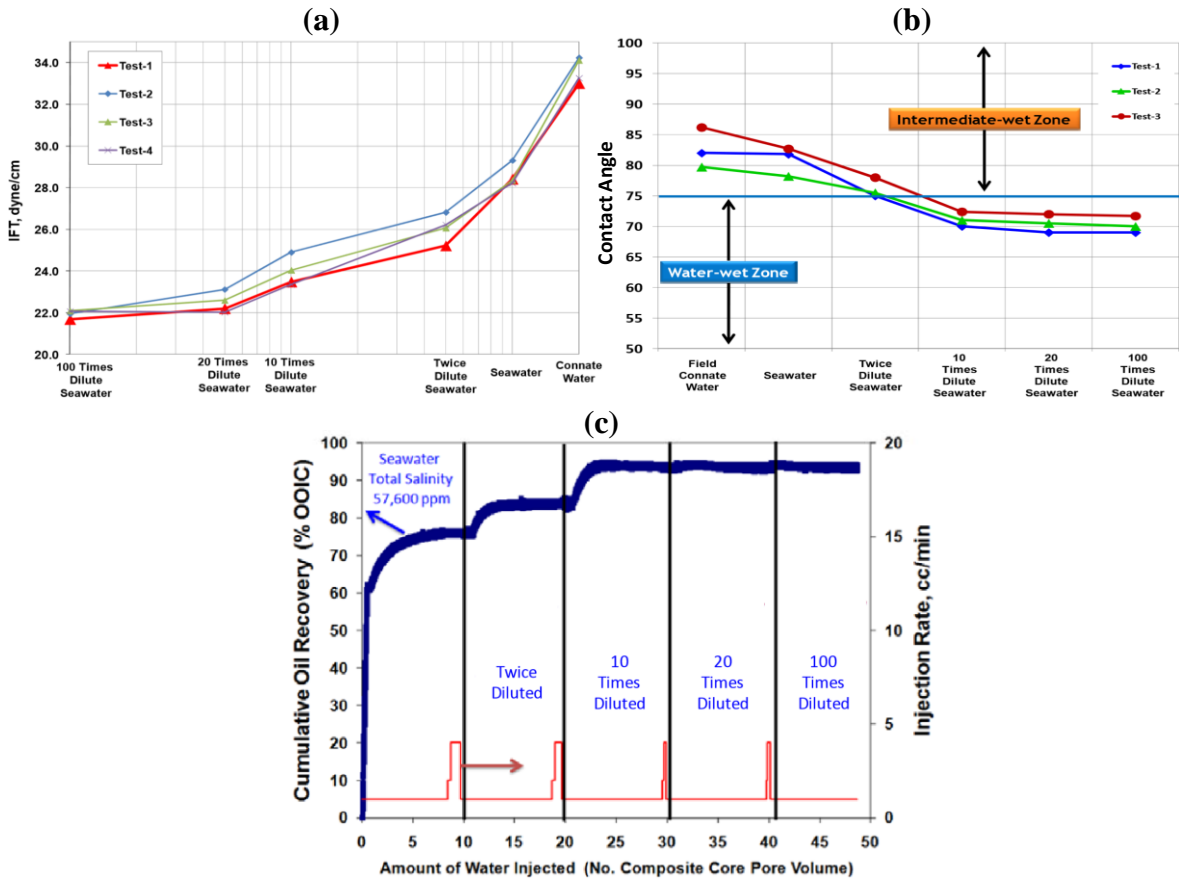


Figure 6. (a) IFT reduction, (b) Wettability change and (c) Incremental oil recovery by LSW injection [144].

Experiments performed by Masalmeh et al. [123] on carbonate cores from some of the Abu Dhabi oil fields showed additional oil recovery by LSWF under secondary mode (12.5%) as well as tertiary injection mode (6.5%) in comparison with formation water injection. The experiments were conducted using live oil and considering reservoir pressure and temperature conditions. In tertiary mode, oil was mobilized after 0.5 PV injection of LSW (Figure 7).

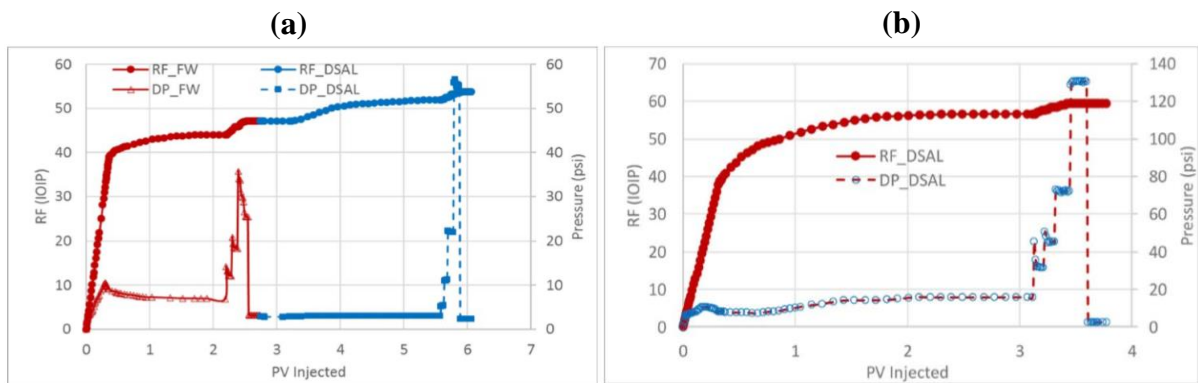


Figure 7. Oil recovery by LSWF in (a) Tertiary injection mode and (b) Secondary injection mode; FW: Formation water (204,201 ppm TDS), DSAL: Low salinity water (241 ppm TDS) [123].

1.6 Hybrid Engineered Water-Polymer Flooding (EWPF)

Literature and field case studies have proven that synergy between two or more EOR techniques provides better results relating to oil recovery and economics. For instance, the combined use of alkali, surfactant, and polymer in the alkaline-surfactant-polymer (ASP) flooding technique results in enhancement of both the macroscopic and microscopic sweep efficiencies, owing to a favorable mobility ratio by the polymer, higher microscopic sweep efficiency due to pH change by alkali, and reduction in IFT by surfactants [150, 151]. Any EOR method involving two or more EOR techniques is known as a hybrid EOR method. Much research is being carried out in the field of hybrid EOR, particularly for chemical methods to increase their applicability. As discussed in previous sections, both PF and EWF have their associated challenges, which limit their field-scale applications. To overcome those limitations and take advantage of the synergetic effects of the two methods, the hybrid EWPF technology comes into play.

Various experiment-based and modeling studies have been carried out in recent years to prove hybrid EWPF as an effective EOR method [5, 15, 152-158]. These studies have shown an average 11% incremental oil recovery by the hybrid method, from different carbonate formations (Figure 8).

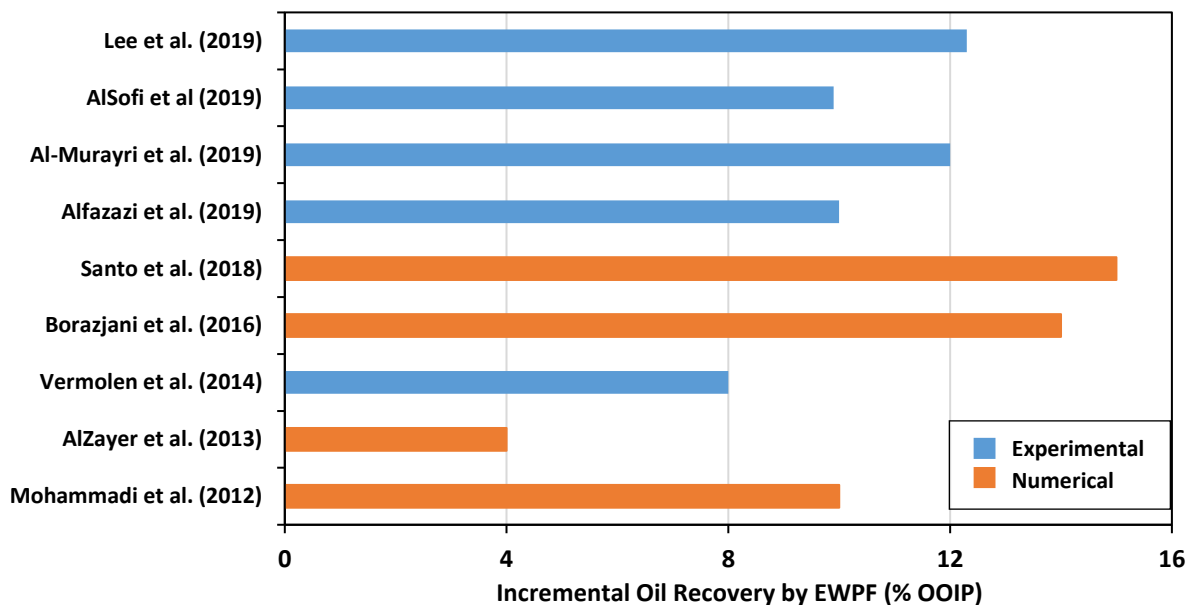


Figure 8. Summary of experimental and simulation studies showing incremental oil by EWPF in carbonates [159].

Rivet [10] and Seright et al. [160] studied the EWPF combined effect in terms of better polymer stability and yield, improved microscopic and macroscopic sweep efficiency, and reduction in chemical cost. A seawater desalination process was developed for combined EWPF application

in an offshore field [161]. EW hybrid methods can provide up to 30% of OOIP incremental recovery [162]. However, there is still more research required to make this hybrid process practically applicable in large scale field projects. One important parameter in this regard is the understanding of principle driving mechanisms responsible for EW effect and how this hybrid process can be designed to get maximum possible oil recovery.

1.6.1 Enhanced Oil Recovery by Hybrid EWPF in Carbonates

The limited literature on the application of EWPF EOR in carbonates shows that it can increase oil recovery equal to or more than the summation of the recovery from each process. Lee et al. [5] performed experiments on carbonate samples using LSW with ion adjustments followed by PF. S_{or} was considerably decreased by low salinity PF (LSPF) compared to conventional high salinity waterflooding and EWF. All designed injection water (IW) solutions (IW-1: pH-7, 1000 ppm SO_4^{2-} , IW-2: pH-7, 4000 ppm SO_4^{2-} , IW-3: pH-4, 4000 ppm SO_4^{2-} , IW-4: pH-7, 100 ppm Ca^{2+} , IW-5: pH-7, 1000 ppm Ca^{2+} , and IW-6: pH-4, 1000 ppm Ca^{2+}) reduced S_{or} , but the neutral low salinity water containing only SO_4^{2-} ions gave the lowest S_{or} (Figure 9a).

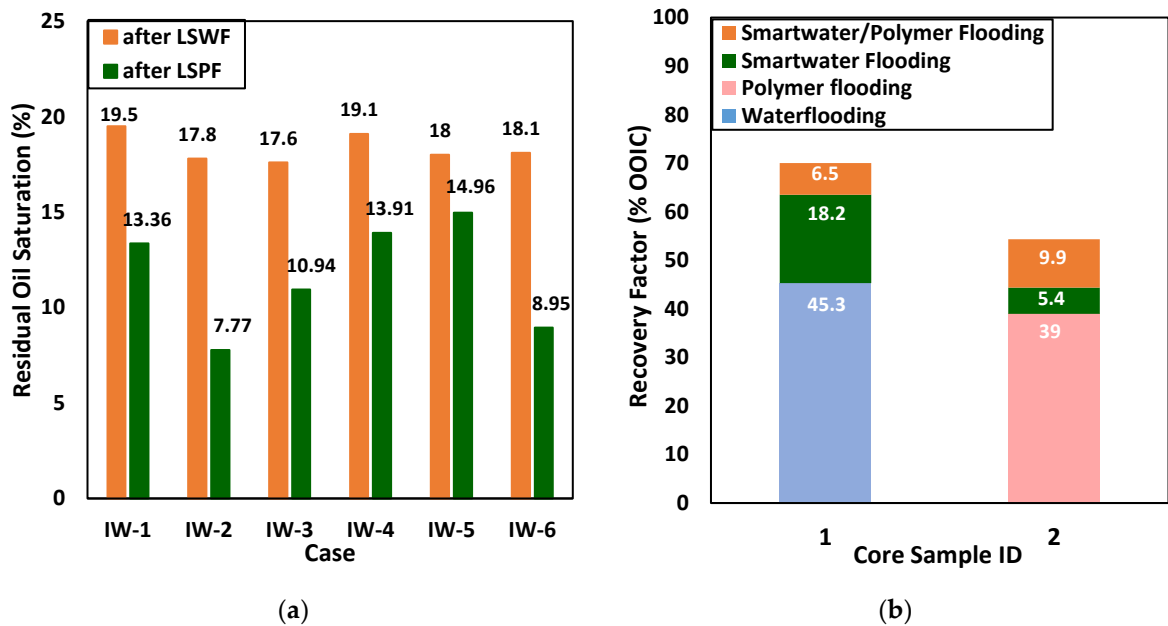


Figure 9. (a) Reduction in S_{or} after LSPF [5] (reproduced with permission from Lee et al., J. Pet. Sci. Eng.; published by Elsevier, 2019); and (b) additional recovery by EWPF in carbonate reservoir cores [163].

Incremental oil recovery by synergy of smart water (SW) and polymer in carbonates was also confirmed by Al Sofi et al. [163]. Hybrid EWPF resulted in an incremental 6–10% OOIP recovery after PF, showing that LSW modifies fluid-rock interactions, creating moveable oil volume, which is displaced easily by polymer in EWPF (Figure 9b). Similarly, Vermolen et al. [152] conducted oil displacement experiments on reservoir cores, and ~ 45% incremental oil

was recovered by LSPF. An incremental 8% OOIP recovery was obtained by further reducing the salinity of water, confirming the synergistic effect of the hybrid process. Hence, different researchers have confirmed synergy and additional oil recovery by combined low salinity/engineered water and polymer in carbonates, but more work is required to fully understand the recovery mechanisms driving incremental oil recovery by the hybrid process and an optimum injection design. The dominant recovery mechanisms for EWPF are discussed in the following section.

1.6.2 Recovery Mechanisms

The hybrid method under study involves the mechanisms of both EW and polymer. EW helps to detach oil from the rock surface, creating a moveable oil saturation in-situ, which is later displaced by polymer flood. Figure 10 shows the mechanisms known to be responsible for EOR by the hybrid method. However, to obtain maximum benefit from this method, there should be an optimum design in terms of EW composition, selection of PDIs to be used in a certain carbonate rock type, polymer concentration, slug sizes for EW and PF, optimum injection rate for PF, and injection scheme for the hybrid process (continuous or slug-wise injection).

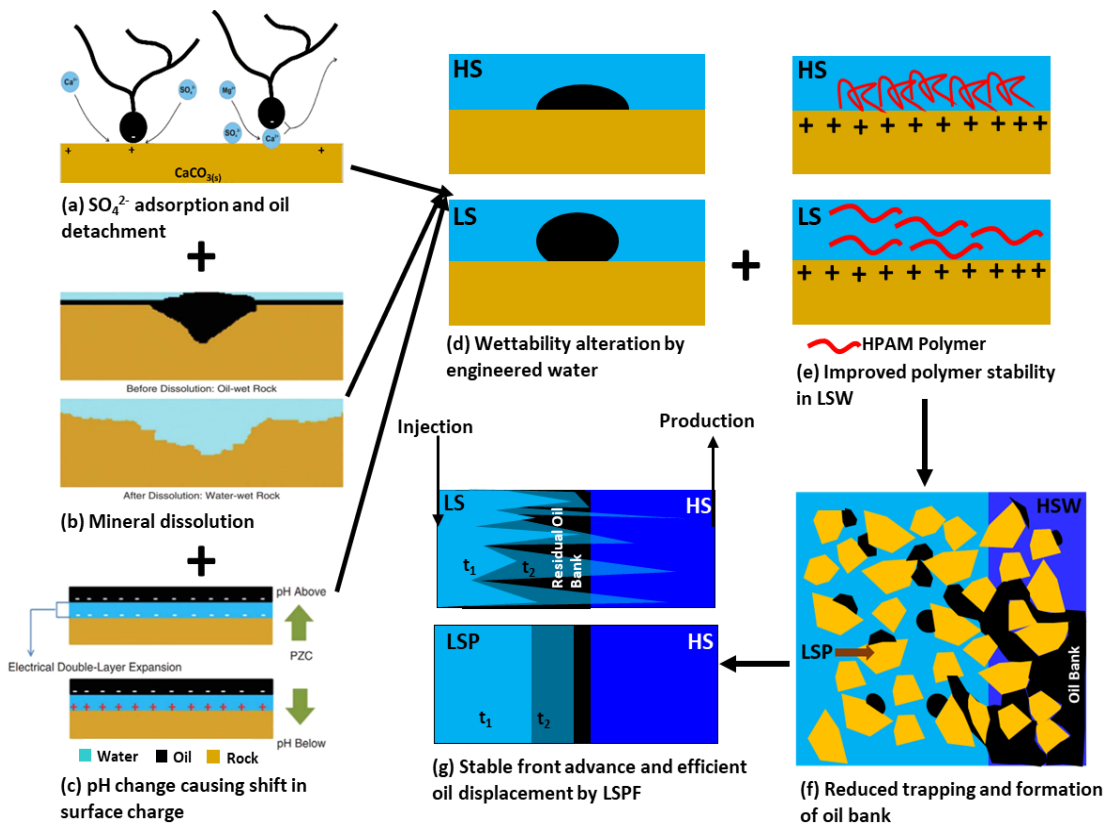


Figure 10. Illustration of governing mechanisms for incremental oil by hybrid LSPF. (a), (b), (c) and (d) depict the functions of LSW [92, 164] (reproduced with permission from Zhang et al., Energy & Fuels; published by American Chemical Society, 2006; and Al Shalabi et al., J. Pet. Sci. Eng.; published by Elsevier, 2016); (e) shows polymer stability in LSW; (f) shows formation of the oil bank [165]; and (g) presents the final outcome of the process i.e. detachment, mobilization, and displacement of the residual oil bank by combined LSPF.

However, to obtain maximum benefit from the hybrid method, there should be an optimum design in terms of EW composition, selection of PDIs to be used in a certain carbonate rock type, polymer concentration, slug sizes for EW and PF, optimum injection rate for PF, and injection scheme for the hybrid process (continuous or slug-wise injection). Mechanisms reported in the literature are briefly discussed in the following section.

Wettability Modification by Engineered Water (EW)

One of the two governing mechanisms for the hybrid process is the effect of ion-adjusted, low-salinity water that changes the wettability of carbonate rock from oil-wet or intermediate-wet to water-wet by disturbing the initial equilibrium of the CBR system [166]. The EW plays its part to enhance the microscopic sweep efficiency by desorption of oil from the rock. Various factors are important to consider while designing the EW for a particular CBR system and polymer type. For example, the selection of PDIs is very critical and must be decided based on the specific rock type (limestone, chalk, and dolomite) under study. The pH of the injection brine is also a critical parameter and must be considered in the design process. The factors which govern the wettability modification mechanism of EWPF are briefly discussed below.

Role of Potential Determining Ions (PDIs)

PDIs in EW polymer solution affect the polymer adsorption and incremental recovery differently. Presence of SO_4^{2-} ions in seawater or EW is the key factor for carbonate wettability modification, as it reduces carbonate rock surface potential, promoting oil detachment by Ca^{2+} and/or Mg^{2+} [95, 138, 167-169]. Lee et al. [5] performed a detailed study to analyze the effect of PDIs and pH on oil recovery by EWPF in a carbonate reservoir. Coreflooding experiments showed that the neutral HPAM polymer solution containing SO_4^{2-} ions resulted in a considerable decrease in S_{or} and less polymer adsorption compared to Ca^{2+} ions (Figure 9a). The incremental oil recovery was 12.3% for this case, the maximum among all cases (Figure 11a). Contact angle measurements by the captive droplet method also confirmed wettability change towards more water-wet condition in the case of the neutral polymer solution with higher SO_4^{2-} concentration (Figure 11b). The reason for lower oil recovery, in case of the polymer solution containing Ca^{2+} ions, is the higher polymer adsorption and permeability reduction due to precipitation of Ca^{2+} ions.

Effect of Brine pH

The pH of the solution also has a strong influence, as it controls mineral dissolution reactions involved in wettability alteration by EW in carbonates. Effluent pH analysis by Lee et al. [5] experiments showed a higher pH increase by acidic solution injection due to calcite dissolution

in acid-base reactions. However, the pH increase must be sufficient (≥ 11) for wettability modification and incremental oil recovery. pH effect on polymer retention and stability was also studied by Lee et al. Polymer adsorption was also significantly increased in acidic medium indicating acidic conditions are not favorable for polymer flooding.

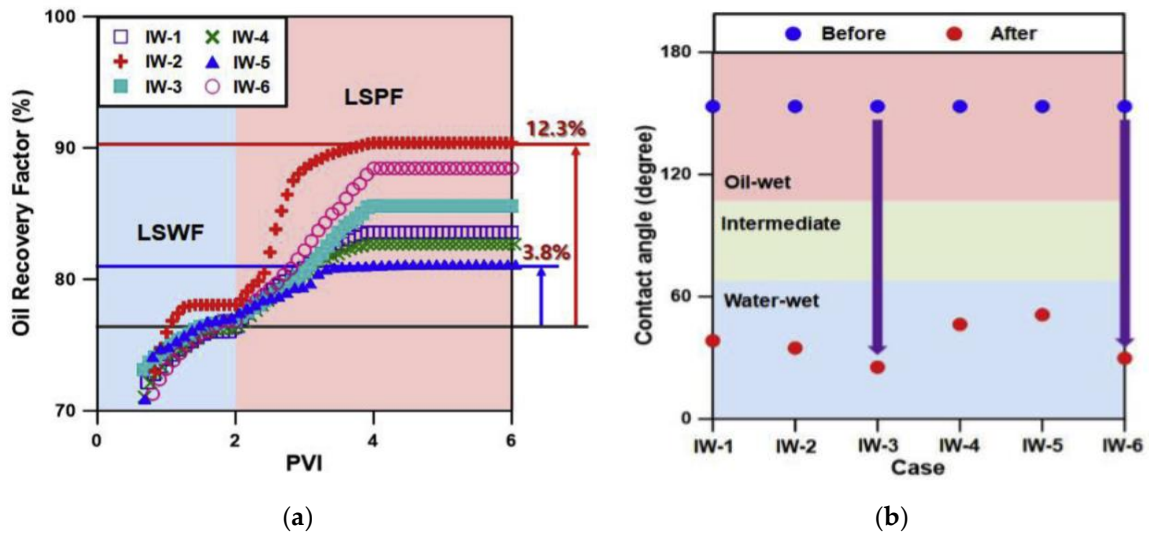


Figure 11. Effect of PDIs and pH of water on (a) oil recovery and (b) wettability alteration by EW [5]. Reproduced with permission from Lee et al., J. Pet. Sci. Eng.; published by Elsevier, 2019.

EW and Polymer Effect on Interfacial Tension

Interfacial tension (IFT) experiments conducted by Al Sofi et al. [158] confirmed that both LSW and polymer have negligible effect on IFT. This is because the IFT reduction should be in the several orders of magnitude to overcome capillary forces and reduce residual oil saturation which is not possible by LSPF. Table 2 shows oil/water IFT measurements for injection water (69,000 ppm TDS), smart water (6,900 ppm TDS) and smart water with polymer from Al Sofi et al. [158] work. It can be observed that IFT values for both injection water and smart water are comparable and are not sufficient to cause any incremental oil production.

Table 2. Oil/water IFT measurements showing negligible effect of smart water and polymer on IFT.

Brine	Polymer (mg/L)	IFT 1 (mN/m)	IFT 2 (mN/m)	IFT 3 (mN/m)	\overline{IFT} (mN/m)
Smartwater	-	37.37	38.99	39.53	38.63
	2000	30.15	29.94	30.26	30.12
Injection water	-	27.3	25.73	25.17	26.07
	3000	27.31	26.94	26.99	27.08

Source: AlSofi, Wang [158]

Favorable Mobility Ratio by Polymer

Another mechanism for EOR by EWPF is the improved fractional flow by polymer. EW alone may not be able to displace the moveable oil; however, by polymer addition, the residual oil

bank formed is easily displaced by the polymer due to stable front movement. Hence, the polymer plays a critical role, and must be compatible with the EW designed for the reservoir. Fortunately, EWPF takes the supplementary benefit of enhanced polymer stability and decreased retention in the presence of EW, leading to higher incremental oil recoveries and cost savings by reducing polymer consumption. Hence, the hybrid EWPF EOR can be successfully applied to carbonate reservoirs with harsh temperature and salinity conditions. However, careful design of EW and polymer must be selected for a field, as the composition of EW can have both positive and negative impacts on polymer performance. Critical factors for polymer performance in the hybrid process include polymer viscosity, retention, degradation, and consumption. These factors and their dependence on EW composition are discussed hereafter.

Enhanced Polymer Stability by EW

HPAM properties are strongly dependent on makeup brine salinity, hardness, pH, and ionic composition. HPAM are the cheapest and most widely used polymers, but start losing viscosity and behave more like Newtonian fluids under high salinity and high temperature conditions, thus, limiting their application to such formations [152]. Low pH promotes HPAM adsorption due to coiling of polymer chains as more molecules are adsorbed onto an available surface area. Similarly, high salinity results in charge screening effect, reducing polymer viscosity and stability. Ca^{2+} ions promote HPAM precipitation, which can have a detrimental effect on rock permeability and polymer degradation. The recommended Ca^{2+} concentration in EW should be below 200 ppm [170]. In contrast, SO_4^{2-} ions, being negatively charged, promote stability of the anionic HPAM polymer in carbonate formations. A number of studies on polymer rheology have shown ~30–50% reduction in polymer concentration [15, 152, 158, 171-174] to achieve the target viscosity when low salinity makeup brine is used (Figure 12).

Lee et al. [175] developed a comprehensive database based on detailed rheological experiments using HPAM polymers. This database clearly demonstrated higher polymer viscosity and enhanced stability by reducing brine salinity and hardness. Vermolen et al. [152] performed coreflooding experiments to assess the LSW impact on polymer concentration and incremental oil recovery and showed a 50% reduction in polymer concentration needed to attain a desired viscosity, mainly because of improved polymer stability and reduced coiling in LSW (Figure 13). The cost savings will be even higher in high salinity formations.

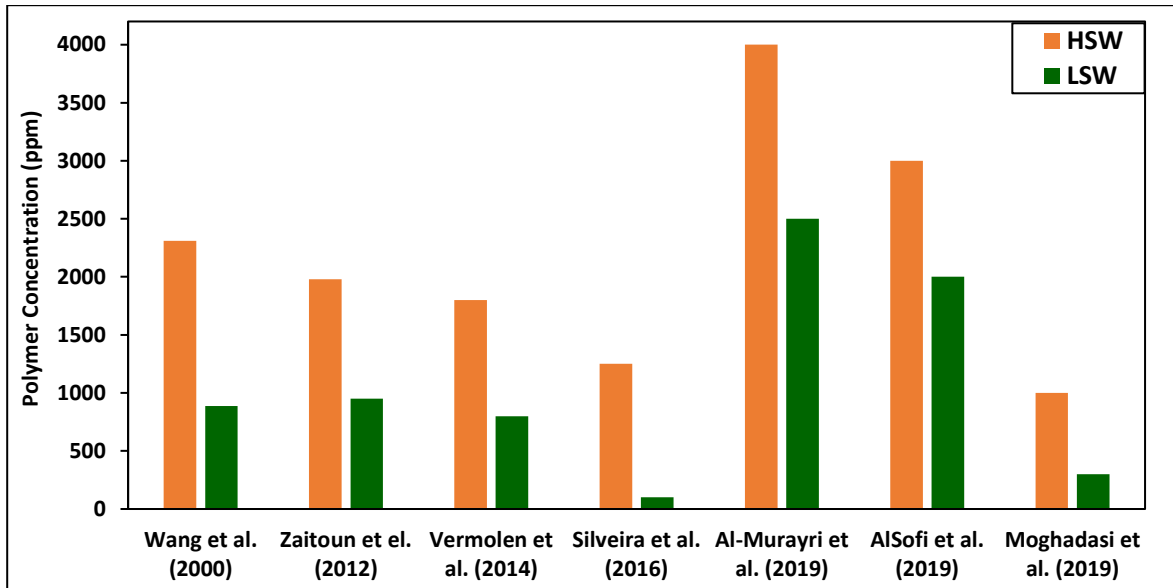


Figure 12. Studies showing reduction in required polymer concentration by LSW.

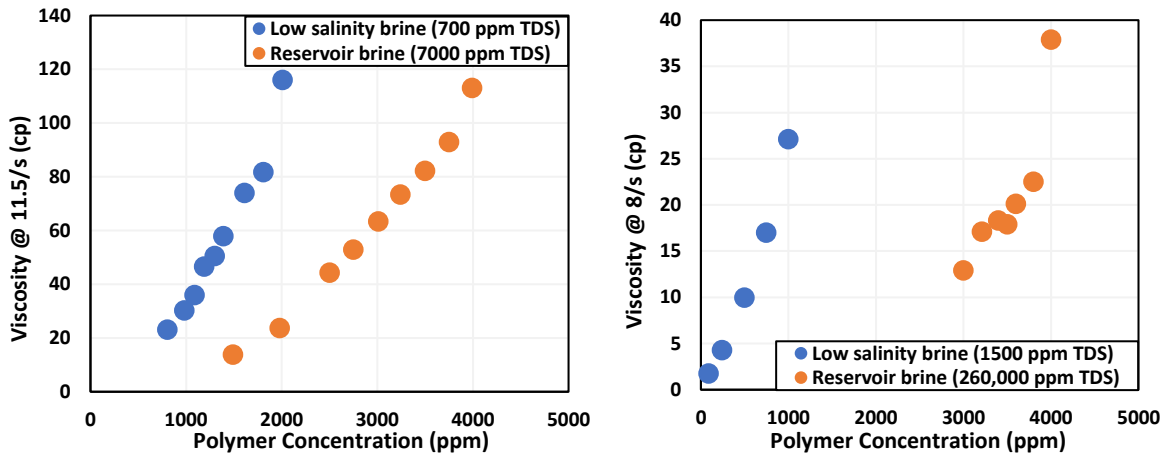


Figure 13. Reduction in HPAM concentration using LSW as the makeup brine [152]. Adapted with permission from Shehadeh et al., published by IPTC, 2014. TDS: Total dissolved solids.

Considering a high salinity and high temperature scenario of Arabian carbonate reservoir with slightly heavy oil (25 °API), Al Sofi et al. [163] showed positive effects of LSW on polymer rheological properties and thermal resistance. The smart water (7,000ppm TDS) resulted in ~30% decrease in polymer concentration to maintain target viscosity and, also, improved the thermal tolerance of the polymer (Figure 14) compared with the injection water (70,000ppm TDS).

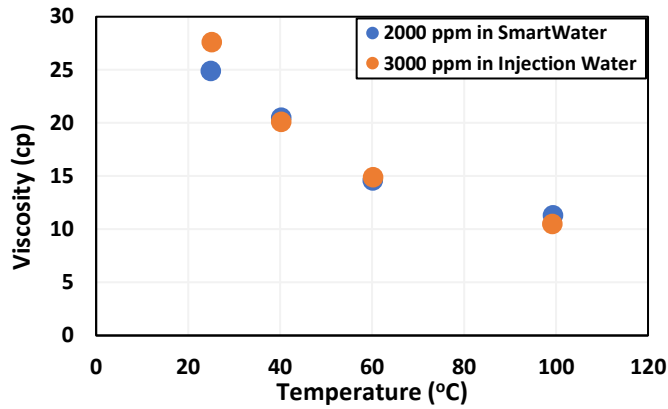


Figure 14. The smart water effect on polymer concentration required for target viscosity [176]. Reproduced with permission from Al Sofi et al., J. Pet. Sci. Eng.; published by Elsevier, 2018.

Improved polymer stability in LSW, spiked with SO_4^{2-} ions (2935 ppm TDS with 1155 ppm SO_4^{2-}) was confirmed by Al-Murayri et al. [15]. The target viscosity of 3 centipoise (cp) was achieved at a relatively lower polymer concentration (2,500 ppm) using LSW compared to high salinity brines (polymer concentration 4,000 ppm). This resulted in ~37% reduction in polymer consumption at reservoir conditions. Similarly, the LS polymer solution also retained 94% of its original viscosity after 188 days of aging at reservoir temperature, showing better thermal stability of the polymer in low salinity makeup water (Figure 15). The results of his work showed that a carefully designed, low salinity polymer (LSP) solution can provide both improved polymer stability and required viscosity for efficient oil displacement at high temperatures, and desired molecular weight for better polymer injectivity in a low permeability carbonate formation. Hence, the PF application envelope can be extended to severe reservoir conditions using LSW, which otherwise may not be technically or economically viable using high salinity formation water.

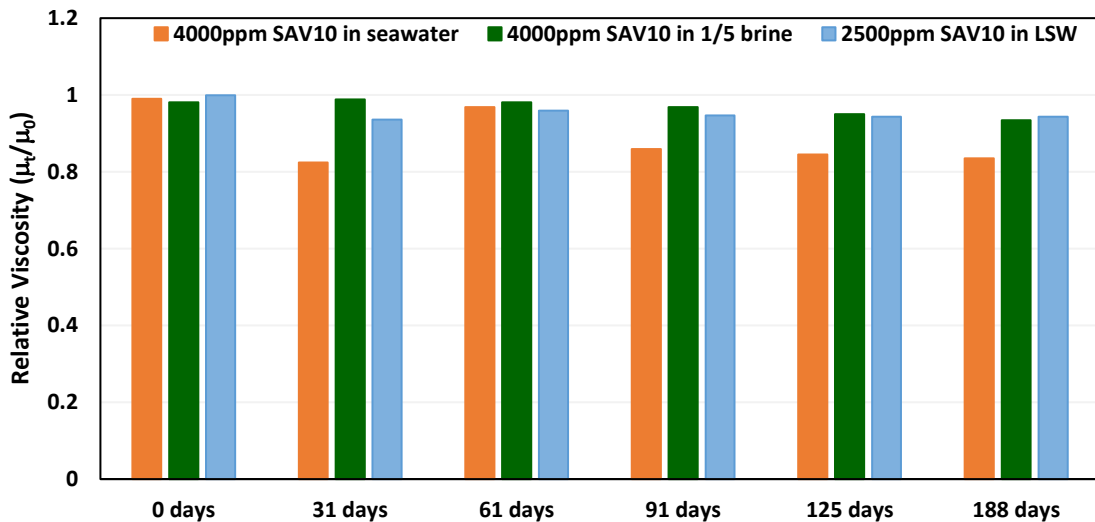


Figure 15. Better thermal stability of SAV10 polymer in LSW at 113 °C. LSW, 1/5 brine, and seawater have 2935, 47,869 and 49,878 ppm of TDS, respectively [15].

EW Effect on Polymer Retention

Alsofi et al. [176] also investigated the effects EW has on polymer adsorption and frontal acceleration under reservoir conditions by performing two injectivity experiments on carbonate cores at a constant frontal velocity of 1 ft/day using polymer solutions prepared in injection water (70,000 ppm salinity), smart water (7,000 ppm salinity), and a tracer. The results were in line with other relevant literature [5, 15, 152] in that EW provided 10-28% reduction in polymer adsorption due to increased polymer coil expansion, which resulted in less polymer molecules required to occupy the surface adsorption sites (Figure 16). Similarly, the larger polymer expansion in presence of LSW resulted in slightly higher inaccessible pore volume (IPV). Hence, there was no significant negative impact of smart water on the polymer front and oil bank acceleration.

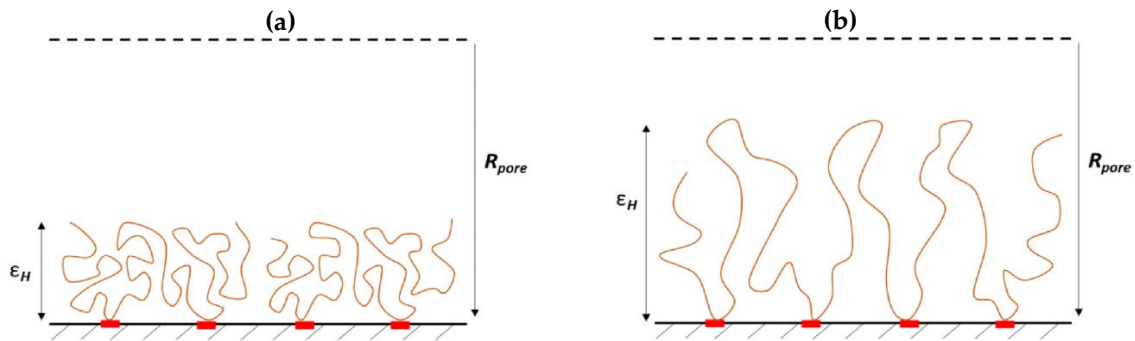


Figure 16. Polymer retention in the presence of (a) injection water and (b) smart water [176]. Reproduced with permission from Al Sofi et al., J. Pet. Sci. Eng.; published by Elsevier, 2018.

A substantial decrease in polymer retention has also been shown in several studies [152, 174, 176-179] in the presence of LSW (Figure 17).

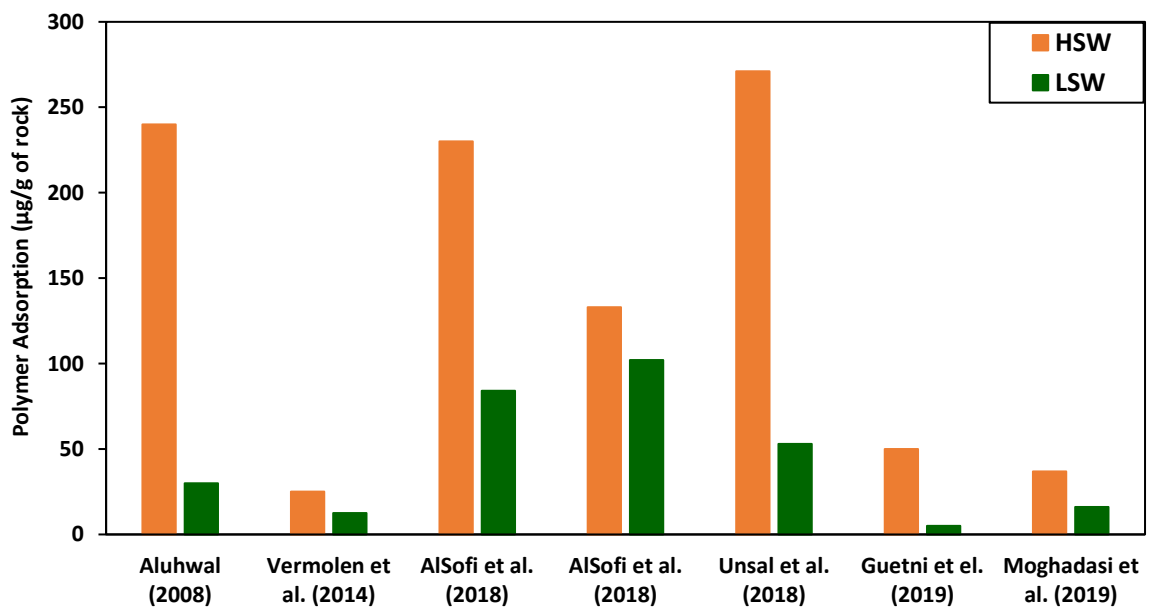


Figure 17. Studies showing reduction in required polymer adsorption by LSW.

Impact of Polymer on EW Performance

While EW improves polymer stability, the polymer can also have positive or negative effects on EW performance, which can be qualitatively assessed by electrokinetic surface potential (zeta potential) and contact angle measurements. Zeta potential is a measure of the overall surface charge in a system and is an indicator for wettability alteration of the system. A higher negative zeta potential in the case of carbonates shows a higher net repulsion force between carboxylic oil material and carbonate surface, resulting in oil detachment and wettability shift towards water wet. In cases where it is not possible to measure the zeta potential, electrophoretic mobility can be used as an indication of wettability alteration, as it is directly proportional to the zeta potential.

Electrophoretic mobility and contact angle experiments were performed by Al Sofi et al. [176] to show the positive impact polymer has on LSW performance. HPAM polymer solution, prepared by using smart water (10 times dilution of injection water), resulted in the highest decrease in electrophoretic mobility and, hence, zeta potential and the greatest wettability shift towards the water wet state (contact angle of 88.9° for smart water-polymer compared to 102.4° for smart water only) for an aged carbonate reservoir material (Figure 18).

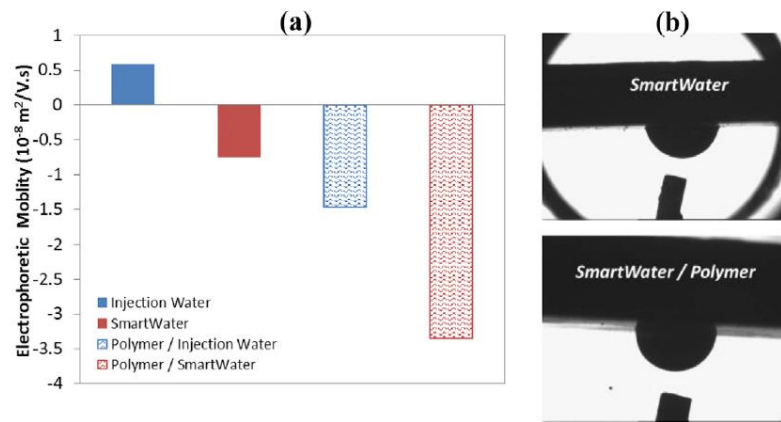


Figure 18. (a) A higher reduction in zeta potential and (b) increased wettability shift to water-wetness in the presence of HPAM polymer in smart water [176]. Reproduced with permission from Al Sofi et al., J. Pet. Sci. Eng.; published by Elsevier, 2018.

The reasons for reduced electrophoretic mobility and contact angle in the presence of polymer can be the negative charges on polymer backbone or adsorption of anionic polymer molecules onto the positive carbonate rock particles suspended in the solution. The PDIs attached to the HPAM backbone in solution and adsorbed polymer on the suspended rock particles might also cause more repulsive forces and a higher negative mobility. These experiments confirmed that polymer has no adverse effects on the LSW capability of wettability alteration; in fact it can slightly enhance the LSW effects.

1.6.3 Potential Risks associated with EWPF

Potential risks associated with EWPF, as investigated by Vermolen et al. [152], are as follows:

- Viscosity of a LSP solution is more sensitive to brine salinity compared to the solution with high salinity water (HSW). A slight increase in brine salinity can reduce polymer viscosity significantly, making it necessary to consider this factor while designing a LSPF project.
- The contamination of LSP slug with already present high salinity formation water also poses a risk for polymer viscosity loss and increased adsorption.
- Another risk in this process is delayed incremental oil recovery due to the higher polymer slug needed to reach required adsorption as a result of lower polymer concentration.
- Reduced injectivity of polymer and chase fluid in the presence of EW can also be a potential limitation involved in this hybrid method [176].

However, these risks can be partially or completely offset by lower maximum adsorption and increased polymer hydrodynamic acceleration in LSW. Vermolen et al. [152] carried out a de-risking study to minimize risks of using LSW for PF and showed that, due to polymer adsorption, a low salinity slug is formed in between HSW and LSP, which prevents direct contact of the polymer with HSW, and thus, polymer slug efficiently displaces the HSW slug without deterioration. Despite the risk of delayed oil production, a two to four times reduction in polymer concentration and the resulting cost savings can be enough to justify the economic feasibility of LSPF, particularly in high salinity formations, which otherwise may not satisfy the criteria for conventional PF.

Several variable rate corefloods were conducted by Al Sofi et al. [176] to assess the smart water effect on polymer injectivity. Resistance factors and residual resistance factors for smart water cases were slightly higher than those for injection water cases, indicating a negative impact of smart water on polymer injectivity. Although polymer and chase fluid injectivity were slightly reduced due to increased polymer chain expansion in smart water, reduced polymer consumption and retention still showed that the hybrid method has potential for successful field-scale implementation in high salinity, high temperature carbonate formations, as it can result in significant cost savings.

1.6.4 Lab-Scale Studies

In order to establish the EOR potential of hybrid EWPF in carbonates, a number of lab-based studies were carried out over the past ten years [5, 157, 180-182]. Vermolen et al. [152] presented a detailed experimental workflow for LSPF design for a field on lab scale. The experiment with an aged reservoir core confirmed that, using LSW in PF can reduce the project cost by lowering polymer concentration and providing additional oil recovery by wettability modification and improved viscoelastic behavior of polymer. Figure 19 shows the recovery and pressure drop profile for sequential injection of three polymer solutions of different salinities and concentrations. LSPF resulted in ~52% additional oil compared to HSW.

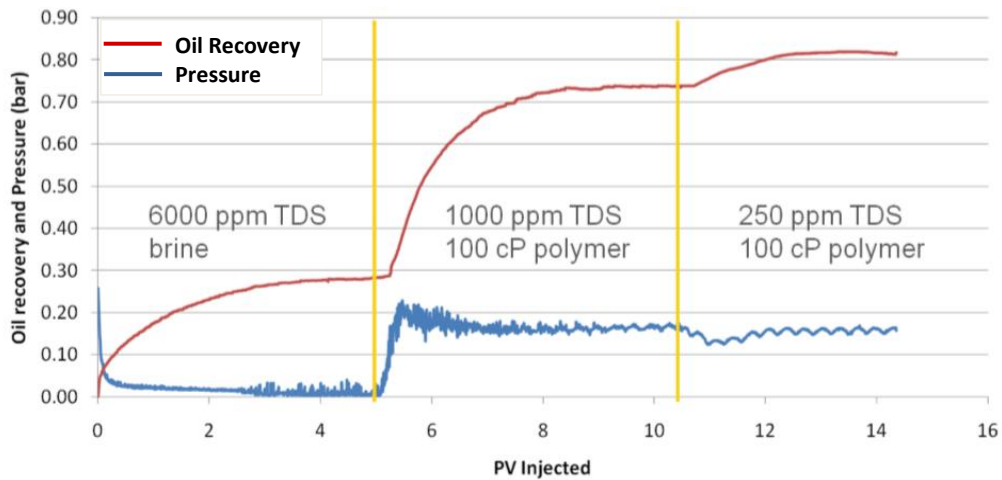


Figure 19. Oil recovery and pressure trend for LSPF using reservoir core [152]. Reproduced with permission from Shehadeh et al., published by IPTC, 2014.

Oil-displacement experiments conducted by Al Sofi et al. [163] at reservoir conditions (99°C) for an Arabian carbonate reservoir aged cores showed ~6 to 10% higher oil recovery for the hybrid LSW and sulfonated polyacrylamide polymer process compared to the recovery obtained from the stand-alone processes (Figure 20). The higher negative zeta-potentials for LSP solutions indicated more repulsive force in the system, which helped to detach the adsorbed oil and increased the recovery factor. Based on their results, oil recovery can be directly related to zeta potential in the sense that higher the negative zeta potential value, higher will be the oil recovery from that system. In addition, the higher recoveries in coreflood-1 were because the pore system in core sample had good connectivity. Laboratory experiments were conducted on a reservoir composite core to assess the feasibility of using SNF polymer SAV10 combined with LSW (2935 ppm TDS) for a high salinity and high temperature carbonate oil reservoir in Kuwait (113 °C and 239,000 ppm) with a relatively low permeability of <10 md [15].

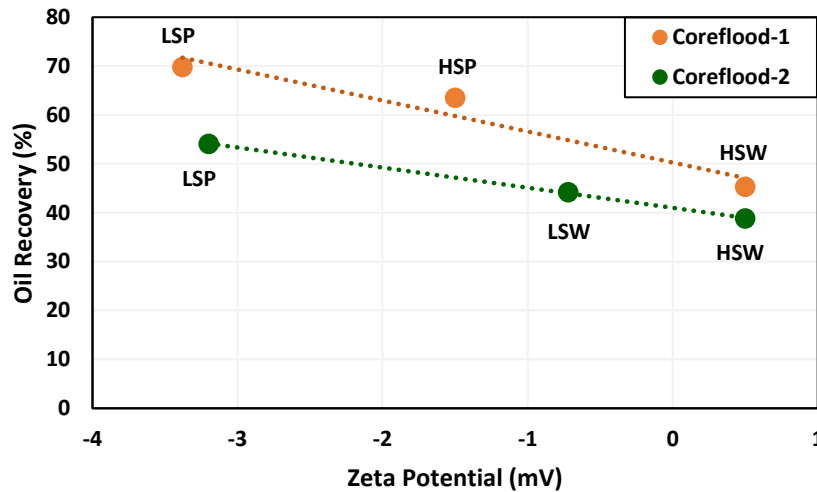


Figure 20. Oil recovery as a function of zeta-potential, showing higher recovery by the hybrid method compared to standalone processes; coreflood-1 shows PF and LSPF comparison while coreflood-2 displays LSW and LSPF comparison [163].

Secondary LSWF reduced S_{or} to 23%, followed by a further 10% reduction by LSPF, whereas the pressure drop data suggested no significant plugging by polymer (Figure 21). The results showed that LSPF can be applied to harsh reservoir conditions and low permeability reservoirs if the process is designed carefully. In addition, critical parameters such as stability and rheology of polymer in presence of LSW is also important and must be considered in selection of a suitable polymer for a specific CBR system [183].

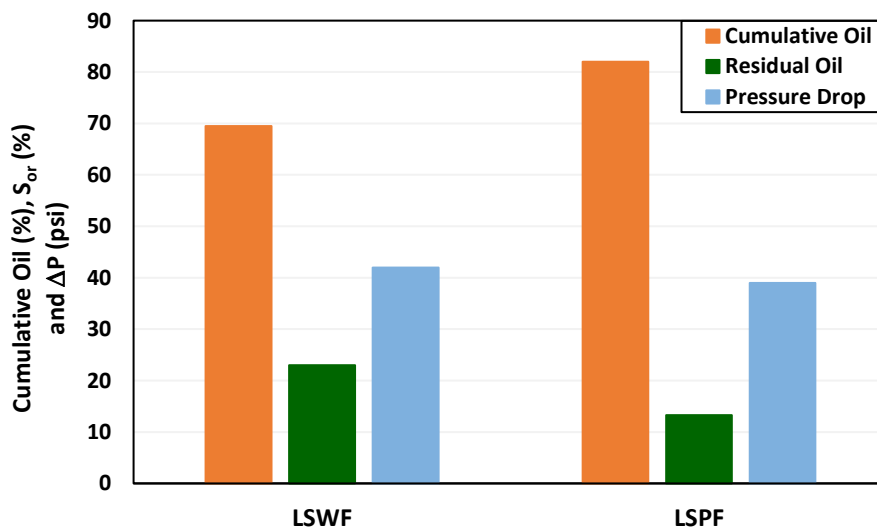


Figure 21. Comparison of oil recovery, S_{or} and pressure drop by LSWF followed by LSPF for a Kuwait carbonate oil reservoir composite core [15].

1.6.5 Numerical Modeling Studies

A systematic analytical and numerical modeling study was conducted to investigate the synergy between LSW and PF [156]. The comparison of conventional WF, HSW/PF and LSW/PF

showed that combined LSPF gave the best results in terms of highest incremental oil recovery and lowest water cut. This can be attributed to the improved fractional flow, stable frontal advance, and reduced viscous fingering by LSPF. Overall, the combined EOR process resulted in an incremental oil recovery of 15–42% and a 11–48% reduction in water cut after one pore volume (PV) of injection, depending on the extent of reservoir layering and heterogeneity. Figure 22 (a) presents the correlation between shock front mobility ratio and cumulative oil production. As the mobility ratio decreased from 1.1 (for high salinity waterflooding) to 0.9 (for LSPF), total oil recovery increased from 48% to 70%, proving the better polymer performance in low salinity environment. The effect of salinity on oil recovery by PF was also studied and the 3D numerical modeling results for different injection water salinities clearly depicted higher ultimate recoveries for low salinity/polymer cases as highlighted in Figure 22 (b). A reduction in salinity from 30,000 to 700 ppm resulted in 23% extra oil production compared to high salinity base case, confirming the synergy between the two processes.

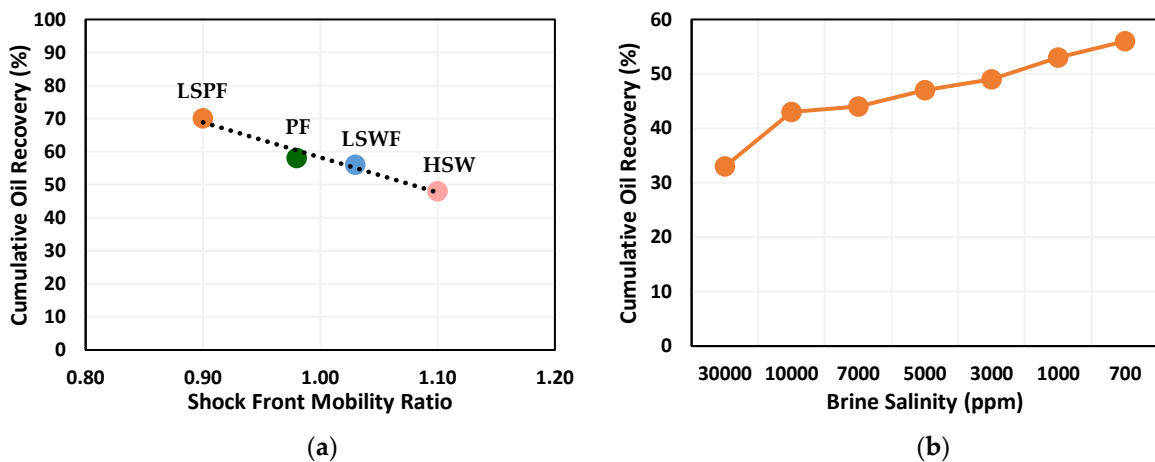


Figure 22. Numerical modeling results showing oil recovery as a function of (a) mobility ratio for different flooding scenarios and (b) brine salinity used for PF [156].

Borazjani et al [155] presented an analytical solution to model LSPF by incorporating polymer non-Newtonian properties, adsorption, and ionic strength of water. Henry’s sorption equation and modified Darcy’s law were used to formulate the model. To study the effect of LSP slug size, a splitting technique presented by Pires, Bedrikovetsky [184] was used to solve problems which were non-self-similar. The results showed ~14% higher ultimate oil recovery by LSPF, delayed water breakthrough, and the lowest water cut (Figure 23). Polymer adsorption was also higher for high salinity polymer (HSP), as polymer breakthrough occurred later (after 8.1 PV) compared to LSPF (after 7.8 PV). The results showed that the hybrid LSPF technique has better performance over conventional PF, both in terms of reduced polymer consumption and higher oil cuts.

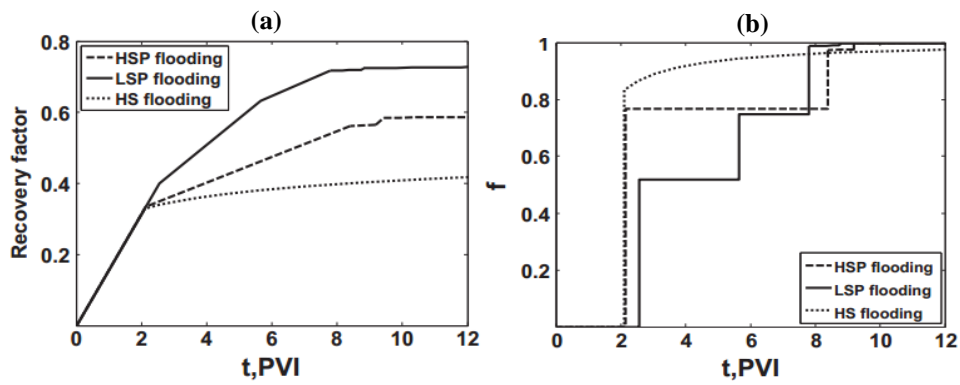


Figure 23. Analytical solution results showing the effect of LSPF on (a) oil recovery and (b) water cut [155]. Reproduced with permission from Borazjani et al., J. Pet. Sci. Eng.; published by Elsevier, 2016.

A comprehensive numerical simulation study using empirical modeling of LSWF was carried out by Mohammadi and Jerauld [153] to simulate the hybrid LSPF process in VIP and CMG-STARS reservoir simulators. Polymer rheology and adsorption was included to model the salinity and hardness effects on polymer viscosity degradation, reduction in permeability, and IPV by polymer retention in porous media. The study investigated the influence of injection sequence, polymer and LSW slug sizes, oil viscosity and heterogeneity of the reservoir on oil recovery (Figure 24). The hybrid method was more beneficial for high viscosity oil. Based on simulation results, the optimum LSP slug size was 0.5-0.7 PV.

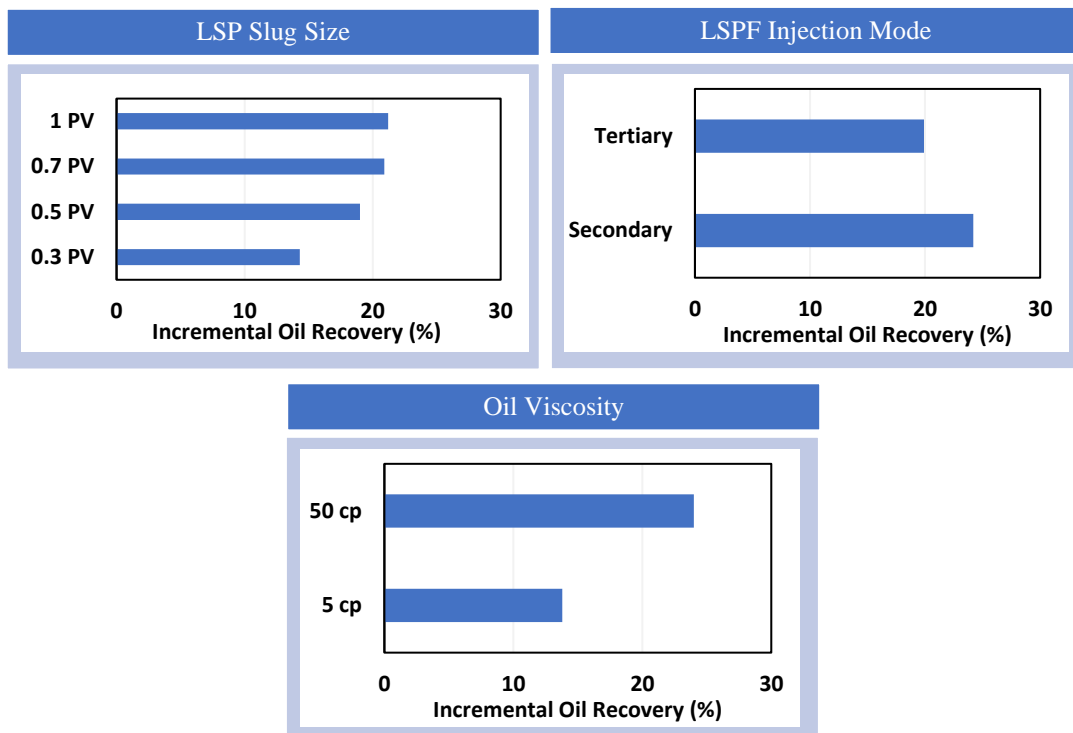


Figure 24. Effect of different design parameters on LSPF performance in terms of incremental oil recovery [153] Additional 20% oil recovery was obtained by LSPF over the conventional WF, mainly due to wettability modification by LSW, better polymer stability, and efficient front displacement by

polymer, improving the overall fractional flow. 1D simulation results showed improved fractional flow and the better performance of the hybrid process compared to LSWF and PF alone. Higher oil recovery and better timing was obtained in secondary mode than the tertiary mode (oil breakthrough at 0.3 PV compared to 0.5 PV for tertiary mode), whereas hybrid process synergy was more pronounced in tertiary mode compared to secondary mode. The study also showed that, due to better performance of polymer in LSW, the chemical cost can be reduced by five times.

Alzayer and Sohrabi [154] conducted a numerical simulation study using a correlation of residual oil saturation after waterflood (S_{orw}) and salinity of water, developed by Webb et al. [185] utilizing the relevant published data in the literature. The objective of the study was to improve oil recovery from a heavy oil reservoir (80 cp and 20°API oil) using LSWF followed by PF. Comparison of different injection schemes showed that combined LSWF and PF provided 4% of OOIP additional estimated ultimate recovery (EUR) with significantly lower injection volumes required compared to both methods simulated separately (Figure 25). The synergetic effects of hybrid EWPF are also confirmed by modeling studies of Hirasaki and Pope [45], Han and Lee [186], and Khamees and Flori [187].

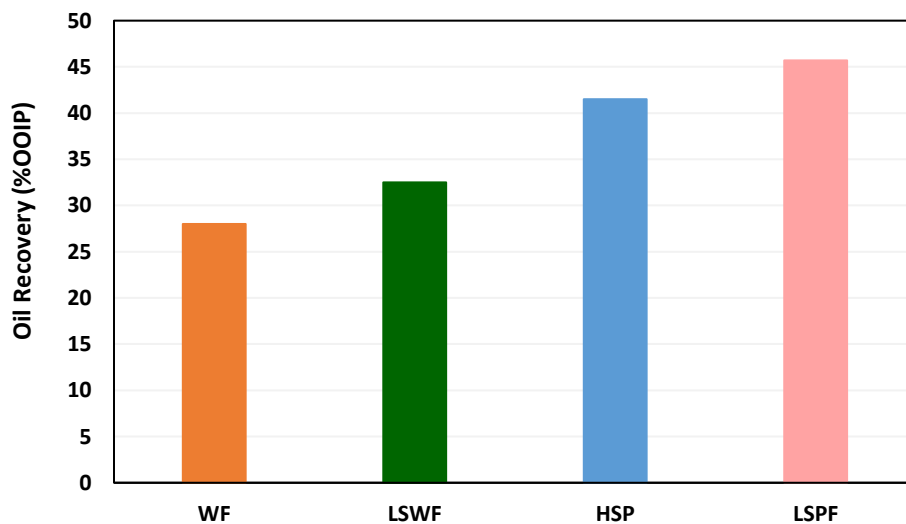


Figure 25. Comparison of LSPF with high salinity WF (50,000+ ppm), LSWF (2000 ppm), and HSP flooding after 0.6 PV injection [154].

Based on this research, the main parameters to be considered for applicability of each EOR technique discussed, are summarized in Table 3.

Table 3. Key conditions for polymer, engineered water and engineered water/polymer flooding.

<i>Parameter</i>	<i>Conditions</i>
<i>Polymer Flooding</i>	
Porous Medium	Mostly Sandstone. Limited application in carbonates mainly due to the high salinity formation water associated with carbonates [25-27].
Formation Water	Salinity should be <100,000 ppm [43]. Chlorides should be <20,000 ppm, Ca ²⁺ and Mg ²⁺ divalent ions must be <500 ppm [62]. Low salinity (LS) is preferred to avoid polymer degradation [59].
Permeability	20 to 2300md. Polymer adsorption can cause permeability reduction [14, 60, 188].
Temperature	Should be < 93 °C. HPAM undergoes thermal degradation at high temperature [32, 61, 64].
pH	High pH is favorable for HPAM due to increased electrostatic repulsion [189, 190].
<i>Engineered Water Flooding</i>	
Oil	Must have polar organic components in order to observe EW EOR effects [123, 141, 191].
Injection fluid	Salinity must be between 2000–5000 ppm [140, 192] but can work up to 33000 ppm [104, 118]. Injection water must have PDIs, Mg ²⁺ and/or Ca ²⁺ and SO ₄ ²⁻ [106, 113, 193].
Temperature	Should be >70°C [126, 141, 142, 193].
Initial Wettability	Oil-wet to mixed-wet [191, 194, 195].
<i>Engineered Water Polymer Flooding</i>	
Formation Water	This method can be applied to reservoirs containing high salinity and high hardness formation water in the range 167,000-239,000 ppm [15, 157].
Injection Water	Salinity should be low as compared to formation water. 300-9750 ppm has been reported in literature [157, 181].
PDIs	Injection water spiked with 4 times SO ₄ ²⁻ ions gives best results. Increase in Ca ²⁺ concentration can cause polymer degradation [5].
Temperature	Can be as high as 120 °C [157].
Permeability	EWPF can provide incremental recovery from low permeability formations (< 10md) as well [15, 180].

1.7 Hybrid Engineered Water-Surfactant-Polymer Flooding (EWSPPF)

The favorable synergy between LSW and surfactant is also proved by various researchers [196, 197]. The IFT reduction by surfactant is adversely affected by high concentration of divalent ions (Ca²⁺ and Mg²⁺) in HSW [198, 199]. Divalent cations also cause surfactant precipitation in the form of sulfonate salts [199]. A low salinity surfactant flood can reduce re-trapping of the oil released by LSW and provide higher recovery compared to standalone EWF or surfactant flooding. Furthermore, LSW can improve surfactant solubility and reduce anionic surfactant adsorption on the carbonate rock surface, making this hybrid method economically viable for harsh reservoir conditions [200, 201]. Consequently, a wider range of cheap and environmentally safe surfactant systems can be considered for low salinity settings.

The displacement experiments performed by Alagic et al. [202] on sandstone cores, using a high AN crude oil (2.84 mg KOH/g of oil), showed around 20% of OOIP incremental recovery by using anionic surfactant under low salinity conditions compared to high salinity conditions. These results also indicate that higher AN oils are favorable for low salinity and surfactant flooding, as lower IFT can be achieved with high amount of acidic components present in crude oil [85]. Zivar et al. [203] developed capillary desaturation curves for different low salinity waterflooding, surfactant flooding and low salinity surfactant flooding (LSSF) experiments available in the literature and showed that LSSF provided lower S_{or} for the similar capillary numbers, compared to individual methods.

One drawback for hybrid LSSF is the unfavorable mobility ratio which can lead to unstable front movement, especially in heterogeneous carbonate formations containing viscous oils. In such cases, combining EWPF with EWSF can improve both macroscopic and microscopic sweep efficiencies and recover the maximum residual oil. The laboratory coreflood experiments were performed by Al-Ajmi [204] on Berea core samples to investigate the effectiveness of hybrid LSW and LS-surfactant-polymer flooding (LSSPF). Additional oil was produced by LSSPF in tertiary mode with the recovery directly proportional to the surfactant slug size. Maximum incremental recovery obtained was 16% of OOIP. Injection of high concentration LSP solution post-LSSPF recovered extra oil, showing the efficiency of the hybrid method. Theoretically, this hybrid method can be equally or even more beneficial for oil-wet carbonate formations, but there is a gap in the literature for its practical implementation. There is hardly any detailed study on this hybrid EOR method for carbonates, as it is a relatively new technique.

1.8 Hybrid Engineered Water-Alkali-Surfactant-Polymer (EWASP) Flooding

Combined alkali-surfactant-polymer (ASP) flooding has been proven the most effective EOR method among various available chemical EOR techniques, with recovery factors of up to 98% OOIP during laboratory experiments [205]. A comparison of different alkali, surfactant and polymer combinations in high salinity, high temperature Berea sandstone samples was performed by Bataweel et al. [206] and the results showed a higher recovery factor for ASP formulation with anionic surfactant compared to other combinations. The residual oil recovered by ASP flooding was ~ 9% higher than the oil recovered by SP flooding. The incremental oil in ASP is recovered by a reduction in IFT due to combined action of alkali and surfactant and a decrease in displacing fluid mobility by polymer. The cost benefit comes from the lower

adsorption of both surfactant and polymer in the presence of alkali, requiring less amount of the chemicals. Despite the encouraging results from various lab-based studies, the pilot and field implementation of ASP flooding is mainly limited to sandstone reservoirs and there is hardly any large-scale application in carbonates because of their geological complexity and harsh reservoir conditions [207]. This can also be attributed to higher project costs because of increased adsorption of chemicals e.g., polymers and anionic surfactants on carbonate surface. Combining conventional ASP flooding with chemically tuned EW can provide significant improvement in terms of chemicals stability in a low salinity environment. This hybrid method can expand the application envelope of ASP flooding to more challenging carbonate reservoirs. Dang et al. [207] developed a robust mechanistic model to fully capture physical and geochemical aspects of ASP process, including phase behavior, polymer rheology, alkali consumption, mineral dissolution reactions, and wettability alteration. The developed model was successfully validated by comparing the model results with experimental data obtained from various lab-scale studies. The validated mechanistic model was then used to simulate ASP flooding on field-scale and evaluate the efficiency of hybrid EWASP flooding. Secondary LSW flooding followed by tertiary ASP flooding resulted in 10% higher oil recovery compared to the case in which HSW was injected in the secondary mode prior to ASP flooding (Figure 26). Hence, this hybrid method can show superior performance on field-scale but needs an extensive analysis to optimize the process design and maximize net present value (NPV) of the project.

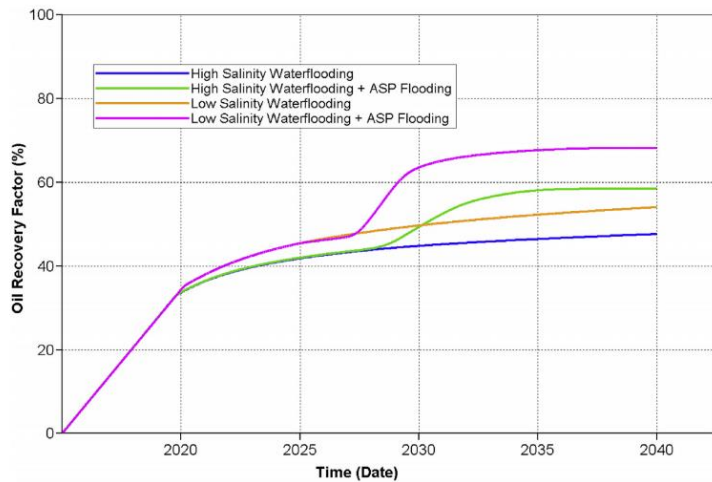


Figure 26. Comparison of EWASP flooding with other flooding scenarios [207].

1.9 Problem Statement

Hybrid engineered water and chemical EOR methods such as EWPF, EWSPF and EWASP can provide both economic and environmental benefits by reducing chemical consumption and cost

while improving sweep efficiency at the same time, but these techniques have not been implemented on field-scale yet due to lack of an appropriate selection criteria and an optimum injection scheme for field applications. Therefore, it requires an extensive experimental and research work to come up with a successful design for a particular CBR system to get maximum benefit from the synergy of the hybrid chemical EOR methods.

Most of the research on hybrid EWPF and EWASP is conducted for sandstones because of the heterogeneity problems and complexity of rock-fluid interactions in carbonates. There is a lack of a comprehensive study on possible application of these methods as potential EOR techniques for carbonate formations in literature.

This research study will address the abovementioned issues by conducting a systematic experimental analysis and evaluating critical design parameters to come up with the best design among different combinations of the EW and chemicals. This study is a continuation of a major research project for selection of best hybrid EOR method for carbonates. During the initial phase of research, an optimum EW composition was designed, and the most suitable polymer and surfactant were screened for the hybrid EWPF and EWSF [183, 197]. In this phase, the coreflood experiments will be performed to assess the incremental recoveries by various combinations of EW and chemicals (alkali, surfactant, and polymer). The experiments will be conducted using carbonate outcrops to address the unexplored and challenging areas related to this topic. Typical Kazakhstan's reservoir conditions (Caspian seawater, Tengiz field formation water and crude oil from West Kazakhstan region) will be used as a reference as majority of the oilfields in Kazakhstan are producing from carbonate formations.

1.10 Research Objectives

The main idea of this study is to develop a hybrid EOR method utilizing an optimum engineered water and EOR chemicals (alkali, surfactant, and polymer) formulation to overcome the limitations of CEOR and EWF by synergy between the two processes. Primary objective of this research is to compare the performance of hybrid EWASP flooding with that of EWPF and EWSPF. Optimization of polymer rheological and viscoelastic properties is a secondary objective to improve PF performance. Another important parameter studied herein, is the effect of initial wettability on the performance of hybrid EWPF method. Hence, a key idea behind this research is to choose and recommend novel and effective design of hybrid EOR approach based on laboratory investigation and consequently expand the application envelope of PF and ASP flooding to harsh reservoir conditions, such as those in Kazakhstan fields.

1.10.1 Main objectives

Based on above discussion, the objectives of this research are given below:

- Analyze the effect of pH on polymer viscosity and viscoelasticity and design an optimum pH for the hybrid EOR process to get the maximum benefit in terms of both viscous and elastic properties of polymers.
- Evaluate the effect of initial rock wettability on the performance of hybrid EWPF.
- Study the application of hybrid EWPF and EWASP flooding to increase the oil recovery from carbonate reservoirs by performing oil displacement experiments.
- Conduct detailed experimentation and design optimum operational parameters and injection scheme to increase oil recovery by the hybrid methods.
- Analyze and compare the performance of different hybrid methods in terms of incremental oil recovery and select the best combination.

1.10.2 Thesis structure

The thesis is organized in a manner to cover all the aspects of research topic and fulfill the set objectives systematically. Following are the main sections/chapters:

1. Introduction

This chapter comprises of a literature review of various EOR methods with focus on EWF and EWPF. The existing gaps in the literature are identified to define the problems and finally, the objectives of the thesis are defined.

2. Methodology

The details of materials and equipment used, and procedures followed during research are provided in this chapter. It also includes the design and sequence of coreflood experiments and contact angle measurements.

3. Results and Discussion

This chapter consists of a detailed analysis of the data obtained from various experiments e.g., rheological experiments, corefloods and contact angle measurements. The results are discussed, and the performance of each hybrid method is evaluated.

4. Conclusions and Recommendations

The thesis is concluded with recommendations based on experimental results for the selection of best hybrid EOR method. The areas requiring further research are also highlighted.

5. References

The references are provided at the end.

2. Methodology

To achieve the thesis objectives, a stepwise methodology is followed starting from rock samples and fluids preparation, polymer rheological characterization, rock, and fluid properties estimation and finally coreflood experiments. The data obtained is then analyzed and results are presented. Hybrid engineered water/chemical EOR methods need a thorough investigation in terms of incremental recovery, chemicals stability and better synergy between EW and a particular chemical (polymer, alkali and/or surfactant). This study is continuation of a major research project for selection of best hybrid EW/CEOR method. During the initial phase of project, our team screened out best polymer based on rheological experiments [183]. Optimum surfactant and EW composition was also selected based on phase behavior, aqueous stability, and contact angle studies [197].

Now, the second phase includes coreflooding experiments to evaluate the recovery efficiency of various combinations of EW and CEOR methods. For this purpose, the entire study is carried out in five stages. In the first stage, the required materials such as carbonate cores, brines and chemical solutions were prepared, and their respective properties were estimated. In the second stage, polymer rheological and viscoelastic properties as a function of pH were estimated and an optimum pH was identified. In the third stage, contact angles were measured to study the effect of aging time, temperature, and polymer on EW wettability alteration capability. The fourth stage included the aging of core samples to achieve reservoir conditions. The coreflood experiments with different combinations of EW and chemicals were then performed in the fifth stage. Finally, the results were interpreted to select the optimum conditions and best combination of hybrid method. The materials used and procedures employed during this study are elaborated in the following section.

2.1 Materials

The materials used for the research, including crude oil, brines, rock samples and chemicals are discussed in this section.

2.1.1 Crude Oil

The objective of this study is to select the best hybrid EOR method for oilfields in Kazakhstan to improve the ultimate recovery factor. For this purpose, crude oil from one of the fields in west Kazakhstan was used for oil displacement experiments and contact angle measurements.

The composition of crude oil is given in Table 4. This crude oil is very viscous and contains high percentage of heavier fractions.

Table 4. Composition of crude oil.

Component	C5	C6	C7	C8	C9	C10	C11	C12	C13	C14	C15+	other
Wt%	0.8	0.43	1.63	7.36	8.7	17.87	5.09	5.44	8.3	6.15	30.55	7.66

2.1.2 Rock Samples

Since the objective of the thesis is to study the effect of hybrid methods on carbonate reservoirs, hence limestone outcrop cores were used as porous media. The analysis of crushed rock sample using Scanning electron microscope (SEM) revealed that it mainly consists of calcite (CaCO_3) with trace amounts of Mg and Si (Figure 27). The results of X-ray Diffraction (XRD) also confirmed that the rock contains almost 99% calcite.

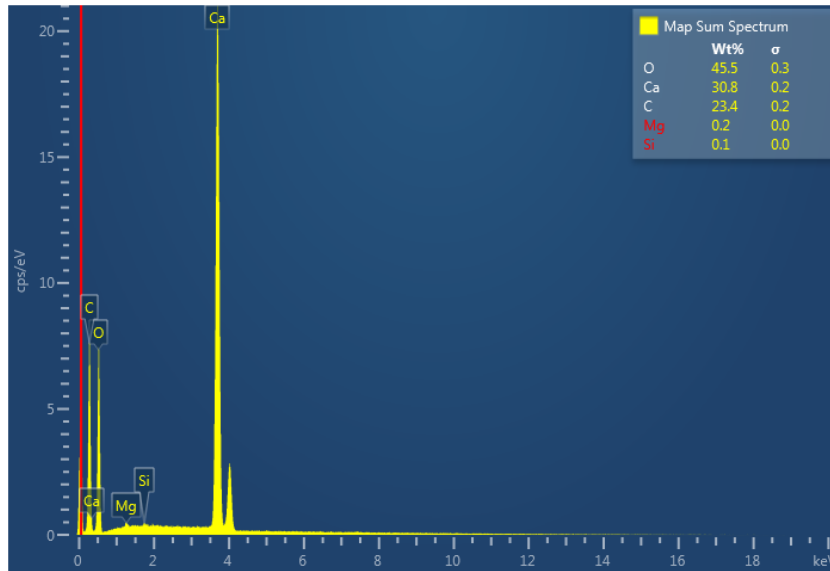


Figure 27. Elemental analysis of crushed rock sample using SEM.

2.1.3 Brines

Three different brines were used in this study as formation water (FW), high salinity water (HSW) and engineered water (EW). The salinities and ionic compositions of the brines were different, and the salts given in Table 5 were used to prepare these aqueous solutions. To mimic Kazakhstani reservoirs, the FW composition was kept the same as Tengiz field formation water with a salinity of around 180,000 ppm. The South Caspian seawater (CSW) was used as high salinity water, having a salinity of 13000 ppm. Finally, 10 times diluted CSW spiked with 6 times SO_4^{2-} , 1 time Mg and 3 times Ca^{2+} (10CSW.6S.Mg.3Ca) was used as EW.

Table 5. Salts used in brines preparation.

<i>Required chemicals</i>	<i>Chemical formula</i>	<i>Purity</i>	<i>Producers</i>
Sodium bicarbonate	NaHCO ₃	≥99.0%	SIGMA-ALDRICH
Sodium sulfate	Na ₂ SO ₄	≥99.0%	SIGMA-ALDRICH
Sodium chloride	NaCl	≥99.0%	SIGMA-ALDRICH
Calcium chloride anhydrous	CaCl ₂	≥99.0%	SIGMA-ALDRICH
Magnesium chloride hexahydrate	MgCl ₂ .6H ₂ O	≥99.0%	SIGMA-ALDRICH
Potassium chloride	KCl	≥99.0%	SIGMA-ALDRICH

This EW recipe was selected as it provided beneficial results in terms of wettability alteration in a previous study by our team [197]. 10CSW.6S.Mg.3Ca reduced the contact angle by 21.3°, making the rock more water-wet [197]. Various studies have also proved the effectiveness of PDIs in addition to reduced salinity for wettability alteration [95, 208]. The low salinity water results in a reduced ionic density near the carbonate surface, making it easier for SO₄²⁻ ions to detach carboxylic oil groups. Mg²⁺ and Ca²⁺ ions then replace these carboxylic groups as they have higher affinity for SO₄²⁻. Another reason for selecting this EW design is its compatibility with other EOR chemicals to be used in this study. 10CSW.6S.Mg.3Ca showed improved performance of surfactant in terms of phase behavior by providing highest microemulsion ratio, and better viscosifying ability of polymer under high temperature high salinity conditions [183, 197]. Owing to these facts, the abovementioned EW was used for this research. The ionic composition for FW, HSW and EW is given in Table 6, whereas the recipe of each brine is given in Table 7.

2.1.4 Chemicals

Three chemicals are used in this study to investigate the potential synergy between various combinations of chemical EOR methods and engineered water. These include polymer, surfactant, and alkali. A brief description of each chemical is given hereafter.

Polymer

Flopaam 5115 (F5115) polymer was used in this study which is a sulfonated hydrolyzed polyacrylamide polymer (HPAM) provided by SNF Floerger. The chemical structure of F5115 is depicted in Figure 28. This polymer is chosen as it is suitable for high temperatures of up to 120 °C and has appropriate resistance to high salinity and divalent ions presence.

Table 6. Ionic composition of different brines used in the study.

<i>Ions</i>	<i>FW (ppm)</i>	<i>HSW (ppm)</i>	<i>EW (ppm)</i>
$Na^+ + K^+$	81600	3240	325
Ca^{2+}	9540	350	105
Mg^{2+}	1470	740	74
Cl^-	90370	5440	544
SO_4^{2-}	-	3010	1806
HCO_3^-	-	220	22
<i>Total</i>	182980	13000	2876

Table 7. Recipe for different brines.

<i>Salt</i>	<i>FW (g/L)</i>	<i>HSW (g/L)</i>	<i>EW (g/L)</i>
<i>NaCl</i>	207.42	4.36	-
<i>Na₂SO₄</i>	-	4.45	2.67
<i>CaCl₂</i>	26.41	0.969	0.29
<i>MgCl₂.6H₂O</i>	12.29	6.18	0.62
<i>KCl</i>	1.32	-	-
<i>NaHCO₃</i>	-	0.3	-

A previous study also confirmed the improved performance of F5115 over other polymers from the same category [183]. Table 8 presents some physical and chemical properties of this polymer.

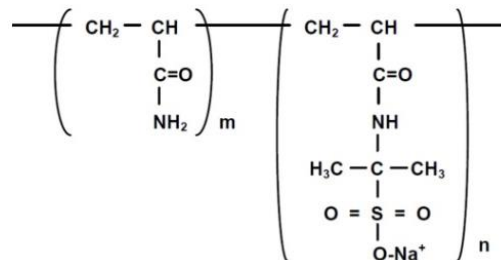


Figure 28. Chemical structure of sulphonated polyacrylamide polymer.

Table 8. Chemical and physical properties of F5115.

<i>Chemical formula</i>	Acrylamide/ATBS/Acrylic acid
<i>Degree of hydrolysis</i>	25 %
<i>Molecular weight</i>	12x10 ⁶ g/mol

Surfactant

To study the potential synergy between surfactant, polymer, and EW, an anionic surfactant of benzenesulfonic acid, Soloterra-113H was used. This surfactant is provided by Sasol company and is thermally stable up to 80 °C. Some of the chemical and physical properties of Soloterra-

113H are given in Table 9. Although the anionic surfactants can have a higher adsorption on positively charged carbonate surface, they are capable to provide ultra-low IFT [209]. Hirasaki performed spontaneous imbibition tests on calcite surfaces using anionic surfactants and sodium carbonate as an alkali and reported appreciable oil recovery [210]. Anionic surfactants are also cheaper and easily available as compared to cationic surfactants. Another precursor for selecting Soloterra-113H was that it provided promising results in a previous hybrid surfactant/low salinity water study conducted by our research team [197].

Table 9. Chemical and physical properties of Soloterra-113H.

<i>Type of surfactant</i>	<i>Chemical Name</i>	<i>Physical state</i>	<i>Density and Viscosity @ 25°C</i>	<i>Flash point</i>	<i>Chemical stability</i>
Anionic Activity: 96.5%w/w	Benzenesulfonic acid, 4-C10-13-sec-alkyl deriv.,	Brown viscous liquid	Density– 1.06g/cm ³ , Dynamic viscosity– 2400 mPas	210 °C	Stable

Alkali

To study possible combinations of chemicals and EW, sodium carbonate (Na₂CO₃), provided by SIGMA-ALDRICH, was used as an alkali. The addition of alkali in surfactant/polymer flooding helps to achieve multiple benefits including in-situ soaps (surfactants) generation by interacting with naturally present organic acids in crude oil, crude oil emulsification, and ultra-low IFT due to synergy between in-situ and added surfactants. Alkali also improves surfactant distribution and arrangement at oil/water interface, reduces adsorption of anionic surfactant due to increased surface negative charge density, provides favorable pH and ionic strength required to lower IFT, and promotes carbonate rock wettability alteration [211-213].

In addition, an alkali causes increased repulsion between HPAM polymer chains resulting in improved rheological and viscoelastic properties of the polymer. The reason for using Na₂CO₃ as an alkali instead of NaOH is that anionic surfactants adsorption on carbonates is considerably reduced in presence of Na₂CO₃ as compared to NaOH, indicating that hydroxide ion (OH⁻) is not a PDI for calcite but carbonate ion (CO₃²⁻) is [210]. Furthermore, Na₂CO₃ also alters the carbonate surface charge from positive to negative by generating CO₃²⁻ ions, making the surface more water-wet.

2.2 Procedures

2.2.1 Brines and Chemical Solutions Preparation

Brines and chemical solutions were prepared for rheological experiments, contact angle measurements, and coreflood experiments. FW, HSW and EW solutions were prepared by mixing appropriate amounts of different salts in distilled water using a magnetic stirrer. The prepared solutions were stored in air-tight containers to avoid contact with air. Polymer solutions were prepared by weighing required amount of dry polymer to prepare a known concentration solution. API standard procedure recommended for polymer solution preparation was followed. The aqueous solution was stirred at a constant speed of 600 rpm to obtain 70% vortex and then dry polymer was added at the vortex shoulder within 30 seconds. The solution was then stirred at a low speed of 100 rpm for 6 to 8 hours and was left overnight to achieve complete hydration and dissolution of polymer in brine. These steps are necessary to avoid fisheyes formed by agglomeration of polymer molecules and to ensure proper hydration of polymer in the solution. Polymer solutions with concentrations given in Table 10 were prepared for different experimental stages.

Table 10. Amount of polymer added for different concentration solutions.

<i>Polymer Concentration (ppm)</i>	500	1500	2000	3000	4500
<i>Amount of polymer added (g/L)</i>	0.5	1.5	2	3	4.5

To perform surfactant/polymer (SP) corefloods, 1 wt% surfactant solution was prepared by gently adding the surfactant to the EW while stirring at 200 rpm on a magnetic stirrer. The solution was stirred for two hours on low speed to avoid foaming and ensure proper mixing. 1 wt% Na₂CO₃ was added to this solution for alkali/surfactant/polymer (ASP) floods. Since alkali addition results in an increase in solution salinity, hence 1.5 times diluted EW was used for alkali-surfactant solutions to keep the overall salinity same as prior to alkali addition. Fresh chemical solutions were prepared for each coreflood experiment. The detailed tests for selection of EW dilution factor for alkali/surfactant (AS) and ASP experiments were conducted by another member of our team, Samanova [214], and can be found in her thesis.

2.2.2 Crude Oil Properties

The viscosity, density and API gravity of crude oil were measured using Anton Paar kinematic viscometer SVM 3001 for temperature range of 20-80 °C and the results are given in Table 11.

The apparatus was first calibrated, and the cleaning status was checked. Crude oil was stirred for 20 minutes to remove any gas bubbles. 1 ml of sample was slowly injected using a 5 ml syringe and the results were displayed on the screen. Figure 29 shows the temperature dependency of oil viscosity and density.

Table 11. Crude oil properties as a function of temperature.

Temperature	Dynamic Viscosity	Kinematic Viscosity	Density	API Gravity
°C	mPa.s	mm ² /s	g/cm ³	°API
20	169.5	187.1	0.906	24.0
30	90.0	100.1	0.900	23.9
40	51.8	58.0	0.893	23.8
50	32.3	36.4	0.887	23.8
60	21.3	24.2	0.880	23.7
70	14.9	17.0	0.874	23.6
80	10.8	12.5	0.868	23.5

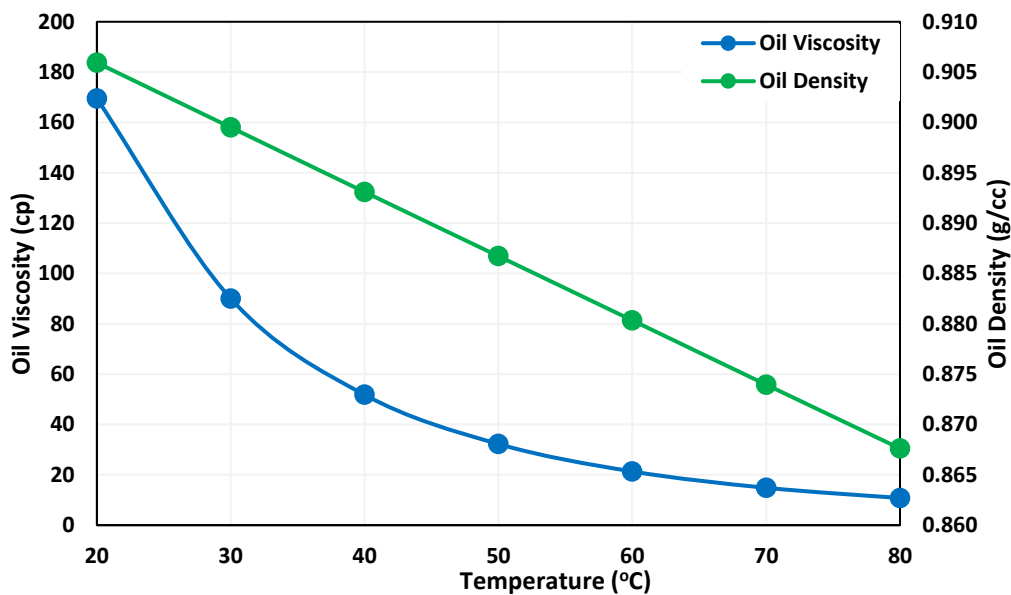


Figure 29. Temperature dependency of crude oil viscosity and density.

One of the most important crude oil parameters used in the screening for ASP and EW flooding is the acid number (AN, mg KOH/g of oil, -COOH group). This parameter represents the amount of acidic components present in crude oil. The rock tends to be more oil-wet if it contains crude oil with a higher AN. It is due to high attraction force between negatively charged carboxyl group (COO⁻) of oil and positively charged carbonate surface. Consequently, oil recovery during waterflooding is low at high AN value. The main mechanism governing EOR by chemically tuned or low salinity water is the change of carbonate rock wettability to more water-wet condition, subsequently improving the relative permeability and fractional flow

of oil. Consequently, higher recoveries can be obtained by EW in reservoirs containing acidic crude oils. Similarly, the oils with minimum AN of 0.3 mg KOH/g of oil can be considered for alkaline/surfactant flooding [150]. However, an AN value of more than 2 mg KOH/g showed higher incremental oil recoveries by alkaline flooding due to positive interaction between acidic groups of oil and alkali components [215]. It was, therefore, important to know the AN of crude oil used in this study to assess its suitability for ASP and EW flooding.

Acid number of crude oil was determined by color-indicator titration as shown in Figure 30. ASTM standard test procedure (D974) was followed for this task. The solvent for titration was prepared by mixing 500 ml of toluene, 495 ml of isopropanol and 5 ml of distilled water. 0.1N KOH solution prepared in isopropanol was used as a titrant. A blank titration was first carried out by taking 100 ml of solvent and adding 0.05 ml of phenol phthalein indicator solution to it.

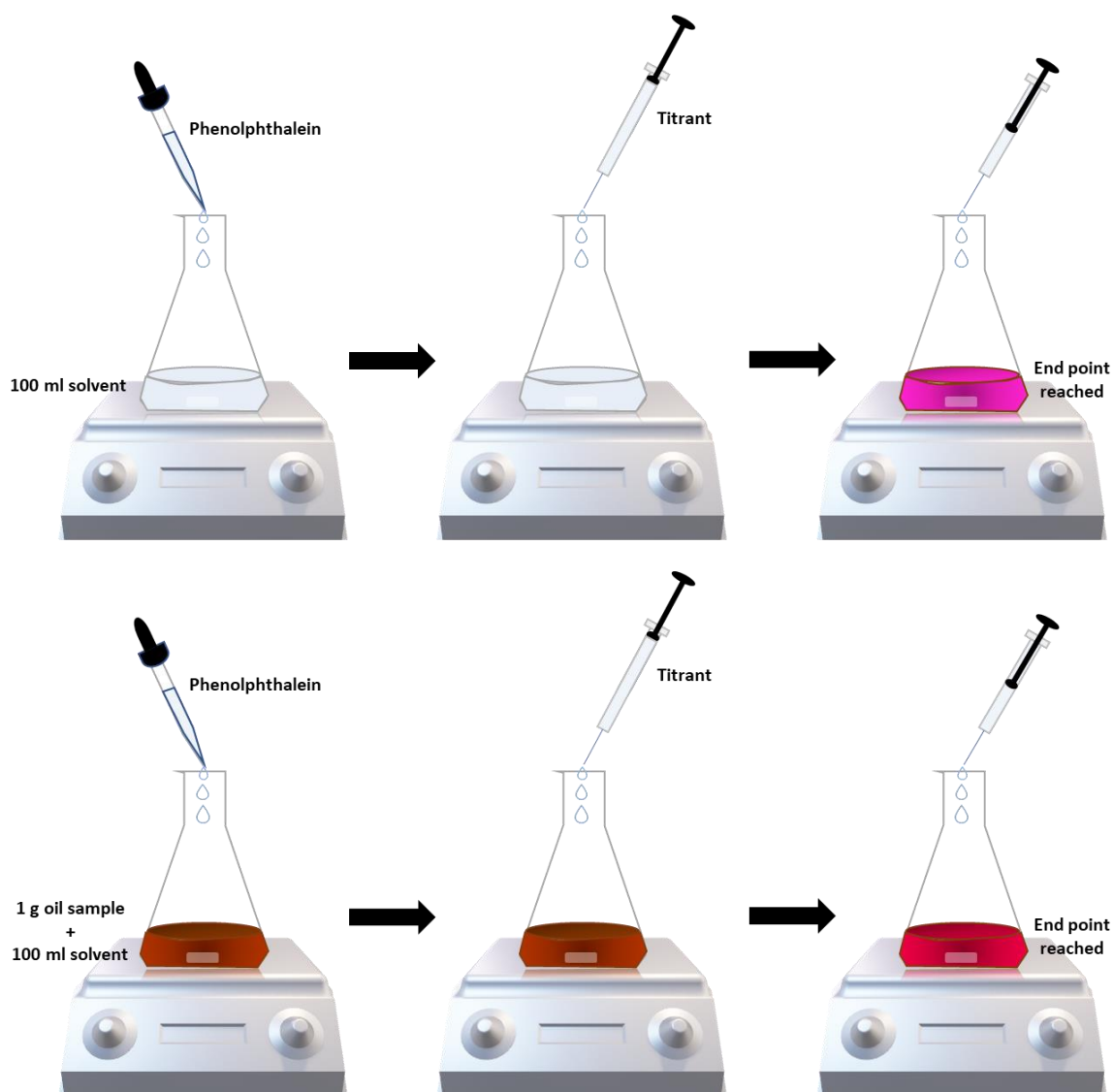


Figure 30. Procedure for determination of crude oil AN.

The solution was stirred for 30 seconds and then titrant was added drop by drop with a 1 ml syringe until the solution turned to pink color. The volume of titrant consumed was noted. Next, the titration was performed with the crude oil sample. 1g of sample was weighed in titration flask and mixed with 100 ml of solvent until the oil dissolved completely. 0.05 ml of indicator solution was added to this mixture and mixed for 30 seconds. The sample was then titrated with KOH solution until the solution changed color from brown to pink. The volume of titrant consumed was noted and AN was determined using Equation 2.

$$AN \text{ (mg KOH/g of sample)} = \frac{(V_{\text{sample}} - V_{\text{blank}}) \times C}{m_{\text{sample}}} \times 56.1 \quad (2)$$

where V_{sample} is titrant volume used for sample, V_{blank} is titrant volume used for blank, C is concentration of KOH solution and m_{sample} is sample weight in grams. The experiment was repeated for 3 samples and the average value was found. The acid number obtained from this titration procedure was around 4.3 ± 0.2 mg KOH/g of oil. The AN indicates that this crude oil is suitable for alkali/surfactant and engineered water flooding.

2.2.3 Rock Properties

Six core samples were cut for coreflood experiments. These cores were first dried in the oven to obtain the dry weight. The porosities were measured using a Vinci Helium Porosimeter. The core samples were then saturated with formation water using Vinci Manual Saturator (AP-007-001-1) and porosities were again calculated by weight method using saturated core weight, dry core weight, formation water density and bulk volume of core sample as expressed in Equation 3 and 4. Table 12 shows the comparison of porosity values obtained from two methods i.e., weight method and helium porosimeter. The values are in the close agreement.

$$V_p = \frac{w_{\text{wet}} - w_{\text{dry}}}{\rho_w} \quad (3)$$

$$\phi_{\text{wt}} = \frac{V_b - V_p}{V_b} \quad (4)$$

Absolute brine permeability and effective oil permeability for each sample were measured using Vinci aging cell apparatus. Darcy's law was used to calculate permeability by incorporating pressure drop, flow rate, fluid viscosity and core dimensions using Equation 5. The absolute and effective permeability values for all samples are given in Table 13.

Table 12. Core samples porosities.

Sample ID	d (mm)	L	W_{dry} (g)	W_{wet}	V_p (cc)	V_b	ϕ_{wt} (%)	ϕ_{He}
A-1	38.10	73.09	187.02	201.60	12.35	83.33	14.83	16.34
A-2	38.10	76.51	195.14	210.57	13.08	87.18	14.99	15.65
A-3	38.12	72.81	187.24	201.56	12.14	83.10	14.60	15.75
A-4	38.10	72.81	185.03	199.60	12.35	83.01	14.87	16.63
A-5	38.08	73.11	185.93	201.09	12.80	83.22	15.38	16.59
A-6	38.09	72.75	186.74	201.27	12.31	82.90	14.85	15.76

$$k = \frac{q\mu L}{A\Delta p} \quad (5)$$

Table 13. Core samples permeabilities.

Sample ID	k_{abs} (md)	k_{eff}
A-1	134.4	117.6
A-2	104.4	84.8
A-3	103.6	80.7
A-4	99.1	75.6
A-5	110.3	100.7
A-6	92.4	75.3

2.2.4 Polymer Shear and Viscoelastic Characterization

One of the objectives of this study is to determine engineered water pH effect on rheological and viscoelastic properties of HPAM F5115 polymer and identify an optimum pH range to get maximum benefit from the hybrid EWPF technique. For this purpose, polymer solutions of 1500, 3000 and 4500 ppm concentration were prepared using EW as make-up brine. The pH of the solutions was adjusted to 2, 4, 6, 8, 10 and 12 using hydrochloric acid (HCl) as an acid and sodium hydroxide (NaOH) as a base to cover the acidic, basic, and neutral range. Anton Paar MCR 301 rheometer with plate-plate geometry was used for measurement of different rheological and viscoelastic parameters. The main steps involved in this experimental stage are schematically described in Figure 31. This phase of study is subdivided in two sections which are discussed below.

Shear Characterization

The objective of the rheological experiments is to assess the effect of polymer concentration, aging time, and pH on F5115 viscosity. The steady shear viscosities were measured at room temperature of 25 °C. A thermal stability study was also performed on 1500 ppm concentration solutions of different pH by placing them in the oven at 80 °C and the viscosity was measured at different aging times. To measure the viscosity, around 1 ml of the sample was placed on the rheometer plate by a pipette and the steady shear profiles were obtained over a shear rate range of 1 to 100 s⁻¹.

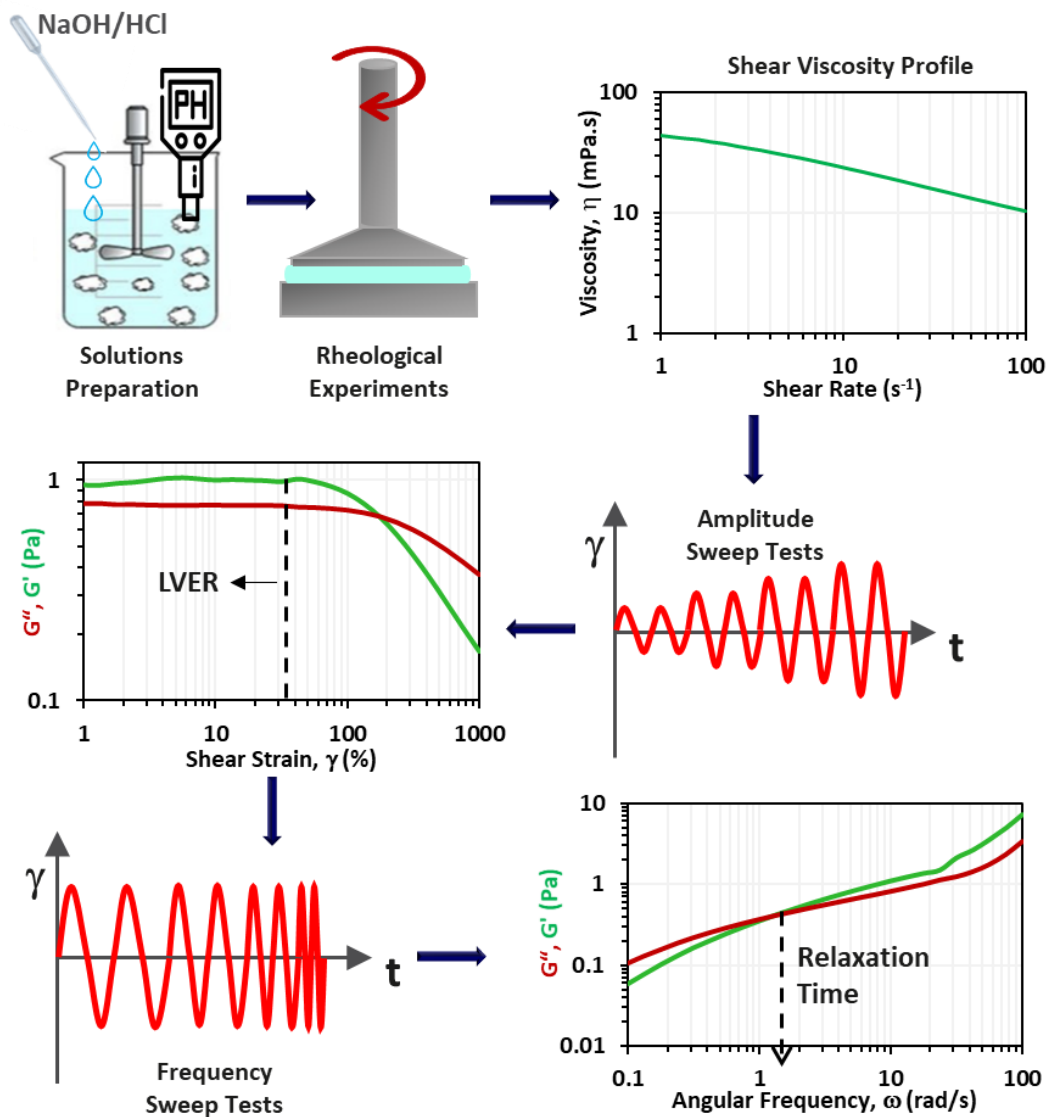


Figure 31. Step-by-step procedure for F5115 rheological and viscoelastic characterization.

Viscoelastic Characterization

This stage of the study was designed to assess if F5115 had viscoelastic characteristics or not. To study the viscoelastic behavior, oscillatory rheological tests namely amplitude sweep test (AST) and frequency sweep test (FST) are performed. An AST is performed by a stepwise

increment in measuring system deflection while angular frequency is kept constant. On the contrary, the shear strain rate is kept constant during an FST while angular frequency is varied in steps. The frequency sweeps are used to evaluate time-dependent properties of a material such as elasticity within a linear viscoelastic region (LVER).

All the oscillatory rheological experiments were performed at 25 °C. Amplitude sweep tests were conducted for pH 6 solutions with three different polymer concentrations (1500, 3000 and 4500 ppm) to determine storage modulus (G') representing the elastic component of polymer structure and loss modulus (G'') indicating the viscous component. The angular frequency (ω) was set at 10 rad/s and shear strain rate ($\dot{\gamma}$) was varied from 1 to 1000 %. The main objective of this test was to obtain the limit of the LVER and select the value of constant shear strain within LVER to perform subsequent FST for solutions under study. The LVER indicates the range in which the test can be conducted without damaging the polymer structure and is indicated as the region to the left side of the dotted-black line in Figure 31.

In the next step, frequency sweep tests were conducted for different pH (2, 6, 8, 10 and 12) and polymer concentrations (1500, 3000 and 4500 ppm) to determine the relaxation times. Relaxation time represents the elastic behavior of HPAM polymers. The longer the relaxation time, the higher the elastic nature of the polymer. For FST, constant shear strain rate of 5% within LVER was used as identified from amplitude sweeps and angular frequency range was set from 0.1 to 100 rad/s to cover both high and low frequencies. Relaxation time was measured by taking the reciprocal of frequency values at the crossover point where G' and G'' intersect as given in Equation 6. The data was interpreted to quantify the effect of pH on polymer rheology and its viscoelastic behavior.

$$Relaxation\ Time = \frac{1}{\omega_{G'=G''}} \quad (6)$$

2.2.5 Contact Angle Measurements

Literature shows that engineered water or chemically tuned low salinity water is capable of wettability alteration in carbonate rocks, however it may not be always true depending upon the characteristics of the CBR system under examination. To confirm that the designed EW is capable to recover additional oil by changing the carbonate rock surface towards more water-wet, and to reproduce the results obtained by our team, contact angle (CA) measurements were performed. The main purpose of CA measurements was to evaluate the effect of initial rock wettability on EW wettability alteration mechanism. Another objective of CA measurement

was to confirm that selected polymer F5115 has no effect on rock wettability or EW performance. For this purpose, 1.5 inch diameter pellets were cut from the same limestone cores used in coreflood experiments. The pellets were then cut in semi-circles, as shown in Figure 32, and saturated with FW to determine the pre-aging contact angles.



Figure 32. Limestone pellets for CA measurements.

OCA 15EC contact angle apparatus by DataPhysics Instruments GmbH was used and CA was measured by captive bubble method. In this method, the pellet is placed into the brine and/or polymer solution and an oil drop is injected by a syringe from the bottom of the pellet. The oil drop rises due to the density difference between oil and water and attaches to rock surface. The oil-water CA is then computed once the oil drop is stabilized. The CA apparatus is schematically presented in Figure 33.

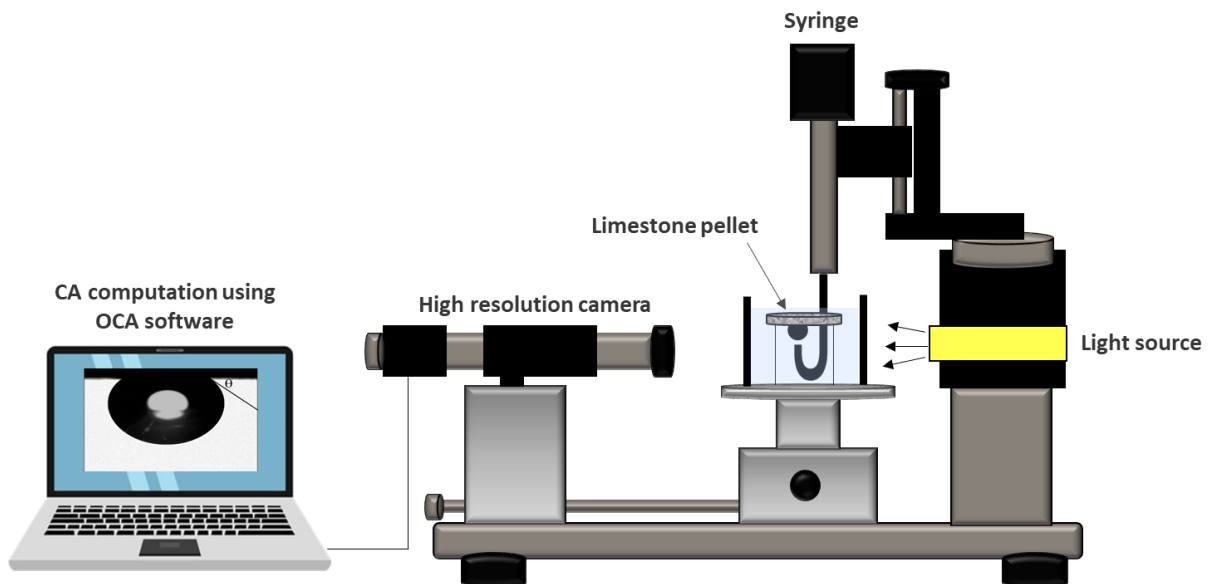


Figure 33. Illustration of OCA instrument for CA measurements.

9 pellets were used for CA analysis. All the pellets were first saturated with FW using Vinci manual saturator and the pre-aging CA of the carbonate rock was measured. The pellets were then kept in the crude oil in a special aging cell and placed in the oven at 80 °C to restore initial reservoir wettability. To check the effect of aging time on initial wettability, the aging time was

set as 1 week, 2 weeks and 1 month for different pellets. After one week of aging with oil, three pellets were taken out of the oven and their post-aging CA were measured. Pellet-1 was then immersed in EW and was kept at room temperature for one week. The final CA was then measured and the change in CA was recorded. Pellet-2 was also exposed to EW for one week, however it was placed in the oven at 80 °C instead of room temperature. Here the objective was to assess the effect of temperature on EW performance to change the rock wettability. Pellet-3 was kept in HSW at room temperature for one week and the final CA was measured.

The same sequence was followed for pellet-4, 5 and 6 with the only difference of aging time with crude oil that was 2 weeks for these pellets. CA measurements for pellet-7, 8 and 9 were also conducted in the similar manner after one month of aging. Once the final CA of pellet-7 was measured post-EW exposure, it was placed in engineered water/polymer (EWP) solution for one week and the CA was again measured to check the effect of polymer on wettability. These CA results were used as a supporting data for the initial wettability state of the core samples used for studying the effect of initial wettability i.e., A-1, A-2, and A-3. The number of pellets and sequence of CA measurements is depicted in Figure 34.

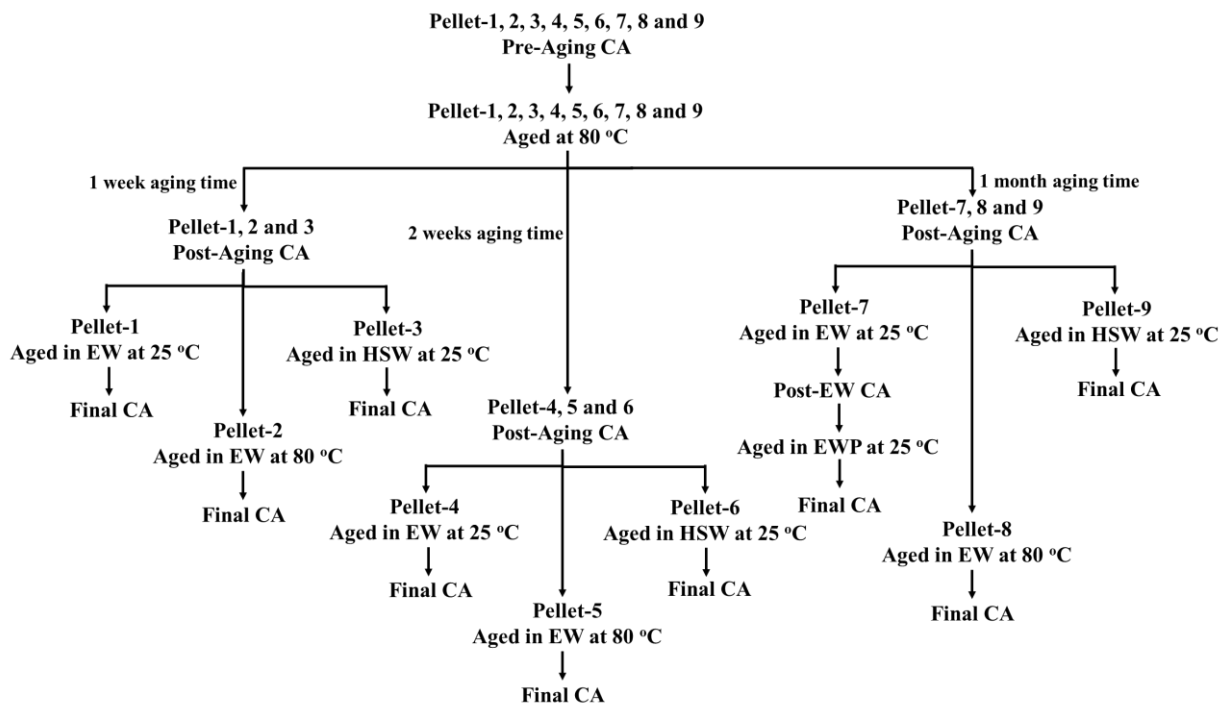


Figure 34. Sequence of CA measurements.

For better accuracy of results, the CA measurement for each case was repeated at least three times and the average value was used for further analysis and reporting. CA was measured for both top and bottom surfaces of a pellet to check the consistency of the results.

2.2.6 Design of Oil Displacement Experiments

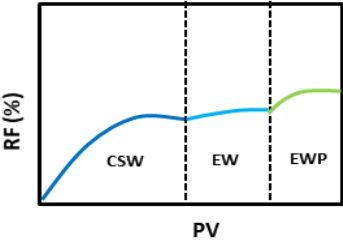
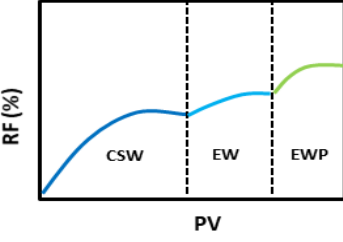
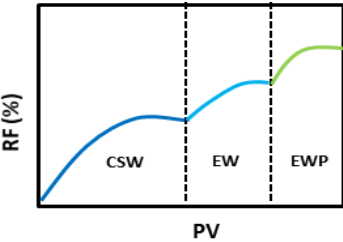
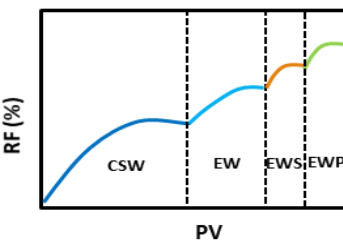
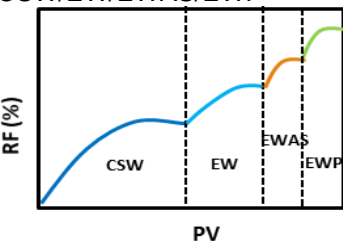
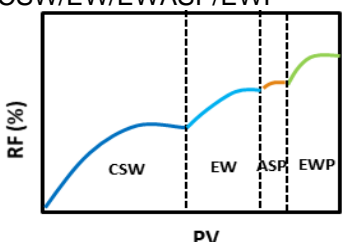
There are various tertiary recovery techniques such as low salinity waterflooding, polymer flooding, and alkali/surfactant/polymer flooding. Each of these EOR methods has its associated limitations which can be overcome by combining the two methods. Previous work by our team showed encouraging results of combining engineered water/polymer and engineered water/surfactant by conducting wettability and sweep efficiency measurements [183, 197]. To investigate the enhanced oil recovery potential of various hybrid EW/CEOR methods, several oil displacement experiments were needed to be conducted. Six coreflood experiments were designed in this phase to investigate various parameters such as effect of initial wettability, best combination of hybrid method and comparison of continuous vs slug-wise injection of alkali/surfactant solution. Core samples A-1, A-2, and A-3 were selected to study the effect of initial wettability by aging them for different times. The flooding sequence for these samples was designed as starting with HSW injection followed by EW injection and then EWPF was carried out.

A hybrid engineered water/surfactant/polymer flooding (EWSPF) experiment was designed for Sample A-4 to compare it with EWPF scenario. The HSW was first injected followed by EWF. The injection fluid was then switched to engineered water/surfactant solution and finally EWPF was conducted. The test designed for sample A-5 was a combination of engineered water and EOR chemicals (alkali, surfactant, and polymer). HSW flooding was initiated followed by EWF. Engineered water/alkali/surfactant flooding (EWASF) was then conducted in continuous injection mode until oil cut was less than 0.1%. Finally, core was flooded with EWP solution to recover extra oil by improving mobility ratio. The similar injection sequence was followed for sample A-6 with slight modification of engineered water/chemical flooding phase. During this stage, a 0.7 pore volume (PV) slug of engineered water/alkali/surfactant/polymer was injected, and a soaking time of 6 hours was given before injecting engineered water/polymer solution. This experiment was designed to compare the effect of slug-wise injection and soaking on the performance of hybrid method. Table 14 presents the designed corefloods along with the sequence of injection for the hybrid methods under investigation.

2.2.7 Coreflooding

After designing all the coreflood experiments to be performed, the standard experimental procedure was followed for each experiment. Some preliminary steps were required to make the samples ready for coreflooding.

Table 14. Design of oil displacement experiments for EW based hybrid EOR methods.

Experiment #	Injection Sequence/Design	Remarks
1. Hybrid EWPF in a weak oil-wet system	CSW/EW/EWP 	The objective of this coreflood was to confirm that EW was not suitable for weak oil-wet systems.
2. Hybrid EWPF in an intermediate oil-wet system	CSW/EW/EWP 	This coreflood was designed to show that EW as well as EWPF works well in intermediate oil-wet systems.
3. Hybrid EWPF in an oil-wet system	CSW/EW/EWP 	This coreflood was designed to show that EW works well in an oil-wet system. Hence, initial wettability of the system is an important consideration for hybrid EWPF application. In addition, the results were compared with surfactant / polymer (SP) and alkali / surfactant / polymer (ASP) experiments.
4. Hybrid EWSPF in an oil-wet system with continuous injection of surfactant solution	CSW/EW/EWS/EWP 	The primary objective of this coreflood was to assess the combined recovery of both surfactant and polymer in presence of EW. The results were compared with those obtained from Experiment-3.
5. Hybrid EWASP flood in continuous injection mode	CSW/EW/EWAS/EWP 	The main objective of this coreflood was to assess the combined recovery of alkali, surfactant, and polymer in presence of EW. The results were compared with those obtained from Experiment-4.
6. Hybrid EWASP flooding in an oil-wet system with 0.7 PV ASP slug injection	CSW/EW/ASP/EWP 	Here, the objective was to analyze the effect of ASP slug injection and soaking time. This gives more time for EWASP slug to contact with crude oil and rock and promote IFT reduction and wettability alteration. The results were compared with Experiment-5 to quantify the benefit of slug-wise injection.

The oven dried core samples were first saturated with FW using Vinci manual liquid saturator. Afterwards, Vinci aging cell apparatus was used in which one sample at a time could be flooded with desired fluid. The coreflood apparatus is schematically shown in Figure 35. After setting the core holder, confining pressure was applied to create overburden on the rock sample. The back pressure was set at 500 psi. The accumulators were filled with the fluids to be injected and the entire setup was then heated at 80 °C for sufficient time. All the corefloods were performed at reservoir temperature of 80 °C.

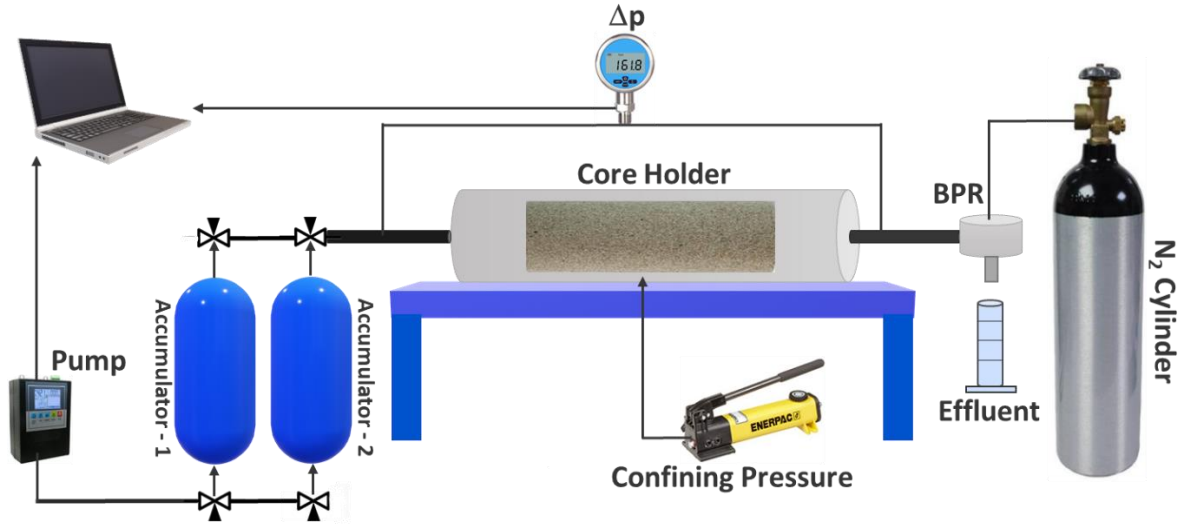


Figure 35. Schematic of Vinci aging cell apparatus used for oil displacement experiments.

The core sample was first flooded with FW at injection rates from 3 cc/min to 12 cc/min and absolute permeability was obtained using pressure drop data. Next, crude oil was injected at a rate of 1 cc/min until effluent water-cut was less than 1%. The flow rate was then increased to 2 cc/min and continued until no water production was observed at the outlet. This procedure was repeated for flow rates up to 7 cc/min to reach initial water saturation (S_{wi}) in the core and measure effective oil permeability using pressure-flow rate data. The effluent water production recovered during oil flooding was measured and S_{wi} was calculated using Equation 7.

$$S_{wi} = \frac{PV - V_w}{PV} \times 100 \quad (7)$$

Both FW injection and oil injection were performed at a temperature of 80 °C. The core sample was then kept in a special aging cell and placed in oven at 80 °C for one month to achieve initial reservoir wettability conditions. The same steps were performed to age all the core samples, however the aging time in the oven for samples A-1 and A-2 were different. Sample A-1 was not placed in oven to mimic weak oil-wet reservoir whereas sample A-2 was kept in the oven for two weeks to replicate an intermediate oil-wet reservoir.

Once the predetermined aging time was completed for a sample, it was ready for main coreflood experiment. Table 2.12 presents the detailed injection sequence performed along with relevant flooding parameters for all five corefloods.

Table 15. Injection rates and chemical concentrations for coreflood experiments.

<i>Experiment No.</i>	<i>Aging Time</i>	<i>Injection Fluid</i>	<i>Concentration</i>	<i>Injection Rate (cc/min)</i>
1	0 days	HSW	-	0.5, 2, 5
		EW	-	0.5, 2, 5
		EWP	1500 ppm	0.5, 2, 5
		EW-Postflush	-	0.5, 2, 5
2	2 Weeks	HSW	-	0.5, 2, 5
		EW	-	0.5, 2, 5
		EWP	1500 ppm	0.5, 2, 5
		EW-Postflush	-	0.5, 2, 5
3	1 Month	HSW	-	0.5, 2, 5
		EW	-	0.5, 2, 5
		EWP	1500 ppm	0.5, 2, 5
		EW-Postflush	-	0.5, 2, 5
4	1 Month	HSW	-	0.5, 2, 5
		EW	-	0.5, 2, 5
		EWS	0.5 wt%	0.5, 2, 5
		EWP	1500 ppm	0.5, 2, 5, 7
		EW-Postflush	-	0.5, 2, 5
5	1 Month	HSW	-	0.5, 2, 5
		EW	-	0.5, 2, 5
		EWAS	Surfactant: 1 wt% Alkali: 1 wt%	0.5, 2, 5, 7
		EWP	1500 ppm	0.5, 2, 5
6	1 Month	EW-Postflush	-	0.5, 2, 5
		HSW	-	0.5, 2, 5
		EW	-	0.5, 2, 5
		EWASP	Surfactant: 1 wt% Alkali: 1 wt% Polymer: 500 ppm	0.5
		EWP	1500 ppm	0.5, 2, 5
EW-Postflush	-	0.5, 2, 5		

The steps that were common for all the coreflood experiments are elaborated below.

- After setting the core sample in core holder, the first step was to inject oil to confirm there was no more water production.
- HSW was then injected at 0.5 cc/min until the oil-cut was less than 0.1%. The injection rate was then increased to 2 cc/min and continued until no more oil was observed at outlet. Finally, the injection rate was increased to 5 cc/min and continued until pressure drop was stabilized and there was no further oil production. These steps were necessary to eliminate capillary end effects and to obtain reliable production data. The oil production at this stage showed the secondary recovery.
- The injection fluid was then switched to EW at a flow rate of 0.5 cc/min. The flow rate was then increased to 2 and 5 cc/min when there was no oil production at a certain rate.
- In the next step, the designed hybrid engineered water/chemical fluid was injected again at the rates of 0.5, 2 and 5 cc/min to minimize capillary end effects and to recover moveable oil volume.
- For hybrid EWSPF and EWASPF cases, there was an additional stage of EWPF after EWSF and EWASP injection. The same injection rate scheme was followed during this stage.
- Each injection stage was continued until oil cut was less than 0.1%. The criterion for changing injection rate was that the oil cut should be less than 0.1% for two consecutive pore volumes and pressure drop across the core is stabilized. An EW post-flush was conducted at the end of each experiment for estimation of resistance factor (RF) and residual resistance factors (RRF).
- The effluents from each injection stage were collected in 10 ml graduated tubes and sufficient time was given for proper separation of oil and water.

After the completion of a coreflood experiment, the oil and water production for each injection stage were measured and the recovery factors were calculated. The effluents for EWPF and EW post-flush were collected to measure effluent viscosities and polymer degradation was estimated using fresh polymer properties. The pressure-production data was analyzed to obtain other useful information such as mobility ratios, capillary numbers, etc.

3. Results

The first section discusses the results of HPAM F5115 polymer rheology and viscoelastic behavior as a function of pH. The objective of this task was to assess the pH effect on synthetic HPAM polymer being used in this study and select an optimum pH range for the best performance of polymer in terms of both viscous and viscoelastic properties. The results of this stage are discussed herein.

3.1 Shear Characterization

To characterize F5115 viscous behavior, the shear rate - viscosity profiles were obtained under different conditions of polymer concentration, pH, and temperature.

3.1.1 Effect of pH on Viscosity

For this purpose, viscosity for 1500 ppm polymer solutions of pH 2, 4, 6, 8, 10, 12 were measured at 25 °C for a shear rate range of 1-100 s⁻¹. The viscosity curves are presented in Figure 36. It can be seen from the graph that as the pH of the solution went towards acidic side, the viscosity decreased considerably (34% of the viscosity of neutral pH solution). This trend was due to the consumption of negatively charged carboxylic groups on polymer backbones by hydrogen ions (H⁺), resulting in reduced stretching of polymer chains. On the contrary, the solution viscosity increased by 14% as the pH increased from 6 to 8.

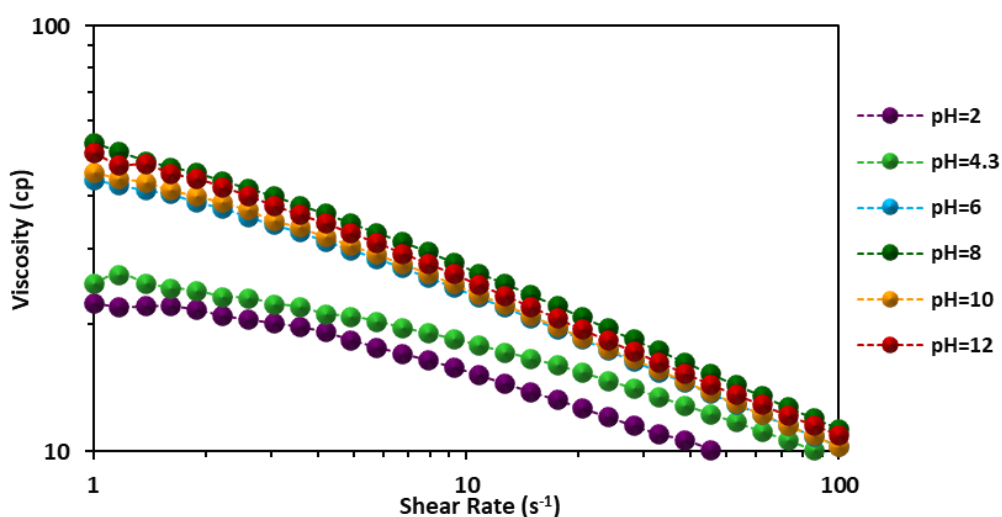


Figure 36. Effect of pH on 1500 ppm F5115 viscosity at 25 °C.

The solutions in the basic range showed higher viscosities than the neutral and acidic pH mainly because of increased hydrolysis in the presence of alkali and higher repulsion among polymer chains. The presence of OH⁻ ions in an alkaline solution increases the dissociation rate of amide

groups on HPAM backbone, generating more carboxylate ions (COO^-). The solution viscosity, in turn, increases due to higher repulsion between molecular chains. The similar behavior was also reported by Gu et al. [216] for HPAM/ Cr^{3+} weak gel, where they observed the highest viscosity of gel in the basic region.

3.1.2 Effect of Polymer Concentration and pH on Viscosity

The same steps were repeated for three different concentrations of polymer (1500, 3000, and 4500 ppm). Figure 37 shows the viscosity as a function of pH and polymer concentration at shear rate of 10 s^{-1} . This shear rate was chosen as it represents the typical shear rates observed in the field. First observation was that as the concentration increased, the solution viscosity also increased significantly. This effect can be attributed to a higher number of polymer molecules present in high concentration solutions, leading to increased repulsion and higher viscosity. The effect of pH was already explained. It was observed that as the pH goes towards highly basic region (>10), the viscosity starts to decrease again possibly due to precipitation of some polymer molecules in excess quantity of NaOH, leading to some viscosity loss. These results indicate that the optimum pH range for this polymer is 7-10.

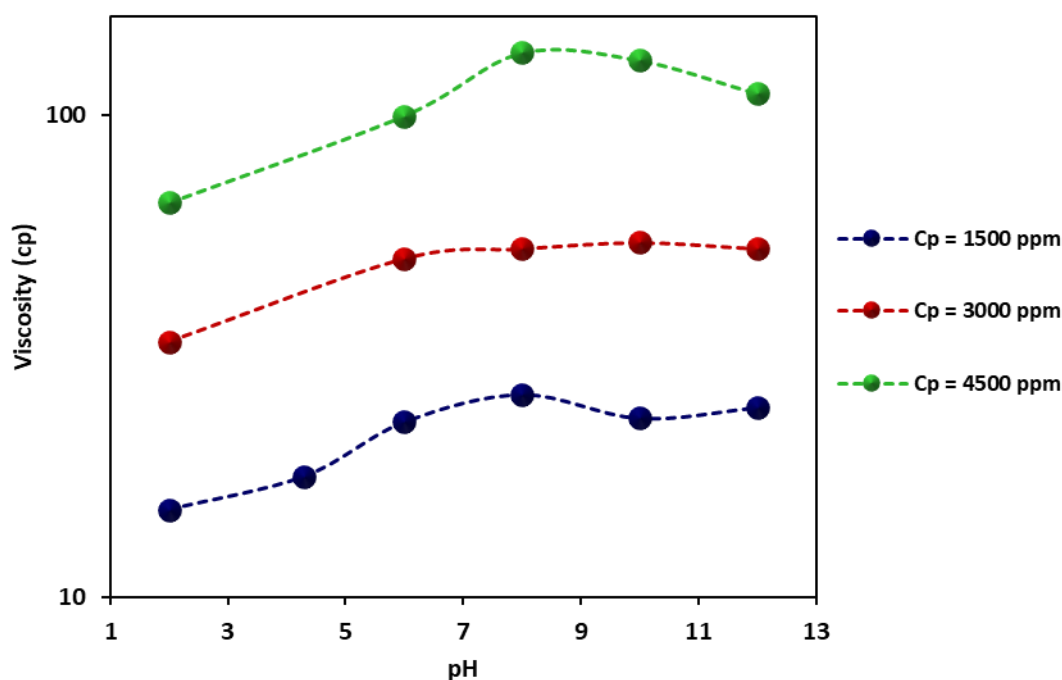


Figure 37. Effect of polymer concentration and pH on F5115 viscosity at 25 °C.

3.1.3 Effect of pH on Thermal Stability

To evaluate the pH effect on thermal stability of F5115, viscosity of 1500 ppm solutions at different pH values were measured at 25 °C. The solutions were then kept in the oven at 80 °C

and the viscosities were again obtained at different aging times. The temperature setting in the rheometer was kept at 25 °C to compare the results with the viscosity of un-aged solutions. **Error! Reference source not found.** presents the results for different pH solutions. The viscosity of acidic solutions of pH 2 and 4 was drastically decreased from 15 and 18 cp to 10 and 4 cp respectively, within 24 hours of exposure to 80 °C. Hence, these solutions were not thermally stable.

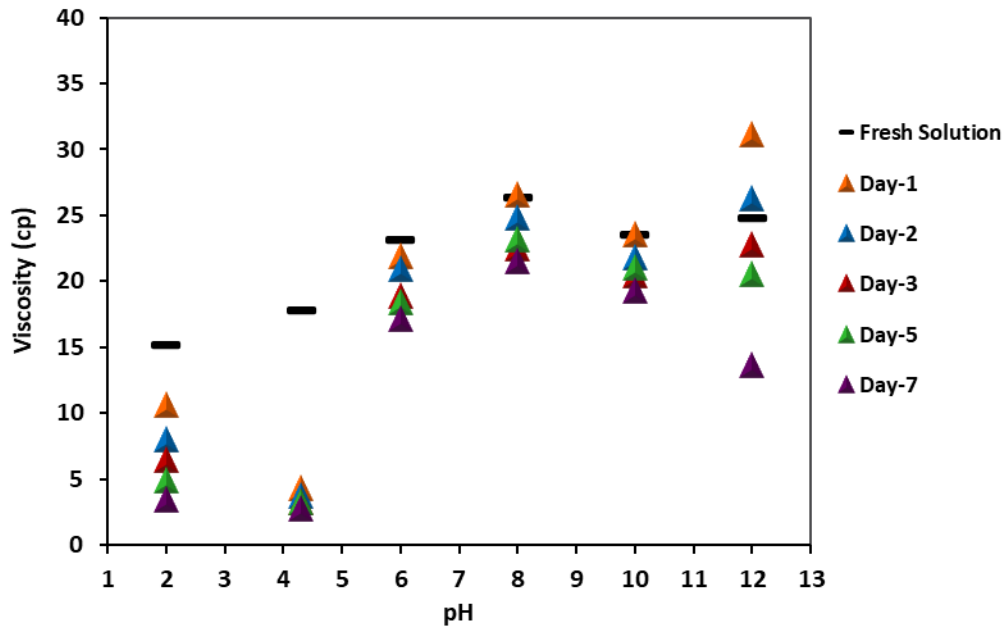


Figure 38. Effect of pH on thermal stability of 1500 ppm F5115. The solutions were kept at 80 °C while the viscosity was measured at 25 °C.

An interesting observation here was that for the 1st two days, the pH 12 solution showed considerable increase in viscosity from 25 to 31 cp. This can be attributed to further hydrolysis and increased repulsion of polymer chains at high temperature. For the solutions in the pH range of 8-10, the thermal degradation in viscosity was lowest and the viscosity for these solutions dropped only by 4-5 cp over one-week aging time. To understand the extent of thermal stability as a function of pH, the viscosity loss for each solution was calculated using Equation 8.

$$Viscosity\ Loss, (\%) = \left| \frac{\mu_o - \mu_t}{\mu_o} \right| \times 100 \quad (8)$$

where μ_o is the fresh solution viscosity and μ_t is the viscosity of the solution after one-week aging time at 80 °C. **Error! Reference source not found.** shows the effect of pH on viscosity loss due to thermal degradation. The viscosity loss under acidic conditions was maximum (~60% higher than the solutions in the basic range). The reason for a rapid decrease in viscosity was the increased reactivity of acid with polymer molecules at high temperature. The H⁺ ions

present in an acidic solution neutralize the HPAM carboxylate ions, leading to reduced repulsion among the polymer chains; the rate of this reaction becomes fast at high temperature. Less number of carboxylate ions on polymer backbones result in a reduction of repulsive forces among molecules, leading to increased entangling and coiling of polymer chains.

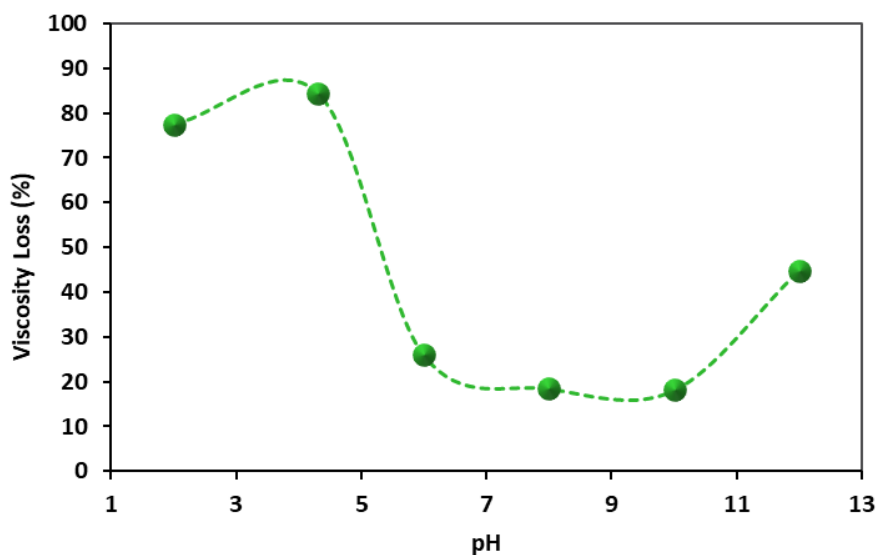


Figure 39. 1500 ppm F5115 viscosity loss as a function of pH after one week aging time at 80 °C.

The solutions in the basic pH range exhibited the lowest viscosity loss (only 18% after 1-week) and maximum thermal stability owing to higher repulsion among the molecules. The reason for the better thermal stability of F5115 in the pH range of 8-10 is that an appropriate amount of hydroxyl ions (OH^-) present in the solution promote stability of the polymer chains by allowing them to expand and repel each other, maintaining the solution viscosity. Interestingly, the pH 12 solution also showed a relatively higher viscosity loss despite being on the basic side. The reason for this trend was the precipitation due to excess amount of NaOH which was not compatible with F5115 above a certain critical concentration. As the concentration of NaOH increased in pH 12 solution, the degree of polymer hydrolysis also increased beyond the required value, resulting in higher viscosity loss. The presence of excess amount of alkali also resulted in increased salinity and cation concentration in the solution which triggered polymer coiling and degradation, causing precipitation by breaking the chains. That is why, the viscosity of pH 12 solution started to decrease on the third day of aging at 80 °C.

The results of viscosity as a function of pH indicate that the viscous properties of F5115 polymer improve with increasing pH but start to degrade again above a critical pH value which is found to be 12 in this case. The optimum pH range for F5115, as identified from shear viscosity measurements, is 7-10. In this range, the polymer exhibited highest viscosity, lowest

thermal degradation, and minimum viscosity loss. It can be inferred from this results that a combination of HPAM polymer and alkali can work better in EOR applications in terms of better polymer stability and reduced adsorption in an alkaline environment.

3.2 Viscoelastic Characterization

The next section discusses the pH effect on viscoelastic properties of HPAM F5115 polymer, as both viscous and elastic components play an important role in enhancing the oil recovery by HPAM-based polymers. Various parameters are available in literature to quantify the viscoelastic effect of a polymer by conducting oscillatory rheology tests i.e., AST and FST. Some of the factors analyzed in this study include storage/elastic modulus (G'), viscous/loss modulus (G''), linear viscoelastic range (LVER), relaxation time, and loss factor ($\tan\delta$).

3.2.1 Analysis of Amplitude Sweep Test

The primary objective of AST was to determine the limit of linear viscoelastic region for HPAM F5115 polymer within which the polymer structure would not be destroyed. Some additional information was also derived from the magnitude of G' and G'' . Figure 40 shows the results of AST for neutral pH solutions of 1500, 3000 and 4500 ppm polymer concentration at 25 °C. The angular frequency for AST was set at 10 rad/s. As expected, both viscous and loss moduli increased with concentration as well as LVER. This can be attributed to increased intermolecular interactions, yielding a high viscosity and elasticity in the solution. At lower concentration, the LVER was relatively unstable indicating lower elastic properties.

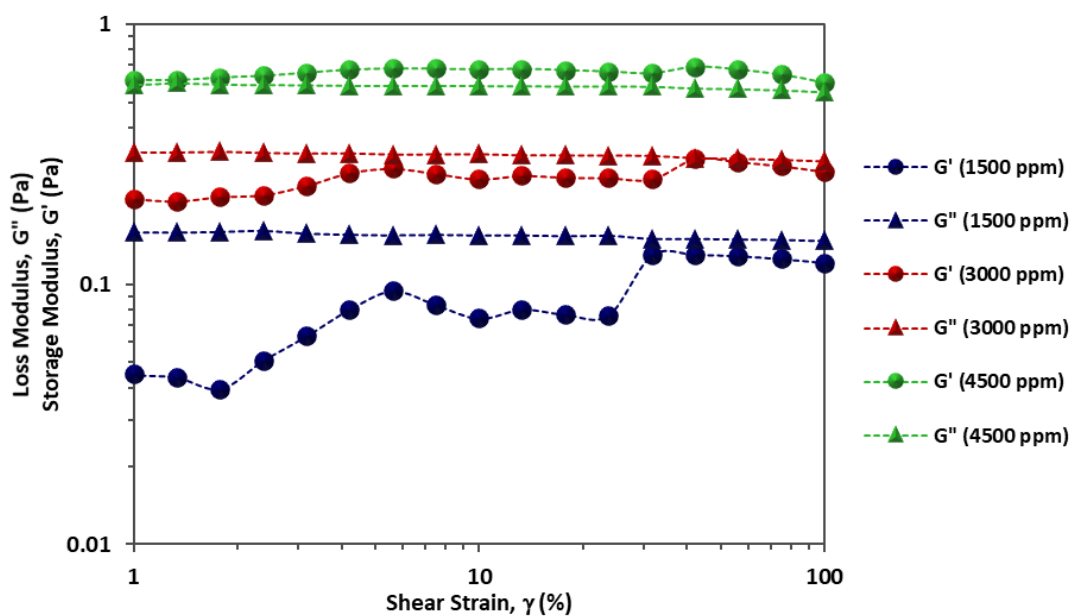


Figure 40. AST results for LVER detection for 1500, 3000 and 4500 ppm neutral pH solutions at 25 °C.

Another observation was that at high shear strain rates, the magnitude of viscous and elastic modulus was almost same, indicating that polymer had equal contribution from viscous and elastic components. Furthermore, for 4500 ppm concentration, the elastic modulus was higher than viscous modulus ($G' > G''$), making the solution more like a weak liquid gel. Hence, both G' and G'' have a direct relation with polymer concentration, however G' is influenced more compared to G'' . It can be because when a large number of molecules are present, number of elastic collisions increases. From this test, limit of LVER was identified as shear strain below 50%, as the elastic modulus was relatively linear in this range. Consequently, the FST were performed at a constant strain rate of 5% within LVER. It is critical to define a constant strain rate for FST based on the LVER identification from AST, so that the polymer molecules do not undergo deformation at high angular frequencies. Elastic or storage modulus can be used to quantify the elastic character of the polymer. Figure 41 shows elastic modulus values within LVER as a function of pH for three concentrations. This graph clearly indicates a direct relation of elastic modulus with polymer concentration. The effect of pH is also visible in Figure 41. Elastic modulus increased with increasing pH and vice versa. The maximum contribution of elastic nature can be observed for the pH range of 8-10. The similar trend was observed for viscous modulus that it increased with increasing pH.

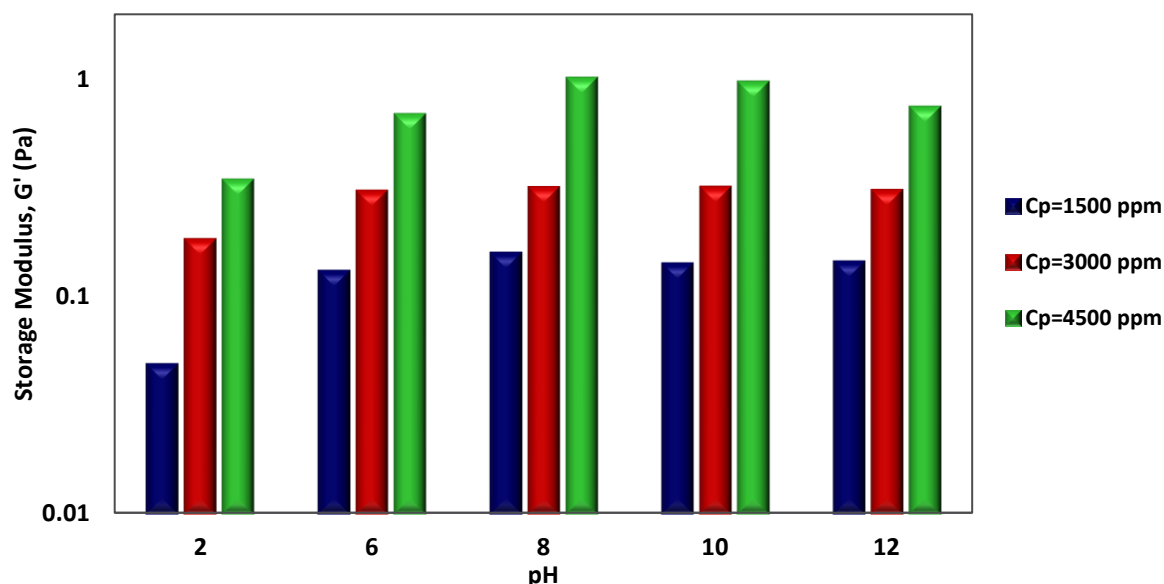


Figure 41. pH Effect on storage modulus for 1500, 3000 and 4500 ppm neutral pH solutions at 25 °C.

3.2.2 Analysis of Frequency Sweep Test

Once the LVER was determined, the frequency sweep tests were performed at a constant shear strain rate of 5% while angular frequency was varied from 1-100 rad/s. In the first stage, the FST was conducted for three concentrations of 1500, 3000 and 4500 ppm while the pH was

kept neutral. The objective here was to check the effect of polymer concentration on G' and G'' .

Effect of Polymer Concentration

Figure 42 presents the results of FST for three different concentration of polymer at 25 °C. As concentration increased, both G' and G'' also increased. An interesting observation was that with increase in polymer concentration, the difference between G' and G'' was significantly reduced, showing a pronounced effect of concentration on storage properties of the polymer solution. An important result from FST is usually the quantification of viscoelastic properties of the polymer. The crossover point (where $G'=G''$) can be used to compare the viscoelastic behavior of different solutions. Once the crossover point is reached, the solution then possesses more elastic character afterwards as angular frequency increases. For the F5115 polymer being studied, the crossover point reached earlier for higher concentration solutions. Additionally, the 4500 ppm solution exhibited higher elastic behavior over a wider range of frequency.

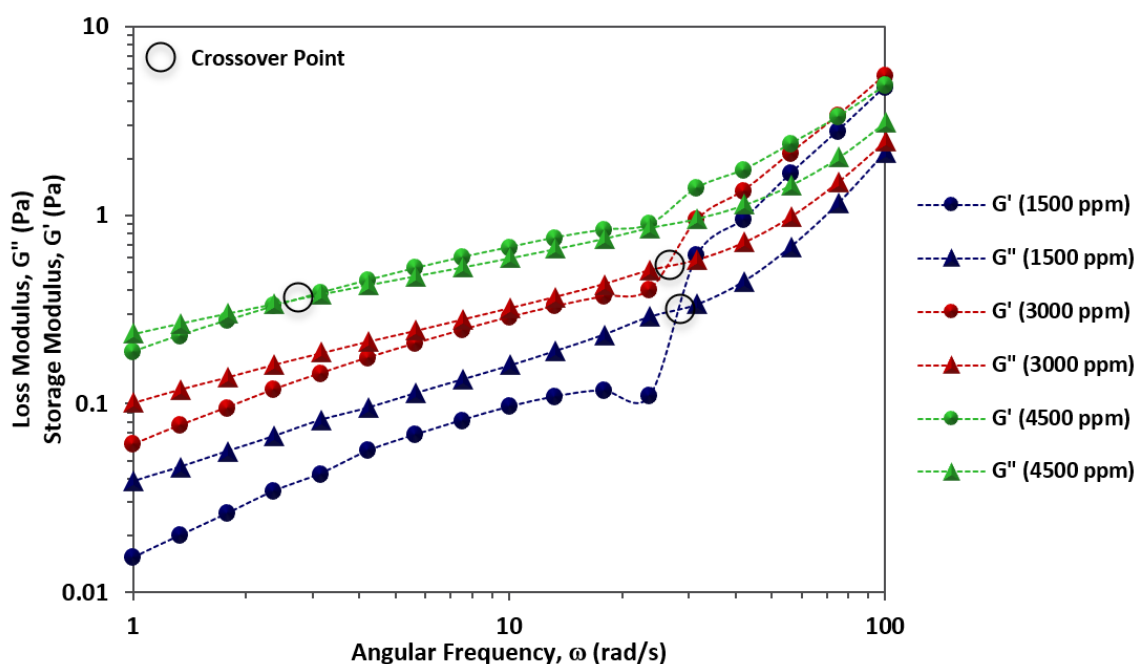


Figure 42. FST results for 1500, 3000 and 4500 ppm neutral pH solutions at 25 °C.

Effect of pH

To analyze the effect of pH on viscoelastic behavior of F5115, frequency sweep test was conducted for 4500 ppm solution at pH 2, 6, and 8. Figure 43 shows the results of FST for this case. For the solution in the acidic range, both moduli showed a decrease and for most of the test conditions, the solutions possessed viscous properties only. This was due to polymer chains coiling and degradation in polymer viscosity and elasticity in acidic medium. However, in the

basic pH range, the G' and G'' considerably increased and there was also the region where elastic component was dominant over viscous component, making the solution more like a weak gel. The crossover point appeared earlier for pH 8 solution which could be due to increased repulsion and stretching of molecules in the presence of OH^- ions. The elastic properties of F5115 were dominated over the viscous properties in the basic pH range.

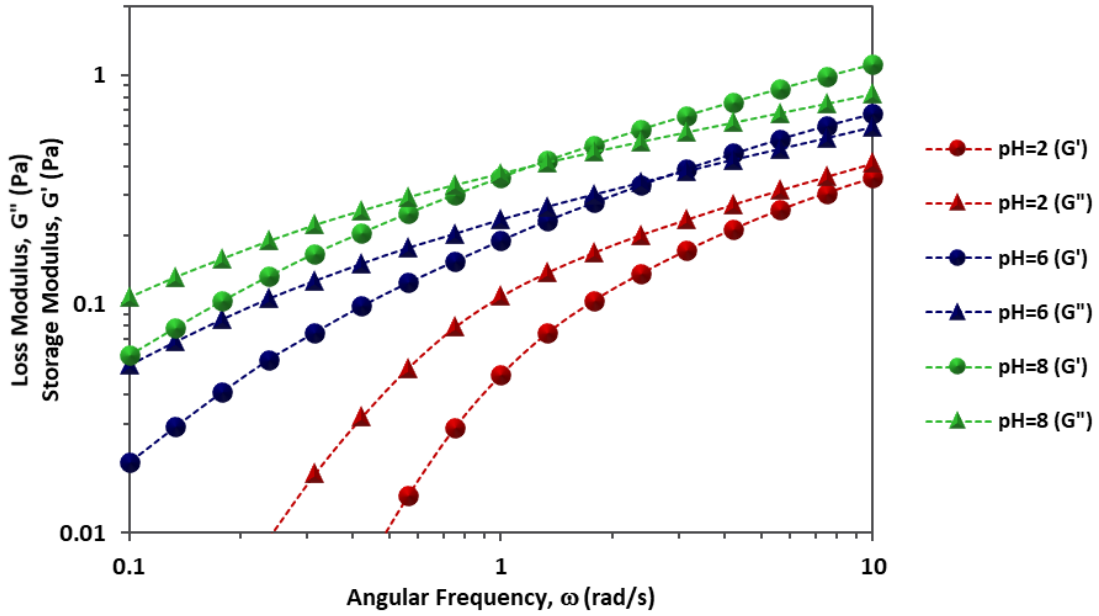


Figure 43. G' and G'' as a function of pH for 4500 ppm solution at 25 °C.

It is also evident from Figure 43 that magnitude of both elastic and viscous moduli was highest for polymer solution of pH 8 throughout the frequency range of interest. Hence, basic conditions can substantially improve HPAM F5115 viscoelastic properties by promoting its elastic character. To adequately quantify the viscoelastic behavior of F5115, a parameter called the relaxation time was estimated using FST data acquired in previous step. The relaxation time indicates the elastic behavior of polymers. The longer the relaxation time, the higher the elastic nature of the polymer. To calculate the relaxation time, the reciprocal of the angular frequency corresponding to the crossover point of G' and G'' is taken, as given in Equation 6.

The relaxation time as a function of pH is graphically presented in Figure 44. It was observed that a high pH significantly improved the relaxation time for all three concentrations, but the effect was more pronounced at higher polymer concentration. Longer relaxation time indicates that more time is required for polymer chains to adjust their alignment. The general trend was similar for all three concentrations that relaxation time increased with increasing pH up to a critical pH of 10. Beyond this pH, the polymer was degraded due to high concentration of alkali and increased salinity, causing the polymer chains to deform and lose elasticity. The highest

relaxation time was obtained for 4500 ppm solution as can also be observed from the crossover point of G' and G'' in Figure 42.

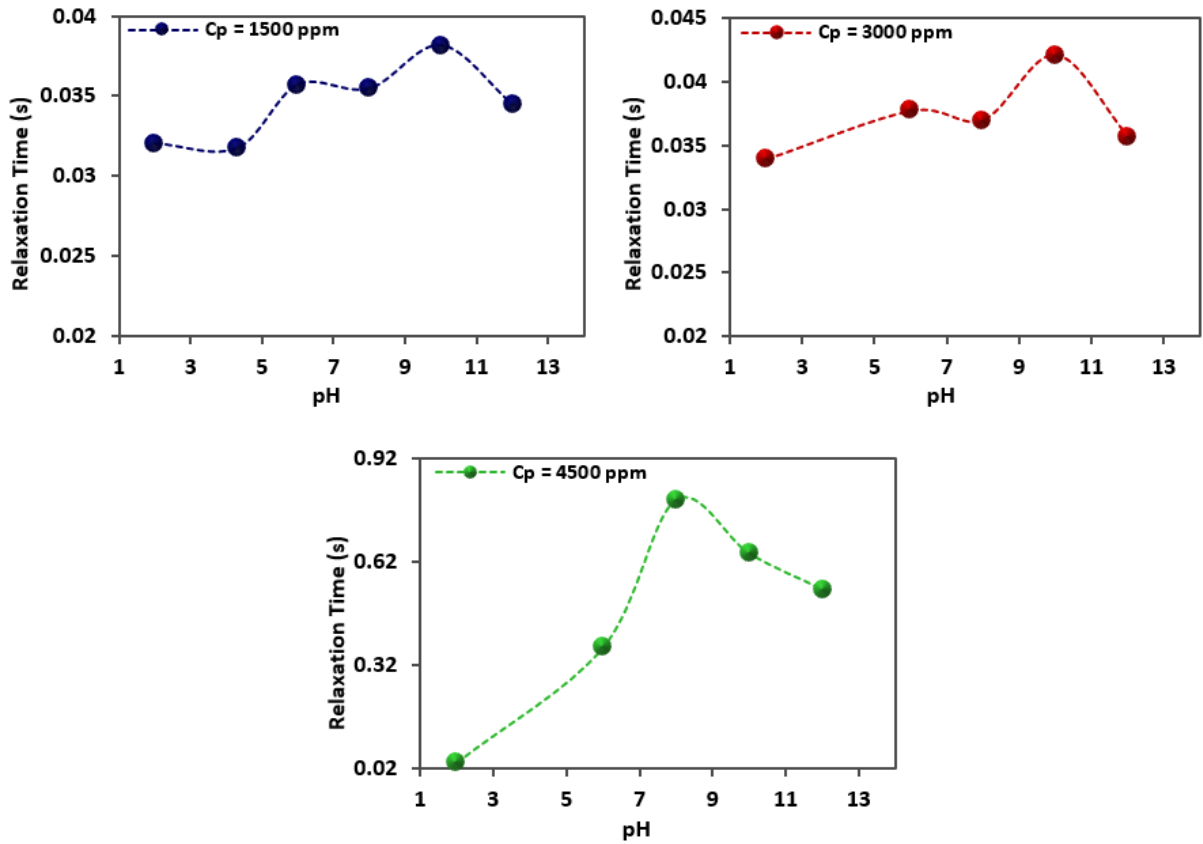


Figure 44. Relaxation time as a function of pH for 1500, 3000, and 4500 ppm solution at 25 °C.

Another useful information obtained from FST was the loss factor ($\tan\delta$) which is a ratio of the loss and storage moduli of the viscoelastic materials (Equation 9).

$$\text{Loss Factor, } \tan\delta = \frac{\text{Loss Modulus, } G''}{\text{Elastic Modulus, } G'} \quad (9)$$

For ideal viscous fluids, the loss component totally dominates the storage component, making δ equal to 90° , and thus the loss factor becomes infinite. On the other hand, the storage component completely dominates the viscous component for a perfectly elastic fluid. δ in this case becomes zero and loss factor is also zero [217]. The elastic modulus of a viscoelastic polymer is higher than the viscous modulus at higher frequencies. However, at the crossover point where G' and G'' are equal, the loss factor becomes 1. Hence, a loss factor value below 1 indicates a higher viscoelastic behavior of the material. Figure 45 shows the effect of pH on loss factor for 4500 ppm polymer solutions. The loss factor for the solution in the acidic range stayed above one, indicating a lower elastic behavior. For the solutions in the basic medium, the loss factor was less than over a wider frequency range, showing a dominance of the elastic

properties of the polymer under these conditions. The loss factor of pH 8 and 10 solutions became less than 1 quite quickly, suggesting it to be an optimum pH range for better viscoelastic behavior of HPAM F5115.

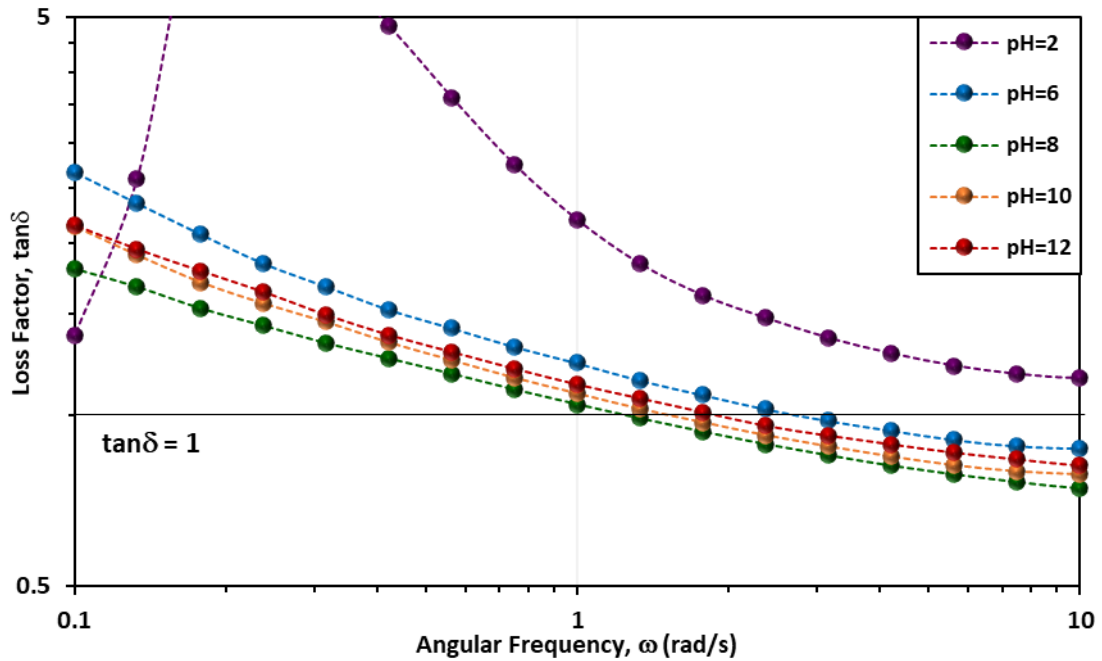


Figure 45. Loss factor as a function of pH for 4500 ppm solution at 25 °C.

The effect of pH on polymer viscosity and viscoelasticity can be summarized by Figure 46. It can be inferred that under high pH conditions, there is increased repulsion and stretching among polymer molecular chains due to presence of negatively charged hydroxyl ions. Conversely, in low pH environment, the charge screening effect is pronounced due to presence of H^+ ions, leading to increased coiling and degradation of polymer chains. Finally, polymer chains possess greater elasticity and have a tendency to stretch more when flowing through pore space under basic conditions. As a result, the polymer molecules are able to go deeper in the pore throats, enhancing the microscopic recovery efficiency by applying a stronger pulling force on the entrapped oil droplet. Hence, polymer viscosity and viscoelasticity increase by adding alkali, which can result in higher oil recovery by polymer flooding in an alkaline setting. This combination can also potentially lower the amount of polymer required, thereby improving the project economics. The improved viscoelastic behavior of polymer with alkali can also reduce S_{or} and increase microscopic efficiency.

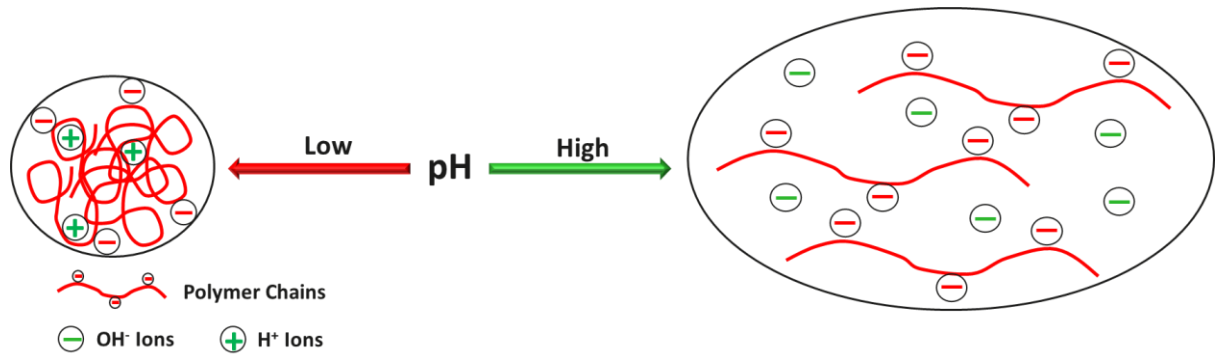


Figure 46. Mechanism for HPAM F5115 performance under acidic and basic conditions.

3.3 Results of Contact Angle Measurements

Contact angles were measured to quantitatively assess the effect of aging time on EW and hybrid EWPF performance. Another purpose of this task was to confirm the results previously obtained by our team [183]. The change in CA by both HSW and EW was also compared to see the effectiveness in altering the rock surface towards more water-wet state. The pre-aging CA for each pellet was measured and was found to be around 10° - 20° , indicating water-wet medium. Post-aging CAs were then measured after 1 week, 2 weeks and 1 month of aging time to analyze the effect of aging time..

3.3.1 Effect of Aging Time on Initial Wettability

On average, the contact angles measured after 1 week, 2 weeks, and 1 month aging time were 134° , 158° , and 160° , respectively. The measurements were repeated three times and the average values were used for further analysis. As the aging time in crude oil increased, the rock surface changed towards strongly oil-wet after 1 month. This is because the carbonate surface, being positively charged, has affinity for negatively charged acidic components in the crude oil. As more time was given for these pellets to contact the oil, almost the entire surface strongly became oil wet. Another reason was a high AN of the crude oil used in this study, leading to more acidic components available for adsorption on carbonate surface. Overall, these results strengthen the point that carbonate reservoirs tend to be oil-wet because the contact angle changed considerably and quickly shifted from more water-wet towards more oil-wet state within one week of aging with crude oil.

3.3.2 Effect of Initial Wettability on EW Performance

After measuring the post-aging CAs for each set of pellets, they were kept in respective fluids (HSW, EW) for one week and the final CA was measured to see the change. The engineered

water was prepared by reducing the salinity of CSW and spiking it with some PDIs, as selected by Sekerbayev et al. as an optimum EW design [197]. South Caspian seawater was diluted 10 times and spiked with 6 times SO_4^{2-} , 1 time Mg^{2+} and 3 times Ca^{2+} (10CSW.6S.Mg.3Ca) to prepare optimized EW. Table 6 shows the ionic composition of this EW. The contact angles were measured using captive bubble method and the profiles obtained for HSW and EW were compared with the initial profiles. Figure 47 shows the comparison of contact angles at different aging times and it can be observed that EW resulted in higher contact angle shift compared to HSW. In fact, the HSW could only slightly change CA after one month aging time.

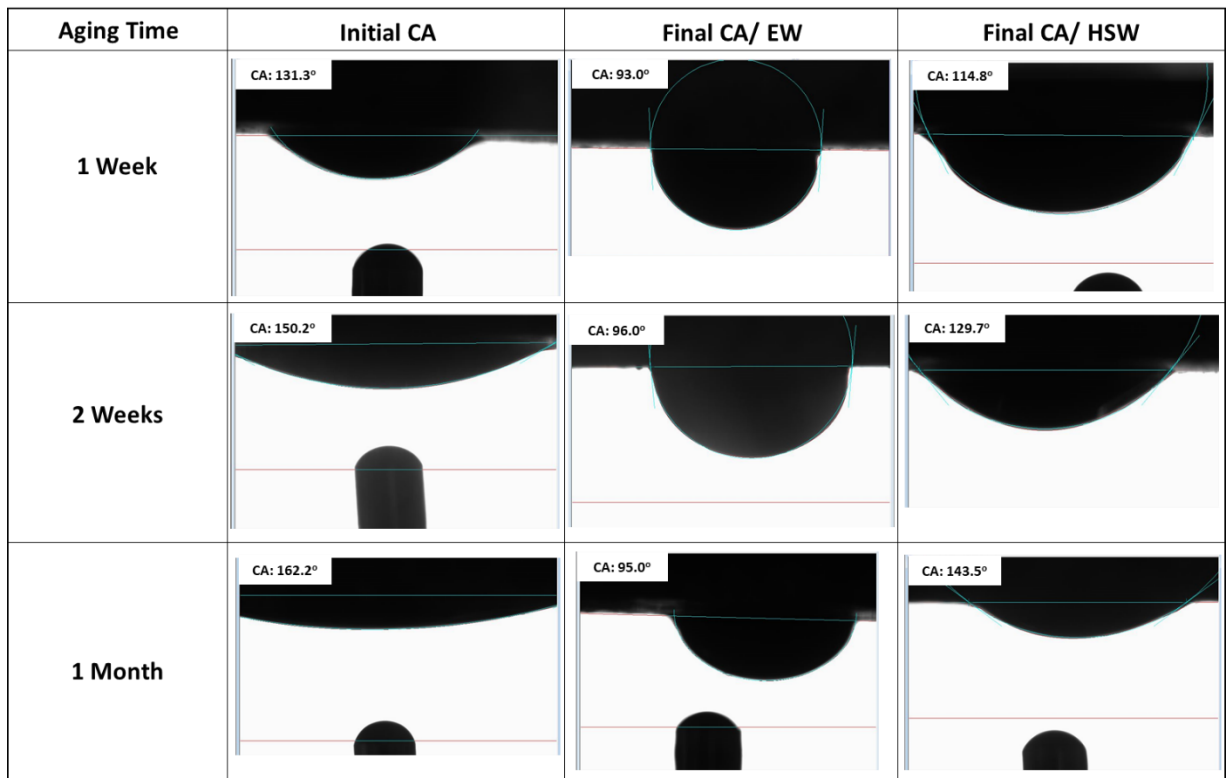


Figure 47. Effect of aging time on wettability change by EW and HSW.

Figure 48 shows the relationship between aging time and change in CA by EW and HSW. As the aging time became more, the change in CA caused by EW also increased because of higher adsorption of crude oil acidic components on calcite surface after one month aging.

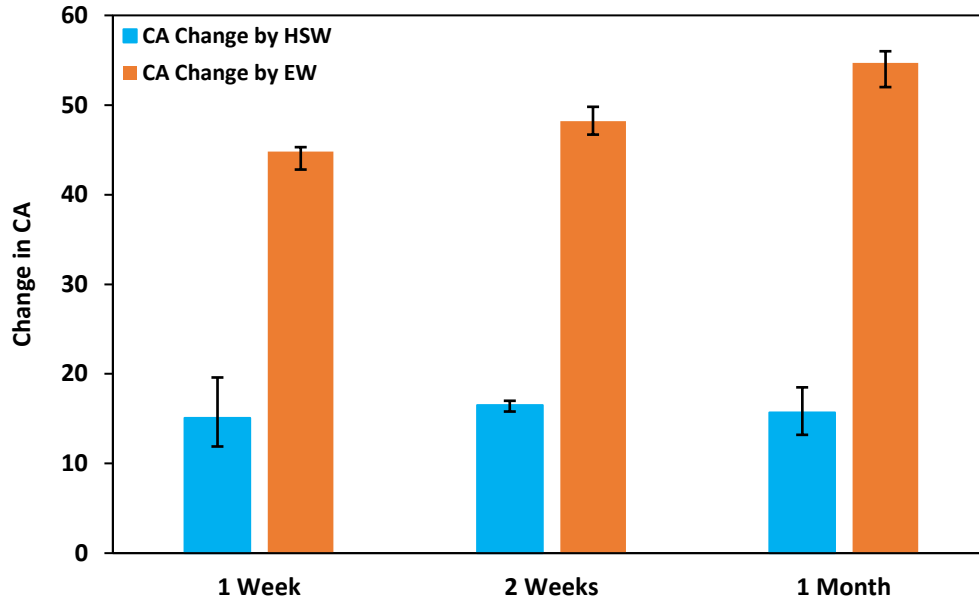


Figure 48. Comparison of CA change by HSW and EW at different aging times.

The change in contact angle by EW was more in case of 2 weeks and 1-month aged pellets. The oil-wet conditions seem to be more favorable for EW to perform its action of wettability alteration as it is easier to detach the larger number of oil components adhered to the surface by disturbing the initial equilibrium state of the surface. HSW was not much efficient in altering the rock wettability in comparison to EW. It can be related to a high concentration of monovalent and divalent ions present in HSW hindering the oil desorption from the calcite surface. On average, the EW reduced the contact angle by 40-55 degrees, making the rock less oil wet. The efficiency of engineered water in altering rock wettability was around 70% higher than high salinity water, making it a profitable choice for oil-wet carbonate rocks. The positive and negative error bars on the Figure 48 indicate the highest and lowest CA change for three repeated measurements on the same pellet.

3.3.3 *Effect of Temperature on Wettability Alteration by EW*

At this stage, the effect of temperature on EW extent of wettability modification was also evaluated by keeping one pellet from each set at 80 °C. The effect of temperature on EW performance is graphically elaborated in Figure 49. It shows the high temperature conditions were more effective in changing the CA towards water wet conditions compared to ambient conditions. After one week of aging, the EW at 80 °C reduced the CA by 60° while EW at room temperature was able to drop the CA by 44°, almost 27% less efficient compared to high temperature conditions.

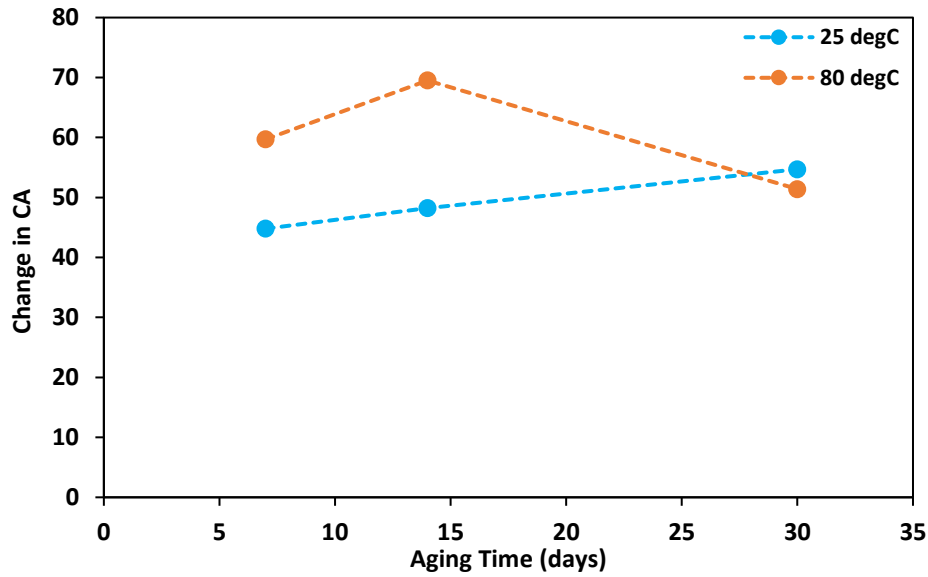


Figure 49. Effect of temperature on CA change by EW at different aging times.

This trend can be credited to increased activity of PDIs, particularly SO_4^{2-} in EW at elevated temperature, as it becomes easier for these ions to substitute carboxylic oil components from the rock surface because Mg^{2+} ions have higher affinity for SO_4^{2-} and can displace Ca^{2+} ions under these conditions [193]. Another contributor to this higher wettability change is the higher calcite dissolution because the rate of mineral dissolution reactions also increases with temperature [218, 219]. However, after one month of aging in crude oil, the change in wettability at high temperature was not as effective as at room temperature. This could be due to a stronger adhesion force between crude oil and carbonate surface after being exposed to oil for one month at 80 °C. In this case, it was difficult for EW to dislodge the oil components and hence the wettability shift was relatively smaller.

3.3.4 Effect of Polymer on EW Performance

To check if polymer has any effect on EW capability to alter rock wettability, one pellet was placed in EWP solution while another pellet was placed in EW only and the CAs were measured and compared after one week. The results, as presented in Figure 50, show that F5115 had no negative impact on EW performance, because the change in CA by EW and EWP was almost same for both the pellets. EW reduced the CA by 30° while EWP reduced it by 28°. It can be said that this CA change was caused by EW, not by the polymer. Al Sofi et al. [158] also measured CAs for LSW and LSP and concluded that polymer had no adverse influence on CA. Hence, the hybrid EWPF approach improves the EOR efficiency of each standalone method, without deteriorating the functionality of individual components involved in the process.

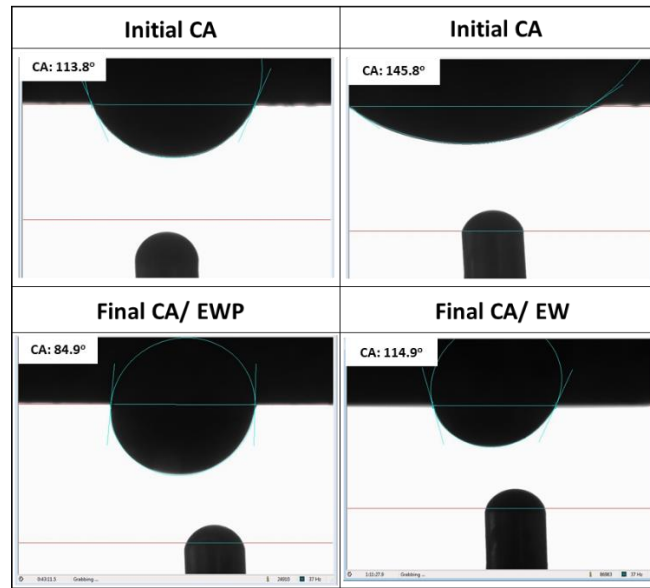


Figure 50. Effect of polymer F5115 on EW wettability alteration extent.

3.4 Polymer Concentration Determination for Coreflood Experiments

Since the viscosity of crude oil to be used in coreflood experiments was 10.8 cp at 80 °C, hence, HPAM F5115 polymer concentration (C_p) was selected based on required viscosity to keep the mobility ratio below 1. This was achieved by conducting shear viscosity measurements at three different polymer concentrations of 500, 1500, and 2000 ppm. The 1500 ppm EWP solution resulted in the target viscosity of 14 cp at 80 °C at the shear rate of 10 s^{-1} , as shown in Figure 51. The shear rate of 10 s^{-1} is chosen as it represents the typical field shear rates. Hence, the optimum polymer concentration for oil displacement tests was chosen as 1500 ppm based on rheological experiments.

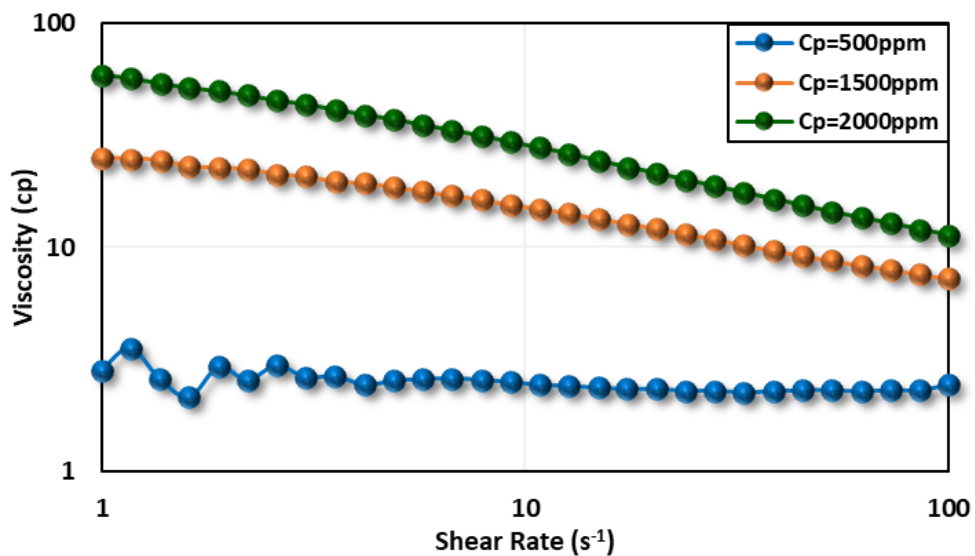


Figure 51. Polymer concentration selection for coreflood experiments.

3.5 Results of Coreflood Experiments

The first step in this phase was to establish S_{wi} in each core sample by flooding the core with crude oil and recording the volume of produced water as shown in Figure 52. The next step was to age the samples at 80 °C to restore initial wettability state.

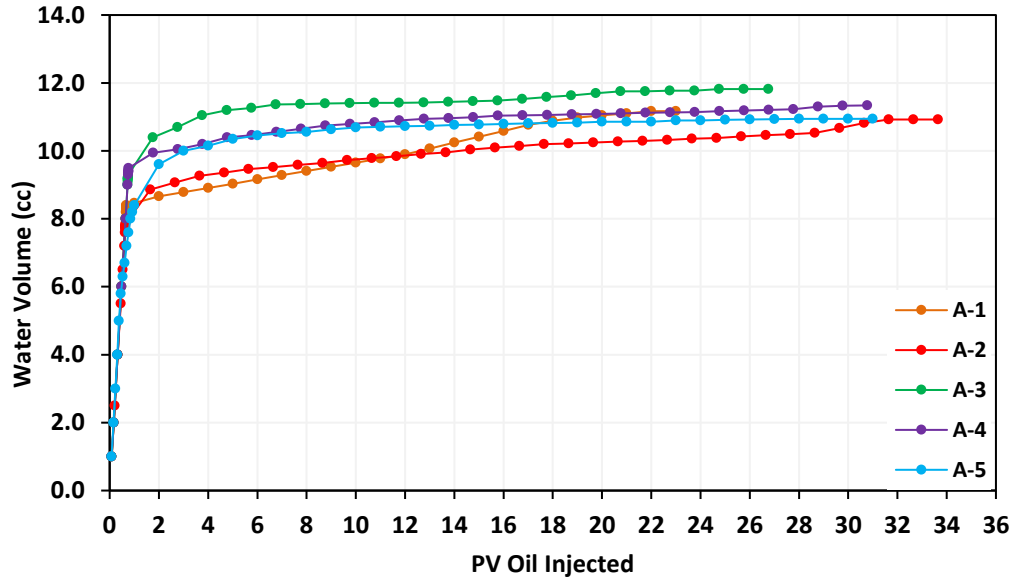


Figure 52. Water production as a function of oil injection for all core samples.

Table 16 shows the S_{wi} values obtained for all the core samples. The coreflood experiments were then performed to evaluate the incremental recovery by different hybrid versions of EWF/cEOR methods. The results of each experiment are discussed in this section.

Table 16. Initial water saturation for core samples.

Sample ID	S_{wi} (%)
A-1	21
A-2	16
A-3	22
A-4	21
A-5	13
A-6	16

3.5.1 Hybrid EW/Polymer Flooding in Water-wet System (Experiment-1)

The oil displacement tests were designed to study the performance of various EW/CEOR combinations. As a first step, the synergy of EW and PF was evaluated by conducting corefloods under different initial wettability states to see the favorable conditions for hybrid EW-based methods. Afterwards, the engineered water and surfactant/polymer combination was tested and finally the formulation consisting of EW/alkali/surfactant/polymer was analyzed. All

these tests were instrumental in achieving the target of this research i.e., the selection of best hybrid EW/CEOR technique. The first test was designed to evaluate the effect of EW in weak oil-wet systems. The pressure drop and oil recovery data for the entire experiment is presented in Figure 53. After establishing S_{wi} , the core was immediately flooded with HSW at 0.5 cc/min without any aging with crude oil. The injection was continued until there was no more oil production. To minimize capillary end effect, the injection rate was increased to 2 and 5 cc/min and extra oil was recovered. 35 PVs were injected in total and the HSW flooding resulted in an excellent oil recovery of 75%. Equation 10 was used to calculate the RF. These results are consistent with similar studies in the literature where HSW provided very good recoveries in water-wet or weakly oil-wet cores. The high RF by HSW can be attributed to the high moveable oil saturation in this core due to negligible tendency of the oil to wet the rock.

$$RF = \frac{V_{oi} - V_{HSW}}{V_{oi}} \quad (10)$$

The injection fluid was then switched to EW at 0.5 cc/min. No oil was produced during this stage even at 2 and 5 cc/min. Total 14 PVs of EW were injected with only 1% increase in oil recovery. This showed that EW or LSW does not give any appreciable recovery in water-wet reservoirs as there is no room for wettability modification. The similar results were observed by Zahid et al. and Skrettingland et al. [94, 145] when they injected LSW in water-wet cores.

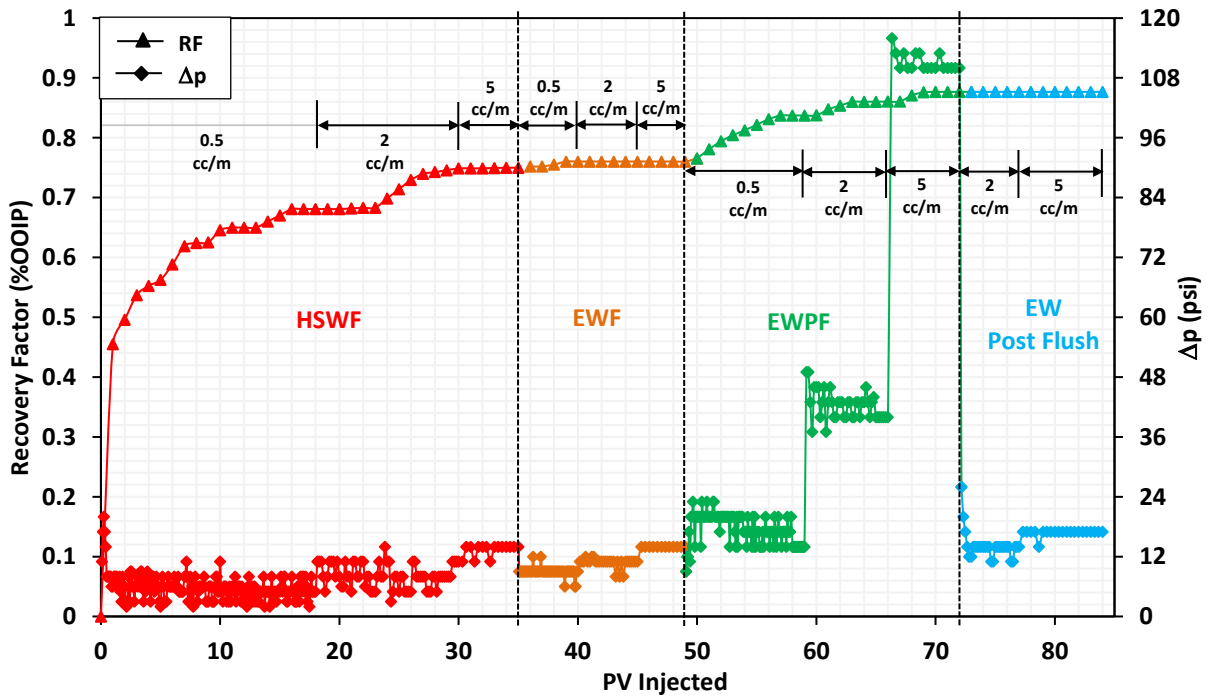


Figure 53. Oil recovery and pressure drop profile for hybrid EWPF experiment in a weak oil-wet system.

Hence, EWF is not an optimum EOR choice for such reservoirs and the initial wettability of the system must be taken into consideration during screening of a reservoir for EWF. The next injection fluid for this core was EWP and its purpose was to improve the mobility ratio and recover extra oil by increasing viscous forces. The oil breakthrough was observed during injection of first PV at 0.5 cc/min, indicating the effectiveness of designed EWP solution in mobilizing the otherwise inaccessible oil volume. The polymer flooding successfully recovered additional 12% of OOIP after injecting 23 PVs. The injection was stopped when there was no more oil production at 5 cc/min. EWPF produced 49% of remaining oil in core after HSW injection. The better performance of polymer in this experiment was due to increased stability and reduced adsorption in presence of EW spiked with SO_4^{2-} ions. The effluents recovered during this stage were collected for viscosity measurement, polymer degradation was estimated using Equation 11 and was around 20-30%. The pressure drop data was used to calculate resistance factor by Equation 12 and was found to be 8.

$$\text{Polymer Degradation} = \frac{\mu_o - \mu_{effluent}}{\mu_o} \times 100 \quad (11)$$

$$\text{Resistance Factor} = \frac{\Delta p_{EWPF}}{\Delta p_{EWF}} \quad (12)$$

The high resistance factor can be attributed to high effective polymer viscosity during flow through porous media and subsequent adsorption on the carbonate surface, causing elevated pressure drop during EWPF [220]. Also, the resistance factor was found to be increasing with injection rate. The pressure drop and resistance factor trends of EWPF indicated a shear-thickening behavior of polymer during flow through the porous media. This behavior is exhibited by HPAM polymers above a particular shear rate also known as critical shear rate or on-set of shear thickening [55, 221]. A reduction in S_{or} has also been reported in literature by HPAM polymers possessing such elastic properties [26, 44]. Finally, an engineered water post-flush was performed to calculate the residual resistance factor (RRF) after EWPF using Equation 13. The value of RRF was around 1.3 for this experiment and observed to be gradually decreasing with increasing injection rate. This can be related to the release of mechanically entrapped polymer during EW postflush, making the EW flow easier at higher rates [222].

$$\text{Residual Resistance Factor} = \frac{\Delta p_{EW-Postflush}}{\Delta p_{EWF}} \quad (13)$$

3.5.2 Hybrid EW/Polymer Flooding in Intermediate Oil-wet System (Experiment-2)

This experiment was part of the test series designed to study the effect of initial wettability on hybrid EWPF performance. For the second test, the core sample was aged for two weeks at 80 °C after establishing S_{wi} . Figure 54 shows the recovery and pressure drop profile for the entire test. Oil flooding was initially carried out in the aged sample to ensure the core was at S_{wi} . HSW injection was then initiated at 0.5 cc/min and early water breakthrough was observed after injecting only 0.2 PV of HSW (after 5 min of HSW injection). The oil production continued till 13 PVs and then the oil cut was less than 0.1%. Injection rate was increased to 2 and 5 cc/min to produce additional oil and reduce capillary end effect. The RF at the end of HSWF was around 50% of OOIP, relatively lower compared to Experiment-1.

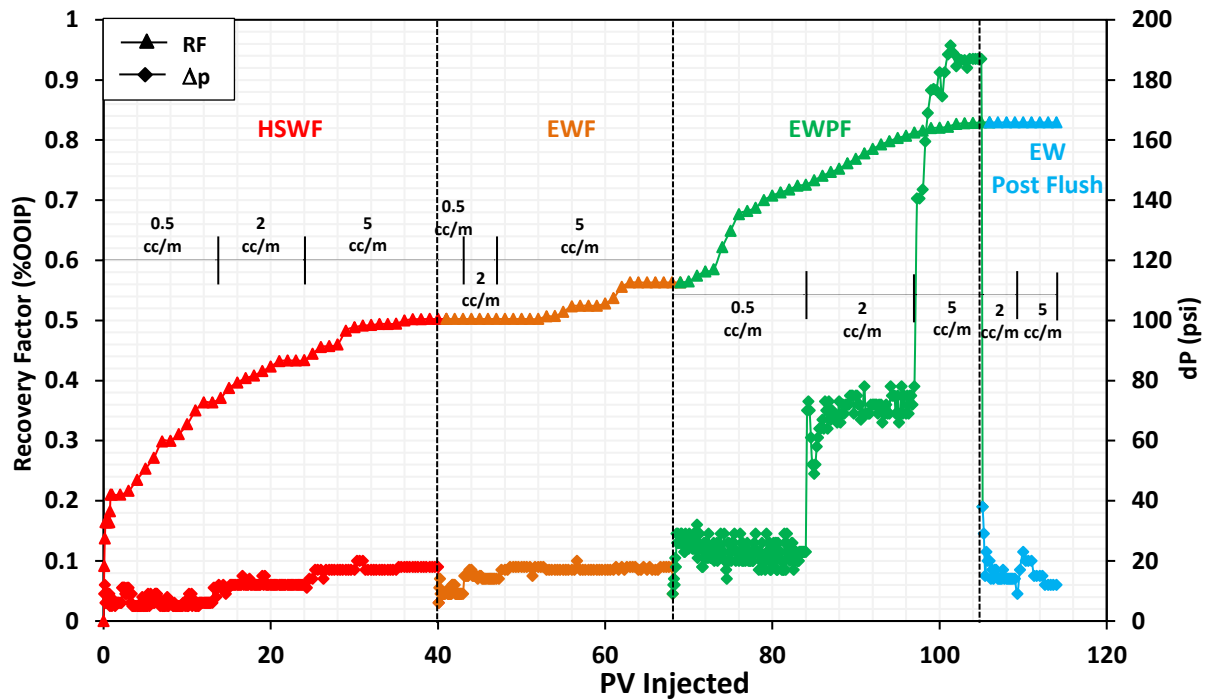


Figure 54. Oil recovery and pressure drop profile for hybrid EWPF test in an intermediate oil-wet system.

The reason for a lower RF was the intermediate-wet nature of the rock due to which a layer of oil was adsorbed on the surface and could not be displaced by HSW. The viscosity of oil was another factor responsible for a low RF. The viscosity of CSW is 0.5 cp at 80 °C, resulting in a viscosity ratio of 21.6. A high viscosity ratio resulted in poor volumetric sweep and early breakthrough of water. The injection fluid was then replaced with EW and flooding was continued at 0.5 and 2 cc/min but no oil was produced. This is because EW needs some time to disturb the oil/rock equilibrium and detach the oil from the surface. Additionally, the desorbed oil volume cannot move until a critical oil saturation is achieved, making an oil bank which is then displaced by EW. That is the reason that there was no oil production for first 14 PVs of

EW injected. The oil breakthrough occurred at 15 PV and additional 6% OOIP oil was recovered by EWF. Clearly, this oil production was due to engineered water wettability alteration mechanism because the viscous forces were insufficient to produce any oil as the viscosity ratio in this case was even higher than HSW case. The EWF stage reduced the S_{or} by 6% and produced 12% of ROIC.

In the next stage, EWPF was started at 0.5 cc/min and the oil production started during injection of third PV of EWP solution. The pressure drop was considerably increased during this stage indicating high viscous forces and formation of oil bank by injected polymer solution. Cumulative 37 PVs were injected and EWPF effectively recovered 27% of OOIP. The S_{or} was further reduced by 27% at the end of this stage. The recovery of remaining oil by EWPF in this experiment was 12% higher compared to Experiment-1, indicating the better performance of this hybrid method in intermediate-wet conditions. The EW postflush was conducted at the end of the test. The resistance factor and residual resistance factor were estimated using Equation 3.3 and 3.4 and were found to be 10 and 1.7, respectively. The relationship of these factors with injection rate was same as observed in Experiment-1. Overall, the hybrid EWPF method showed better results in intermediate oil-wet state compared to weak oil-wet conditions.

3.5.3 Hybrid EW/Polymer Flooding in Strongly Oil-Wet Condition (Experiment-3)

In the third experiment, the synergy of engineered water and polymer in a strong oil-wet medium was assessed. Figure 55 shows the recovery factor (RF) and pressure drop profile for the entire experiment. The aged carbonate core was first flooded with crude oil to ensure the core was at S_{wi} . The high salinity CSW was then injected to obtain the recovery by waterflooding and to reach residual oil saturation (S_{orw}). Total 34 pore volumes (PV) were injected and the RF after HSW flooding was around 51%. The reason for a low RF by conventional WF is the strong oil-wet nature of the carbonate rock. A considerable fraction of oil became adsorbed onto the rock surface and could not be mobilized by HSW.

As in Experiment-2, an early water breakthrough was observed after 7.3 min of HSW injection (at 0.3 PV). The HSW performance observed in intermediate and strong oil-wet conditions was quite different than that in water-wet condition (Figure 56). In intermediate oil-wet case, small amount of oil was continuously produced for a longer period. The recovery factor after first PV was highest for water-wet case and lowest for the intermediate oil-wet case. That was another reason of higher incremental recovery by EWPF in intermediate oil-wet core as HSW could not produce reasonable oil volume, leaving a higher residual oil saturation in the core.

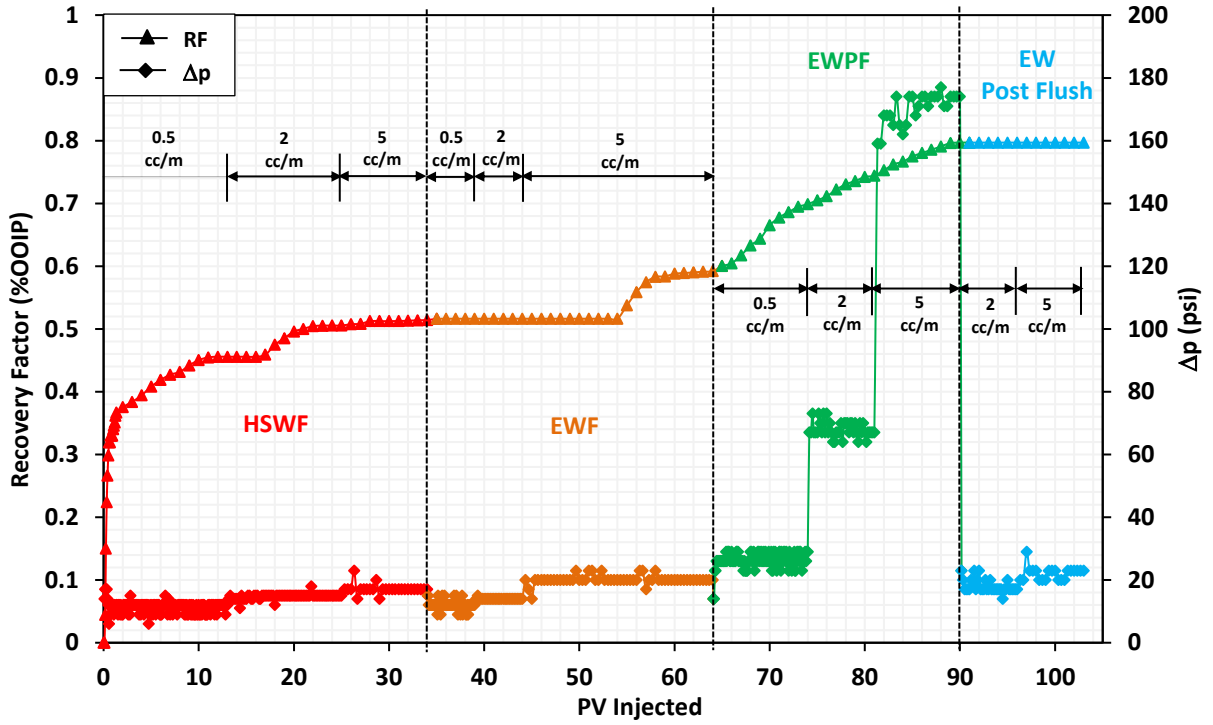


Figure 55. Oil recovery and pressure drop profile for hybrid EWPF in strong oil-wet medium.

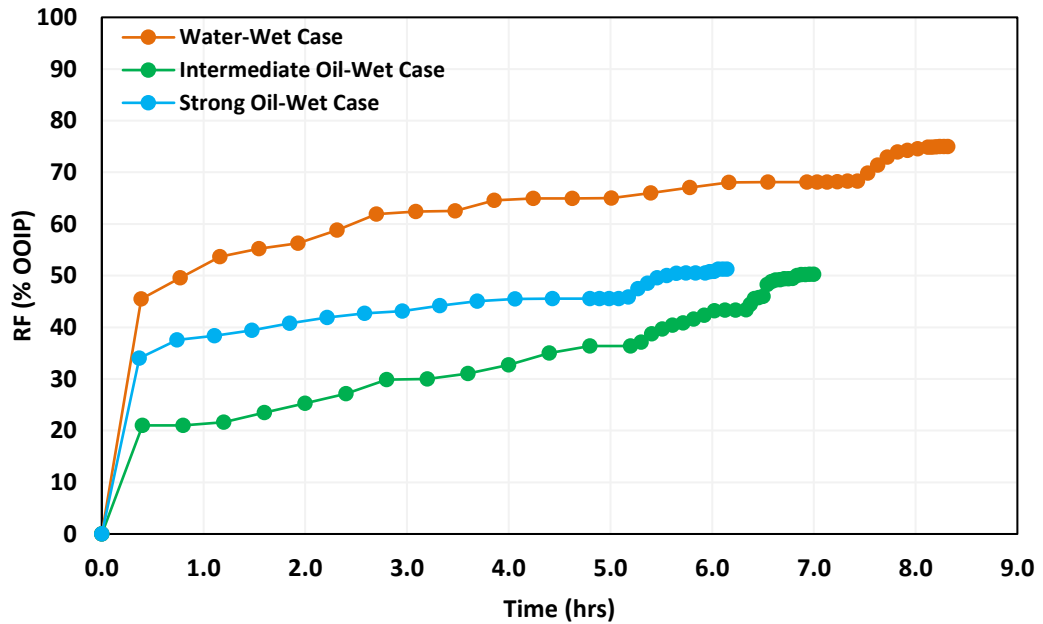


Figure 56. Effect of initial wettability on oil recovery by HSWF.

The injection fluid was then switched to EW and no oil was recovered at 0.5 and 2 cc/min. This is because EW required some time to perform its wettability modification action. The oil breakthrough occurred at 21 PV and additional 8% OOIP oil was recovered by EWF. EW successfully recovered 16% of remaining oil in core after WF, reducing the S_{or} by 7%. These

results are consistent with similar studies in the literature where EW recovered additional oil in strong oil-wet carbonate formations [94, 96].

After EWF, the core was flooded with EWP solution and the oil production started during injection of first PV at 0.5 cc/min. EWP was able to recover maximum oil which could not be displaced by HSW and EW due to adverse mobility ratio. At the end of EWPF, 20% OOIP incremental oil was recovered and the S_{or} was further reduced to 20%. The very good oil recovery by EWPF can be attributed to favorable viscosity ratio of 0.7, improving the macroscopic sweep efficiency. Furthermore, the residual oil bank formed by EW in the previous step was successfully displaced by viscous polymer flood. The pressure drop across the core sample was also considerably increased which was another indication of high viscous forces during EWPF. The test was concluded with an EW postflush to estimate RRF. The resistance factor and residual resistance factor for this experiment were around 8 and 1.3 respectively and followed the similar trend as in Experiment-1 and 2.

3.5.4 Hybrid EW-Surfactant Polymer Flooding (Experiment-4)

This coreflood experiment was designed to evaluate the performance of combined SP flooding in presence of EW. The results of this coreflood were compared with other hybrid combinations. The core was aged with crude oil for one month. In the first step, HSW was injected to achieve residual oil saturation after WF (S_{orw}). The oil recovery and pressure drop profile for this experiment are presented in Figure 57. HSWF resulted in oil recovery of ~ 64% OOIP. A significant amount of oil was still left in the core because of unfavorable mobility ratio and oil-wetting nature of the rock. EW was then injected continuously for almost 29 PV to promote wettability alteration and recover residual oil. This stage recovered 5% OOIP, reducing the S_{or} by 5.3%. As expected, EW alone could not produce all the remaining oil because of its very low viscosity.

The core was then flooded with engineered water surfactant (EWS) solution, at the optimized design, in continuous injection mode for 28 PV. The surfactant solution effectively recovered maximum residual oil volume by reducing the IFT between oil and water. The S_{or} was dramatically reduced to only 7% at the end of EWSF. However, it was quite challenging to estimate the oil recovery of this step as the produced oil was strongly emulsified in surfactant solution. The effluents were placed in the oven to promote separation of oil from aqueous solution and the visible oil volume was noted to estimate recovery by EWSF, which was around 19% of OOIP. In terms of remaining oil in core, the EWSF successfully recovered 63% of it.

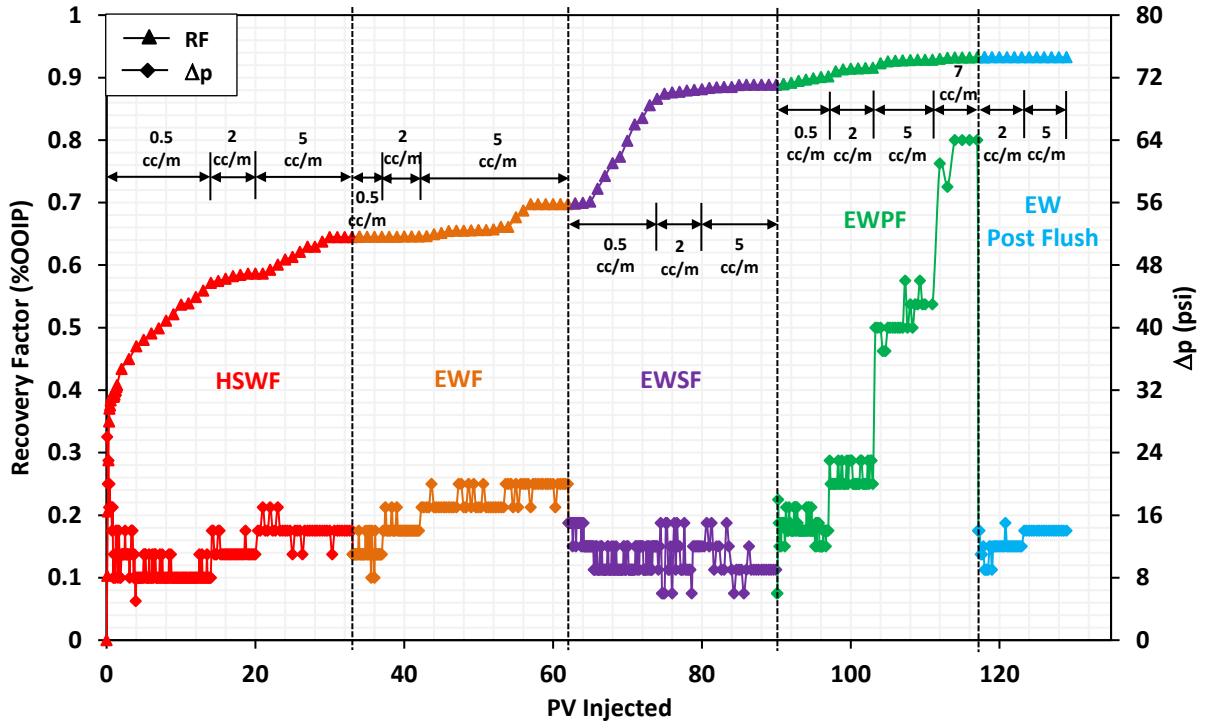


Figure 57. Oil recovery and pressure drop profile for hybrid EWSPF experiment.

The EWP solution was then injected continuously for 27 PV to produce any moveable oil by providing favorable mobility ratio. Very little amount of oil was produced during this stage and the pressure drop trend of EWPF was also quite different compared to the previous experiment. The injection rate was increased to 7 cc/min to overcome capillary end effects, but only 4% OOIP was recovered, and pressure drop was relatively lower than that expected by EWPF. The possible reason was that the S_{or} at the end of EWSF was already very low and there was not enough oil volume for polymer front to displace. The experiment was finally terminated by injecting an EW post flush for calculation of RRF of polymer flooding for this experiment. The resistance factor and RRF were 4 and 1.1 respectively, relatively lower than rest of the tests and possibly due to a low S_{or} at the start of PF stage. The incremental recovery factor by hybrid EWSPF was 81% of remaining oil in core (ROIC), 23% higher than that of hybrid EWPF case (Experiment-3). The only drawback of this hybrid method was the tough emulsions produced by EWSF. Precipitation of surfactant was also observed in the effluents during surfactant injection.

3.5.5 Hybrid EW-ASP Flooding - Continuous Injection (Experiment-5)

In the fifth experiment, a combination of EW and EOR chemicals i.e., alkali, surfactant, and polymer was studied to assess the potential of hybrid EW/ASP flooding and to compare its results with hybrid EWSPF (Experiment-4) and EWPF (Experiment-3). The pressure drop and

oil recovery data for the whole test is presented in Figure 58. The experiment was started with oil flooding in the aged core sample to ensure the core was at S_{wi} . High salinity CSW was then injected continuously for 9 PVs at 0.5 cc/min. The injection rate was increased to 2 and 5 cc/min to minimize capillary end effect. Total 24 PVs were injected and the HSW recovered 61% OOIP. During this stage, the small amount of oil produced continuously, reflecting the typical production profile of an oil-wet reservoir [223, 224]. The injection fluid was then changed to EW at 0.5 cc/min but no oil was produced. Similar to former experiments, the oil breakthrough by EW occurred after some time when the injection rate was 5 cc/min. An appreciable incremental oil recovery of 8.3% of OOIP was obtained by EWF after injecting 23 PVs and the S_{or} was also reduced by 8% at the end of this stage.

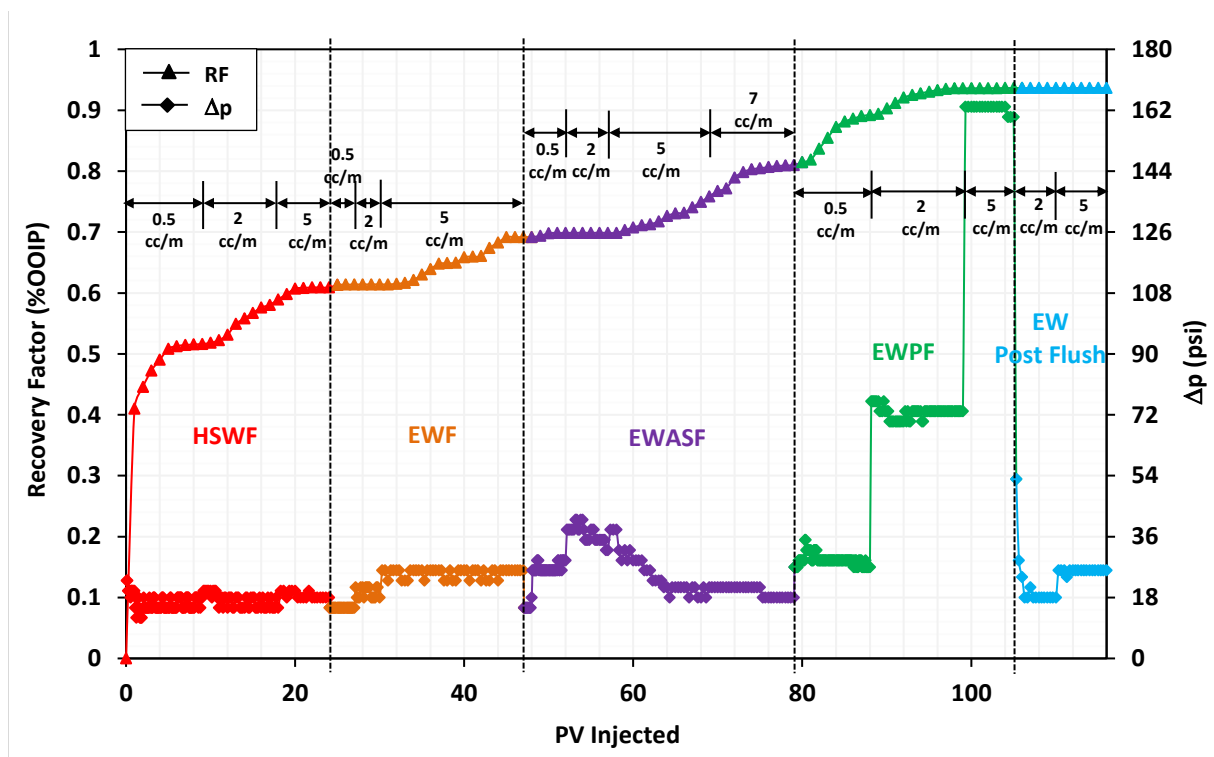


Figure 58. Oil recovery and pressure drop profile for hybrid EWASP experiment in continuous injection mode.

In the next stage, an alkali-surfactant (AS) solution was continuously injected for almost 32 PVs. The oil production started during 12th PV, showing the AS formulation required some time in achieving IFT reduction and residual oil mobilization. Appreciable incremental oil recovery of 12% OOIP was obtained and S_{or} at the end of AS flooding was only 19%. The pressure drop was relatively higher during first couple of PVs of AS injection due to formation of microemulsion by injected and in-situ generated surfactant. However, the same drawback of tough emulsions was also present in this case and it was a bit difficult to estimate the oil

recovery during AS injection. Furthermore, some alkali-surfactant precipitates were also visible in the effluents recovered, indicating chemical degradation during flow through porous media. Once there was no more oil production by AS flooding even at 5 cc/min, the injection of EWP solution was initiated at 0.5 cc/min. The incremental recovery was considerably higher during this stage as some moveable residual oil volume generated by AS flooding could not be displaced due to unfavorable mobility ratio and was available to be produced by EWPF. The total RF after injection of 26 PVs of EWP solution was 94% of OOIP, 13% additional recovery by EWPF. The S_{or} at the end of the EWPF was 6.4%. The test was terminated after injecting EW postflush for estimation of RRF. The hybrid ASP flooding in continuous injection mode resulted 4% higher incremental oil recovery compared to hybrid EWSPF. The resistance factor and RRF for this test were around 8 and 1.2, respectively.

3.5.6 Hybrid EW-ASP Flooding - Slug Injection (Experiment-6)

The last experiment performed in this research study was a combination of EW and EOR chemicals i.e., alkali, surfactant, and polymer. The objectives of this test were to assess the EOR potential of hybrid EW/ASP flooding, effect of ASP slug injection, and comparison of this test with hybrid EWASP flooding in continuous injection mode (Experiment-5). Figure 59 shows the RF and pressure drop results obtained for this case. The flooding started with injection of HSW until there was no oil production at the outlet. Almost 31 PV were injected in total and 59% of OOIP was recovered by HSWF. The S_{or} at this point was around 41%. The EWF was then initiated and continued till 18 PV. Like previous experiments, the EWF started to mobilize released oil volume after a certain period and helped to recover additional 9% of OOIP (21% of ROIC). The pressure drop during EWF was slightly higher than the pressure drop observed in HSWF, indicating the formation of moveable oil bank in-situ by wettability change. The effluents recovered also got slightly turbid just before the oil breakthrough, showing some mineral dissolution mechanism was also there.

Having reached S_{or} after EWF, a 0.7 PV slug of engineered water-1 wt% surfactant-1 wt% alkali-500ppm polymer (EWASP-slug) was injected into the core and a soaking time of 6 hours was given for the ASP slug to contact the residual oil, reduce IFT and alter rock wettability. After 6 hours soaking period, the core was flooded with 1500 ppm EWP solution and an excellent oil recovery was obtained during this stage. The EWPF successfully recovered the residual oil bank created by ASP slug. A high pressure drop during EWPF depicted the better performance of polymer in this design.

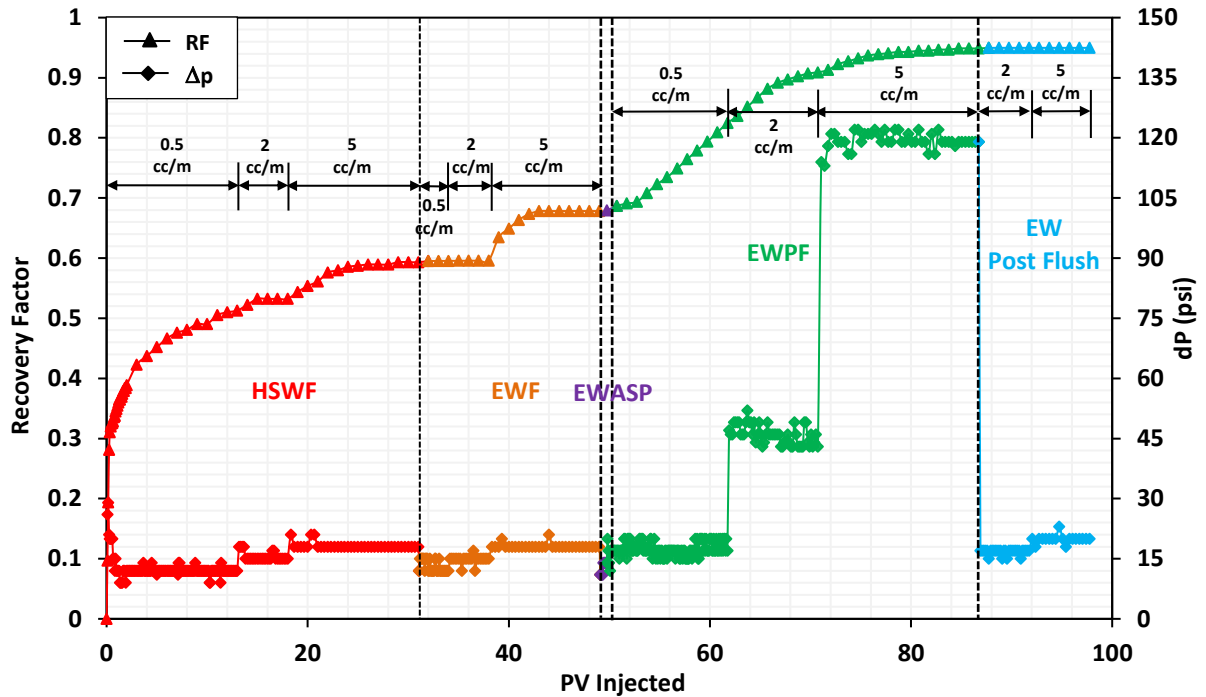


Figure 59. Oil recovery and pressure drop profile for hybrid EWASP slug-wise injection mode.

The total incremental oil recovered during this stage was around 27% of OOIP (84% ROIC). It is worth mentioning here that this incremental recovery included the combined effect of alkali, surfactant, and polymer. Alkali and surfactant helped in reducing oil-water IFT by the action of injected and in-situ surfactant, alkali promoted stability of both surfactant and polymer and finally EWPF efficiently displaced the mobilized residual oil by providing a favorable mobility ratio. A schematic representation of EWASP EOR mechanisms is presented in Figure 60.

Another benefit of this hybrid method was that the incremental produced oil was easily separated from the aqueous solution by density difference. There was no tough emulsion produced as only a small slug of ASP was injected in this case. The S_{or} was only 5% at the end of EWPF, showing promising results of this hybrid formulation. The EW post flush was conducted at the end to estimate polymer RRF and assess the performance of EWPF. The resistance factor and residual resistance factor were found to be 7 and 1.1, respectively. The polymer degradation for Experiment-1 and 2 was around 30-40%, as estimated by Equation 11. However, for tests conducted in strong oil-wet cores, the degradation was 50-60%. The higher degradation factor in strong oil-wet medium can be due to oxidation reactions between polymer carboxylate ions and crude oil acidic components, causing additional viscosity loss. Despite a high viscosity loss, the HPAM polymer resulted in excellent recovery of remaining oil in all the tests. The slug-wise EWASP flooding provided 4% additional oil recovery compared to continuous ASP flooding (Experiment-5) and required lesser amount of chemicals (alkali and

surfactant), making it an optimum hybrid combination of EW and EOR chemicals. Overall, the hybrid EW/ASP tests resulted in the highest reduction in S_{or} and maximum incremental oil recovery. The higher recoveries in Experiment-5 and 6 were partly due to enhanced polymer viscous and viscoelastic behavior in an already created alkaline environment during AS/ASP-slugs injection. The pH of AS and ASP solution was ~ 9 which is within the optimum pH range for F5115 polymer to have maximum viscoelastic properties, as already discussed in Sections 3.1 and 3.2. Hence, the combined action of engineered water, alkali, surfactant and polymer resulted in the best performance of this hybrid formulation.

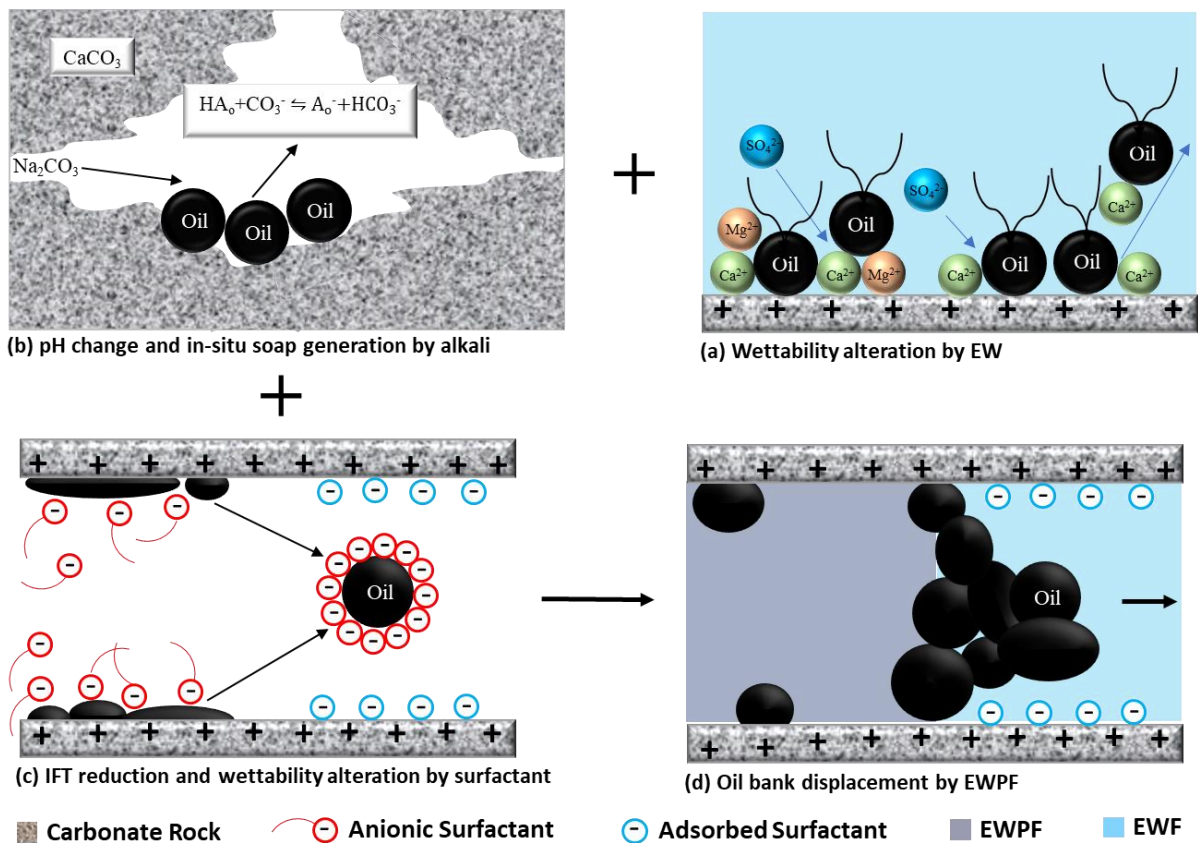


Figure 60. Mechanisms involved in incremental oil recovery by hybrid EWASP flooding.

3.6 Effect of Initial Wettability on EWF and Hybrid EWPF Performance

The analysis of the first three coreflood tests shows that for water-wet systems, the HSW combined with PF can result in a comparable oil recovery as with EWPF, thus hybrid EWPF may not be an optimum choice for such systems. However, in medium to strong oil-wet reservoirs, the S_{or} after HSW flooding is quite high and EWF and EWPF provides very good incremental recoveries under these conditions. The incremental recovery factors for the three

EWPF experiments having different initial rock wettability are given in Table 17. The results clearly indicate that engineered water can recover the residual oil only in intermediate to strong oil-wet reservoirs. The synergetic behavior of EW and PF is also pronounced under these conditions, particularly in intermediate oil-wet case. This can be explained by EW ability to change contact angle between oil and carbonate surface. In case of very weak oil-wet rock, maximum moveable oil is already produced by HSWF, and EWF cannot recover residual oil by wettability change as the rock already has affinity for water. Thus, all the incremental oil produced by EWPF is due to the improved fractional flow and increased viscous forces by polymer. When EW comes into contact with an intermediate oil-wet surface, it becomes easier for EW to detach the carboxylic oil material as the affinity of oil towards the rock surface is not too strong. As a result, a higher residual oil saturation is present that can be easily displaced by subsequent EWP front. For this reason, a higher incremental recovery is obtained by EWPF in the intermediate oil-wet scenario.

Table 17. Summary of oil recoveries by hybrid EWPF under different initial wettability conditions.

<i>Process</i>		<i>HSW</i>	<i>EW</i>	<i>EWPF</i>	<i>Total</i>
<i>EWPF (Weak Oil-Wet Case)</i>	RF (%OOIP)	75	76	88	-
	Inc. RF	-	1	12	13
	RF (%ROIC)	75	4	49	-
<i>EWPF (Intermediate Oil-Wet Case)</i>	RF (%OOIP)	50	56	83	
	Inc. RF	-	6	27	33
	RF (%ROIC)	50	12	61	
<i>EWPF (Strong Oil-Wet Case)</i>	RF (%OOIP)	51	59	80	
	Inc. RF	-	8	20	28
	RF (%ROIC)	51	16	50	

The comparison of incremental oil recoveries as a function of extent of oil-wetting nature of the rock is presented in Figure 61. It can be said that EW performed best in strong oil-wet conditions while the hybrid EWPF scenario showed best results in the intermediate oil-wet state. Hence, the optimum wettability state for hybrid EOR methods utilizing EW is intermediate to strong oil-wet condition. In the third experiment, when EW encountered a strong oil-wet surface, it could not desorb as much oil as it did when the surface was moderately oil-wet. This is because the oil material was strongly clung to the rock surface and a higher

change in the surface forces was required to release the oil. Consequently, a relatively lower residual oil saturation was available for EWPf to move out of the core compared to intermediate oil-wet condition. Hence, EWF is not an optimum EOR choice for water-wet reservoirs and the initial wettability of the system must be taken into consideration during screening of a reservoir for EWF.

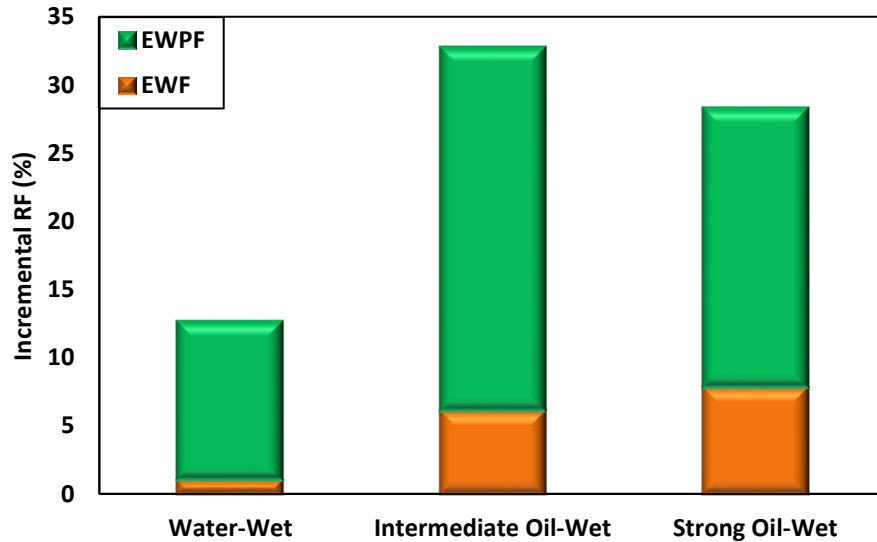


Figure 61. EW and EWPf oil recovery comparison for different wettability conditions.

The mechanism of EW in different wetting mediums is schematically represented in Figure 62. As aging time increases, the contacted surface area between crude oil and rock also increases, making it difficult to detach the oil droplet from the surface. In Figure 3.7, $L_4 > L_3 > L_2 > L_1$, indicating that best condition for hybrid EW/CEOR methods is the intermediate oil-wet condition. However, for EWF, both intermediate and strongly oil-wet conditions are favorable.

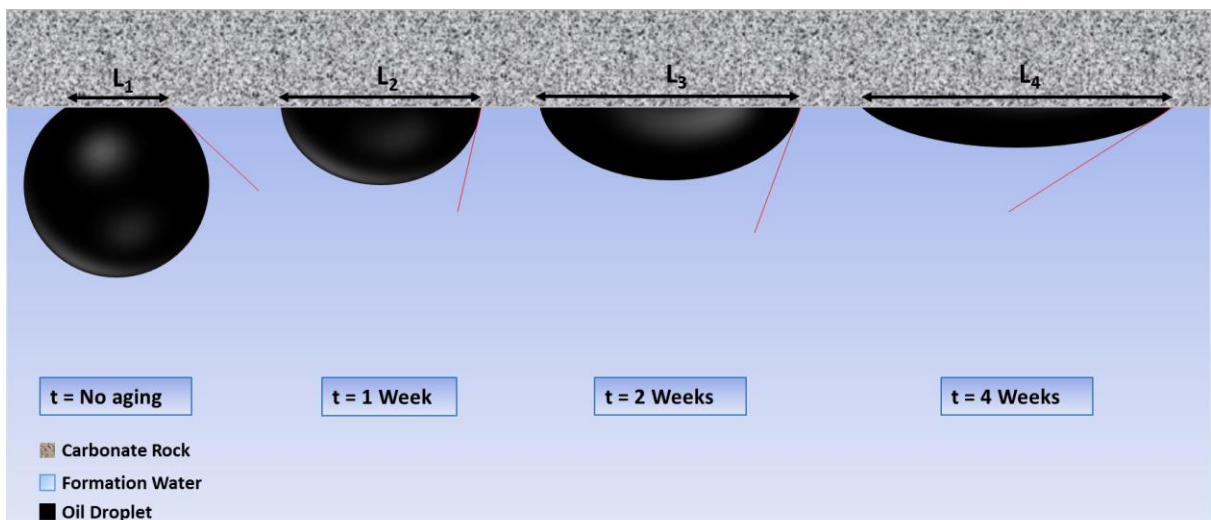


Figure 62. Effect of aging time on contact angle and rock wettability.

3.7 Comparative Analysis of Oil Recovery by Different Hybrid Methods

Table 18 summarizes the recovery factors for all four coreflood experiments performed with different EW/CEOR combinations. It is obvious from these results that hybrid EWASP method gave the highest incremental oil recovery in both continuous and slug-wise injection modes. However, the slug-wise injection seems to be economically more viable as it can reduce chemical cost and oil separation treatment cost considerably.

Table 18. Summary of oil recoveries by various hybrid EWF/CEOR combinations.

Process		HSW	EW	EWSF/EWASP	EWPF	Total
EWPF	RF (%OOIP)	51	59	-	80	-
	Inc. RF	-	8	-	20	28
	RF (%ROIC)	51	16	-	50	-
EWSPF	RF (%OOIP)	64	70	89	93	-
	Inc. RF	-	5	19	4	29
	RF (%ROIC)	64	15	63	40	-
EWASP (Continuous Injection)	RF (%OOIP)	61	69	81	94	-
	Inc. RF	-	8	12	13	33
	RF (%ROIC)	61	21	38	67	-
EWASP (Slug-wise Injection)	RF (%OOIP)	59	68	68	95	-
	Inc. RF	-	9	0.1	27	36
	RF (%ROIC)	59	21	3	84	-

The performance of each method is compared in terms of incremental oil recovery after waterflooding and the total incremental recovery by different hybrid methods for each experiment is plotted in Figure 63. This figure again shows the best performance of hybrid EWASP method, both in continuous and slug-wise injection modes.

3.7.1 Effect of Hybrid EW/CEOR Methods on S_{or} : Capillary Desaturation

Capillary desaturation is the process of recovering capillary-trapped residual oil. Generally, conventional PF is considered to affect only the macroscopic efficiency. On the other hand, conventional SF can only improve the microscopic sweep efficiency. A typical procedure for examining the microscopic sweep efficiency of any improved oil recovery (IOR) process is to construct a capillary desaturation curve (CDC) by performing corefloods at different rates.

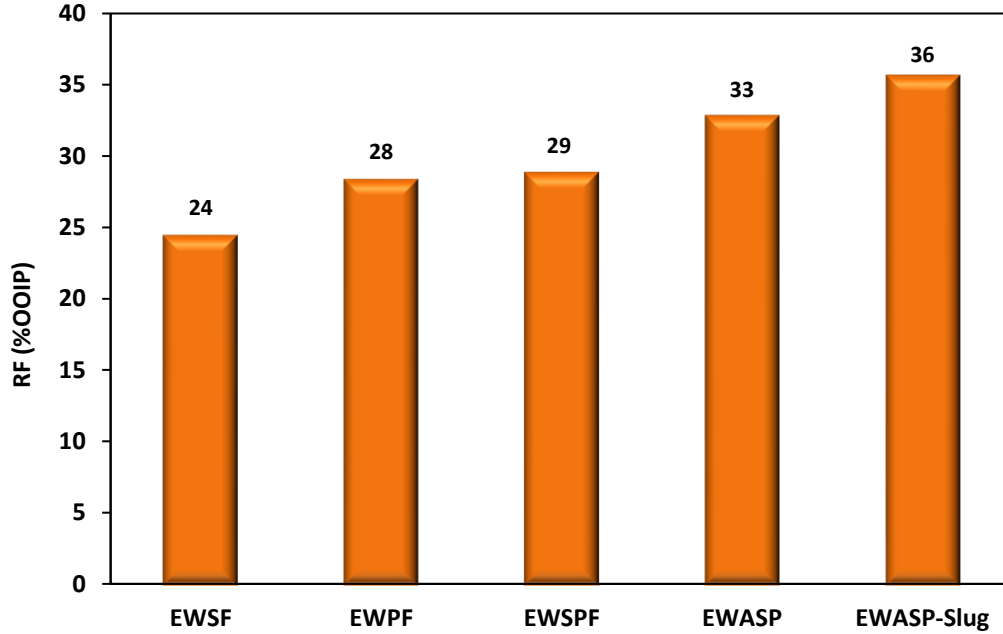


Figure 63. Oil recovery comparison for different hybrid EW/CEOR methods.

Residual oil saturation at the end of each stabilized pressure interval is plotted against the capillary number (N_c) [225, 226]. The capillary number is the ratio of viscous to capillary forces [227-232], as given in Equation 14 [233]:

$$N_c = \frac{K\Delta p}{\sigma L} \quad (14)$$

where K is absolute permeability, $\Delta p/L$ is the pressure gradient across the core and σ is the oil-water IFT. Equation 14 shows that to have an acceptable range of N_c , either the pressure gradient should be high enough or IFT should be extremely low, both of which are generally not achievable by conventional waterflooding (WF) and PF. By the CDC curve, critical N_c can be identified for the process under study. The critical N_c is usually in the range of 10^{-4} to 10^{-3} [228, 234], whereas the typical N_c obtainable by WF and PF in the field ranges from 10^{-7} to 10^{-5} [235]. Analysis of CDCs from different coreflood studies has shown that the typical field operating constraints for PF are generally not sufficient to cause any reduction in capillary-trapped residual oil [33, 236-239].

A comparison of the capillary desaturation tendency of conventional PF [54, 240, 241], SF [242-244], and ASP flooding [245, 246] with that of hybrid EWPF, EWSF, EWSPF and EWASP flooding has been made by plotting the coreflood end-points from each EOR injection stage in six experiments studied, and it is observed that hybrid EW/CEOR methods have resulted in a significant S_{or} reduction, even at smaller values of N_c (Figure 64). The three

highlighted points in Figure 64 indicate the EWPF stage of Experiment-4, 5 and 6. A significant reduction in S_{or} in these cases is due to the combined effect of alkali/surfactant/polymer, depending upon the design of each experiment. There is also a possible contribution of viscoelastic properties of polymer in achieving low S_{or} in these cases because of high pH environment created by the alkali/surfactant flooding stage. Basic conditions promote HPAM viscoelastic behavior, causing a reduction in S_{or} . Recently, it is suggested by some researchers that viscoelastic properties of polymers can cause a reduction in S_{or} by stripping the trapped oil [58, 240, 247-254]. The results of CDC comparison also show hybrid EWASP flooding in slug-wise injection mode resulted in lowest S_{or} for similar N_c values. Another interesting observation in this graph is that most of the EWF and hybrid EWPF points are below the conventional PF CDC, showing the effectiveness of these methods in reducing the remaining oil saturation with quite lower capillary numbers.

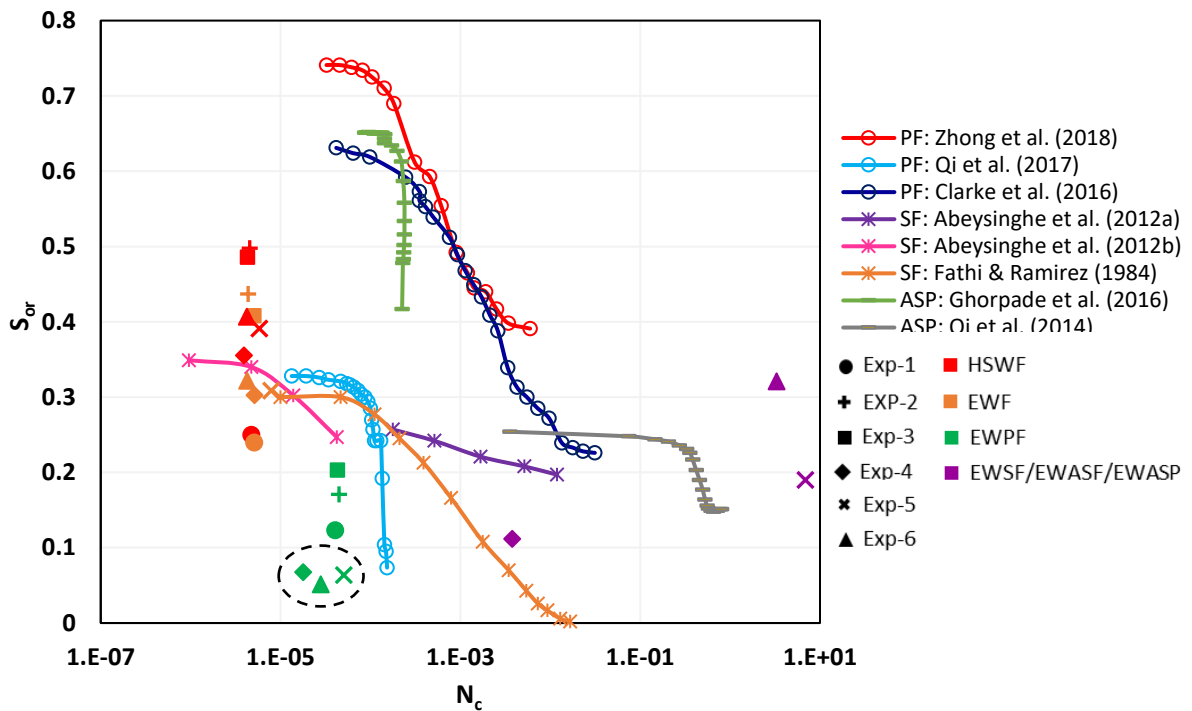


Figure 64. Comparison of capillary desaturation tendency of hybrid EW/CEOR methods with conventional ones.

Almost all the points in Figure 64 fall below conventional CDCs, indicating that S_{or} is lower than standalone methods, and the hybrid EWASP method is the most effective in recovering trapped oil. This can be attributed to synergetic effects of IFT reduction by alkali and surfactant, wettability modification by EW and efficient oil-bank displacement by polymer. For the calculation of N_c , typical IFT value of 30 dynes/cm, reported in literature [158], is used for EWF and EWPF. For surfactant and alkali/surfactant combinations, IFT obtained from phase

behavior study by my team member Samanova [214], is used which is around 0.02 and 0.000027 dynes/cm, respectively. Hence, this research study has confirmed synergy and additional oil recovery by combined low salinity/engineered water and chemicals in carbonates, especially the hybrid EWASP process, but more work is required to fully understand the recovery mechanisms driving incremental oil recovery by the hybrid process.

3.7.2 Recovery Efficiency of Different Hybrid Processes

To clearly observe the recovery efficiency of each hybrid combination studied in this research, a parameter E is defined as the ratio of viscosity and IFT for the overall process. For each hybrid method, the highest viscosity and the lowest IFT among all the fluids involved in EOR stage are used. For instance, in case of EWPF experiment, polymer viscosity and oil-water IFT is used in calculating E. Figure 65 shows a relationship between parameter E, change in S_{or} , and recovery factor in terms of ROIC for each hybrid method. It is evident from Figure 65 that higher the parameter E for an EOR process, higher will be the incremental recovery and lower will be the S_{or} by that method. Hybrid EWASP flooding in slug-wise injection resulted in highest value of E and consequently the maximum incremental oil and minimum S_{or} among all the methods. This again supports the idea of combining two or more EOR techniques and develop a design that is both technically and economically optimum for a given fluid and rock system. The results of this study show that hybrid EWASP flooding has the potential to achieve these objectives while providing some additional benefits as well e.g., lower operational and processing expenditures, reduced environmental footprint etc.

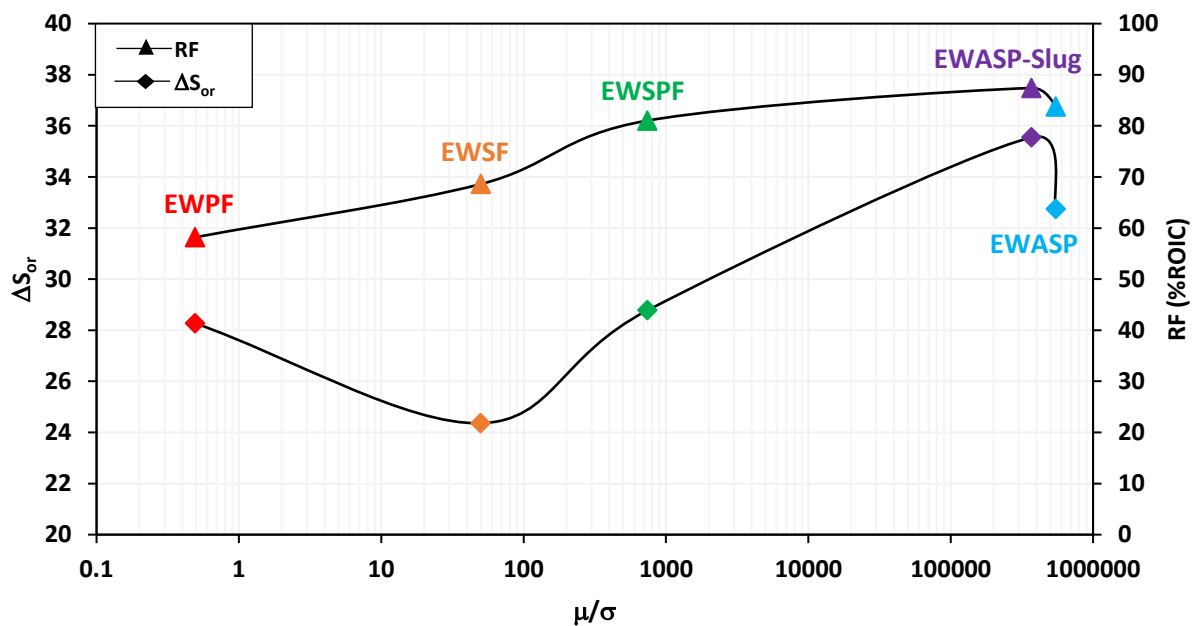


Figure 65. Recovery efficiency of different hybrid methods as a function of viscosity and IFT.

Displacement efficiency (E_d) for each hybrid method studied herein was also calculated using Equation 15. As expected, hybrid EWASP technique in slug-wise injection mode provided the maximum displacement efficiency as can be seen from Figure 66. The second-best method in terms of E_d was hybrid EWASP in continuous injection mode.

$$E_d = \frac{S_{oi} - S_{or}}{S_{oi}} \times 100 \quad (15)$$

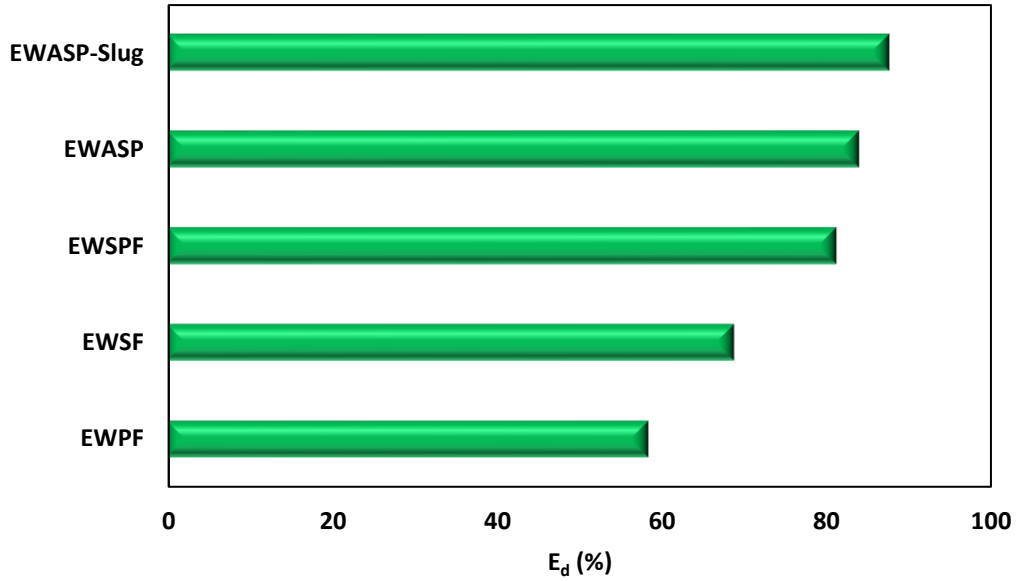


Figure 66. Comparison of displacement efficiency of different hybrid methods.

3.7.3 Calculation of Mobility Ratio for Hybrid Methods

To recover the remaining oil in the reservoir after WF, it is beneficial to design EOR methods that can provide simultaneous mobility control and recovery of capillary trapped residual oil. The capillary desaturation tendency of hybrid EW/CEOR methods has already been discussed. This section will provide some insight into the effectiveness of each method in terms of mobility control. Mobility ratio for each hybrid EOR experiment was calculated using Equation 1. The permeabilities were obtained by Darcy's law using pressure drop data for the respective coreflood. Table 19 presents the mobility ratios obtained for each hybrid combination. The high mobility ratio (26-28) during HSW flooding resulted in early breakthrough of water after injecting only 0.2-0.3 PV in all corefloods. Another reason for early water breakthrough could be the presence of high permeable streaks in carbonate rocks, providing least-resistance path for water flow [157]. The EWPF stage in each experiment successfully decreased the mobility ratio by 93-98% compared to HSWF, enhancing the volumetric sweep efficiency. The results indicate that the hybrid methods with better mobility control were able to provide higher

incremental oil recovery. Hence, mobility control and capillary desaturation are equally important for recovering the remaining oil, especially in heterogeneous carbonate formations where unfavorable mobility ratio can lead to unstable front progression and early water breakthrough.

Table 19. Mobility during HSWF and chemical flooding stages.

Experiment ID	Mobility		
	HSWF	EWSF/EWASF	EWPF
3	27.5	-	0.5
4	28.1	35.1	1.9
5	23.5	29.3	0.5
6	26.3	-	0.7

The critical relationship between mobility ratio and recovery of remaining oil is graphically presented in Figure 67. It can be clearly seen in that lower mobility ratio resulted in higher recovery of remaining oil. The data also reveals that almost similar incremental recoveries were obtained by EWPF and EWSPF, highlighting the value of both microscopic and macroscopic sweep efficiencies.

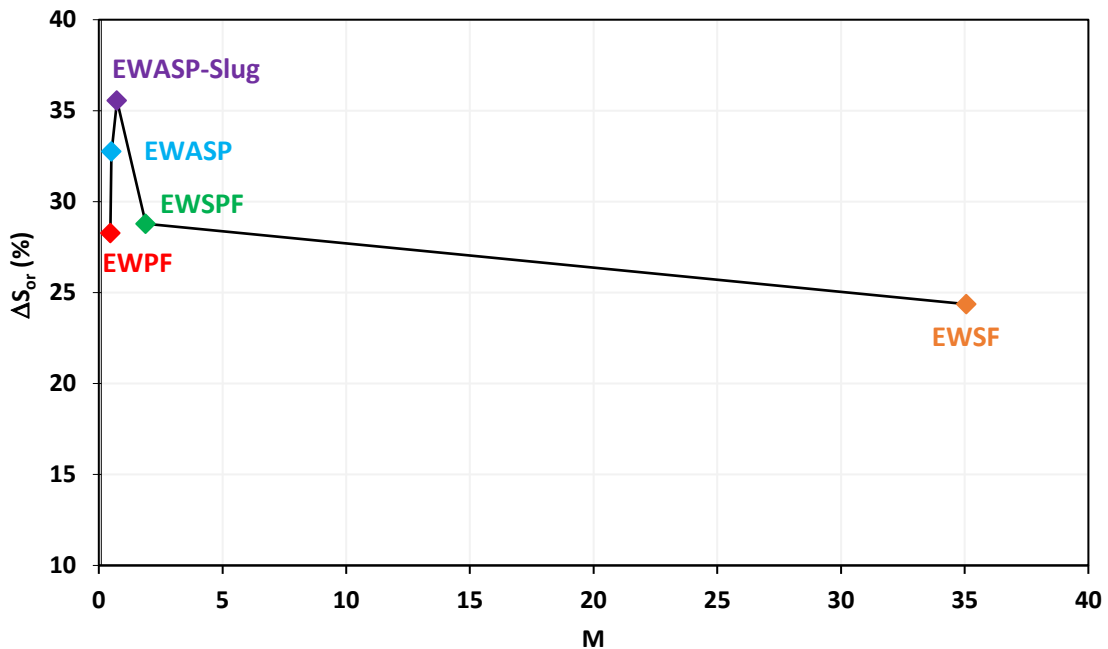


Figure 67. Relationship between mobility and recovery of remaining oil.

3.7.4 Oil Breakthrough during EWF

During the EWF stage of almost all hybrid EOR experiments, the oil breakthrough was delayed by a couple of PVs. To estimate the time required for EW to interact with the adsorbed oil

components, release them and create a moveable oil bank, the oil production by EWF was plotted against time for each experiment (Figure 68). Interestingly, the oil breakthrough in most of the experiments occurred after 1.5 to 2 hours. Hence, it can be inferred from that EW required at least 1.5-2 hours to perform its EOR function i.e., wettability alteration. However, for hybrid EWPF test in strongly oil-wet medium, the oil breakthrough occurred after 2.5 hours. The longer delay in this case could be due to strong oil-wet nature of the surface, hindering the interaction between EW and adsorbed crude oil. Since these experiments were designed to serve as a baseline for selection of best hybrid EOR method, hence slug-wise injection of EW was not studied. However, based on the results depicted in Figure 68, it can be said that a slug-wise injection of EW followed by a soaking period of 1.5-2 hours can result in similar recoveries as obtained by continuous EW injection in laboratory corefloods. This will further reduce the volume of water required and treatment cost to produce EW, making the hybrid methods more favorable for field scale applications.

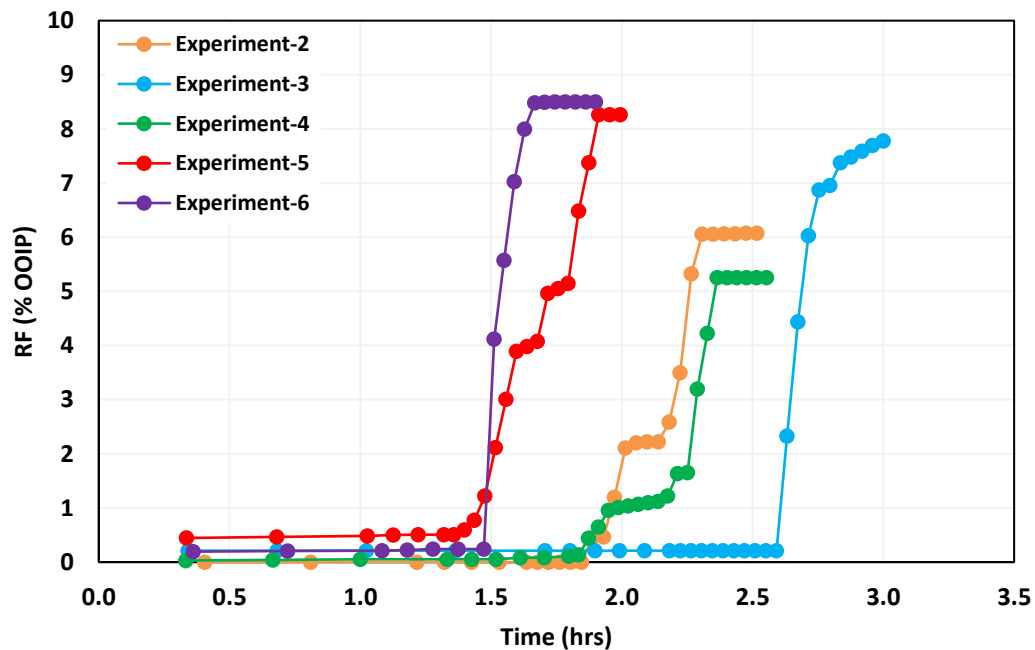


Figure 68. Oil breakthrough time during EWF stage of different tests.

4. Conclusion and Recommendations

The objectives of this research were to analyze the performance of various hybrid EW/CEOR scenarios, compare the incremental recoveries, and select the best design. The mechanisms involved in recovery of remaining oil by each method were investigated and the selection criteria for the optimum hybrid EW/CEOR design was presented.

The HPAM F5115 has shown an improved viscous and viscoelastic behavior in the presence of alkali and the optimum pH range of 7-10. The contact angle measurements show a 40-55° reduction in contact angle by engineered water in oil-wet pellets, indicating a wettability shift towards water-wet state. The change in CA by EW is further pronounced at high temperature of 80 °C. The synergy of optimized engineered water and chemical EOR methods has been proved by conducting several oil displacement experiments. All the hybrid combinations including EWSF, EWPF, EWSPF, and EWASPF have shown higher reduction in S_{or} with lower capillary numbers, compared to conventional standalone EOR methods. The EWPF tests conducted in an oil-wet medium have recovered 16-20% OOIP additional oil compared to the test performed in a water-wet system. The hybrid EWSPF scenario (Experiment-4) has caused 23% higher recovery of remaining oil after waterflooding compared to EWPF test (Experiment-3). Finally, the hybrid EWASPF in slug-wise injection mode (Experiment-6) has provided the highest incremental oil recovery of 36% OOIP, 8% higher than EWSPF (Experiment-4) and 3% higher than EWASP flooding in continuous injection mode (Experiment-5).

HPAM F5115 polymer possesses viscous as well as elastic properties and has exhibited pronounced viscoelastic behavior by increasing brine pH. For heterogeneous oil-wet carbonate formation having high S_{or} after waterflooding, the injection of viscoelastic polymers under alkaline conditions can recover residual oil in addition to mobility control and improved volumetric sweep efficiency. Hence, a properly designed polymer solution can provide multiple benefits when combined with EW and other chemicals such as alkali and surfactant.

The results of this study indicate that mobility control is as critical as IFT reduction and wettability alteration to obtain maximum oil recovery by any EOR approach. The hybrid EW/CEOR combinations including both polymer and alkali/surfactant have shown the better incremental oil recovery and lower S_{or} at the end of the test, indicating higher viscous forces and reduction in capillary force. This can be attributed to the combined actions of the constituents involved in the process such as wettability alteration by EW in a strong oil-wet medium, lower capillary forces due to IFT reduction by injected and in-situ generated

surfactant, reduced surfactant adsorption in presence of alkali, mobility control and improved fractional flow by polymer, and further reduction in S_{or} by polymer viscoelastic behavior in an alkaline environment. The hybrid EW/ASP flooding in slug-wise injection mode has showed overall best performance in terms of incremental oil recovery and chemicals consumption. Based on the coreflooding results, the best hybrid method is the EW/ASP formulation in slug-wise injection.

The different factors influencing the recovery of hybrid EW/CEOR methods have been analyzed in this research. One of the critical parameters in this regard is the initial wettability. Initial wettability of the system is an important factor to be considered for EW-based oil recovery techniques. The contact angle measurements and oil displacement tests carried out in this research study indicate that intermediate to strong oil-wet reservoirs are the best candidate for EWF and hybrid EWPF because of significant wettability shift caused by EW under these conditions. EWF does not provide any incremental recovery in water-wet or very weak oil-wet reservoirs as the recovery by waterflooding is already quite satisfactory from these reservoirs.

Reservoir temperature is another important parameter to be considered during screening stage. CA results of this study prove that high temperature carbonate formations are the best candidates for EW-based EOR techniques. Although, EW has caused a wettability shift at ambient conditions as well, however the CA change is higher at elevated temperature. This is because EW provides better results at high temperatures due to increased reactivity between PDIs and calcite surface.

Another important factor is the impact of polymer on EW wettability alteration mechanism. It is confirmed by CA measurements that polymer F5115 does not affect EW performance and has no negative role in wettability alteration. Hence, all the factors studied herein confirm the successful synergy between EW and CEOR by providing higher oil recoveries and increasing the stability of the EOR chemicals. The screening criteria for application of hybrid EW-based methods must, therefore, include the critical parameters discussed herein, including initial wettability, reservoir temperature, and compatibility between designed EW and alkali/surfactant/polymer selected for EOR application.

Based on the study outcomes, a few recommendations for future work are presented. The analysis of oil breakthrough time during EWF stage showed that at least 1.5 to 2 hours were required for EW to alter the wettability and create moveable oil saturation. Based on these results, a sensitivity study will be instrumental to assess the effect of slug-wise injection of EW

followed by some soaking time. This can further reduce the project cost by lowering the produced water treatment expenses. Similarly, the results of this research study can be utilized, and the selected hybrid EW/ASP method can be further optimized by conducting simulation study and performing sensitivity analysis on various ASP design parameters.

5. References

1. Ahmadi, A. and M. Moosavi, *Investigation of the effects of low-salinity waterflooding for improved oil recovery in carbonate reservoir cores*. Energy Sources, Part A: Recovery, Utilization, and Environmental Effects, 2018. **40**(9): p. 1035-1043.
2. Mwangi, P., P.V. Brady, M. Radonjic, and G. Thyne, *The effect of organic acids on wettability of sandstone and carbonate rocks*. Journal of Petroleum Science and Engineering, 2018. **165**: p. 428-435.
3. Chilingar, G.V. and T. Yen, *Some notes on wettability and relative permeabilities of carbonate reservoir rocks, II*. Energy Sources, 1983. **7**(1): p. 67-75.
4. Treiber, L. and W. Owens, *A laboratory evaluation of the wettability of fifty oil-producing reservoirs*. Society of petroleum engineers journal, 1972. **12**(06): p. 531-540.
5. Lee, Y., W. Lee, Y. Jang, and W. Sung, *Oil recovery by low-salinity polymer flooding in carbonate oil reservoirs*. Journal of Petroleum Science and Engineering, 2019. **181**: p. 106211.
6. Bernard, G.G. *Effect of floodwater salinity on recovery of oil from cores containing clays*. in *SPE California Regional Meeting*. 1967. Society of Petroleum Engineers.
7. Hallenbeck, L., J. Sylte, D. Ebbs, and L. Thomas, *Implementation of the Ekofisk field waterflood*. SPE Formation Evaluation, 1991. **6**(03): p. 284-290.
8. Sylte, J., L. Hallenbeck, and L. Thomas. *Ekofisk formation pilot waterflood*. in *SPE Annual Technical Conference and Exhibition*. 1988. Society of Petroleum Engineers.
9. Austad, T., S. Shariatpanahi, S. Strand, C. Black, and K. Webb, *Conditions for a low-salinity enhanced oil recovery (EOR) effect in carbonate oil reservoirs*. Energy & fuels, 2012. **26**(1): p. 569-575.
10. Rivet, S.M., *Coreflooding oil displacements with low salinity brine*. 2009, University of Texas at Austin.
11. Khaledialidusti, R. and J. Kleppe, *Significance of geochemistry in single-well chemical-tracer tests by coupling a multiphase-flow simulator to the geochemical package*. SPE Journal, 2018. **23**(04): p. 1,126-1,144.
12. Mahani, H., A.L. Keya, S. Berg, and R. Nasralla, *Electrokinetics of carbonate/brine interface in low-salinity waterflooding: Effect of brine salinity, composition, rock type, and pH on ζ -potential and a surface-complexation model*. Spe Journal, 2017. **22**(01): p. 53-68.
13. Khaledialidusti, R. and J. Kleppe, *Surface-charge alteration at the carbonate/brine interface during single-well chemical-tracer tests: surface-complexation model*. SPE Journal, 2018. **23**(06): p. 2,302-2,315.
14. Chang, H.L., *Polymer flooding technology yesterday, today, and tomorrow*. Journal of Petroleum Technology, 1978. **30**(08): p. 1,113-1,128.
15. Al-Murayri, M.T., et al. *Low-Salinity Polymer Flooding in a High-Temperature Low-Permeability Carbonate Reservoir in West Kuwait*. in *SPE Kuwait Oil & Gas Show and Conference*. 2019. Society of Petroleum Engineers.
16. Pye, D.J., *Improved secondary recovery by control of water mobility*. Journal of Petroleum technology, 1964. **16**(08): p. 911-916.
17. Sandiford, B., *Laboratory and field studies of water floods using polymer solutions to increase oil recoveries*. Journal of Petroleum Technology, 1964. **16**(08): p. 917-922.

18. Mungan, N., *Rheology and adsorption of aqueous polymer solutions*. Journal of Canadian Petroleum Technology, 1969. **8**(02): p. 45-50.
19. Gogarty, W., *Mobility control with polymer solutions*. Society of Petroleum Engineers Journal, 1967. **7**(02): p. 161-173.
20. Manrique, E., M. Ahmadi, and S. Samani, *Historical and recent observations in polymer floods: an update review*. CT&F-Ciencia, Tecnología y Futuro, 2017. **6**(5): p. 17-48.
21. Gao, C.H., *Scientific research and field applications of polymer flooding in heavy oil recovery*. Journal of Petroleum Exploration and Production Technology, 2011. **1**(2-4): p. 65-70.
22. Needham, R.B. and P.H. Doe, *Polymer flooding review*. Journal of Petroleum Technology, 1987. **39**(12): p. 1,503-1,507.
23. Zhang, Y., *Survey and data analysis of polymer flooding pilot and field applications in China*. 2015.
24. Al-Saadi, F.S., et al. *Polymer Flooding in a large field in South Oman-initial results and future plans*. in *SPE EOR Conference at Oil and Gas West Asia*. 2012. Society of Petroleum Engineers.
25. Saleh, L.D., M. Wei, and B. Bai, *Data analysis and updated screening criteria for polymer flooding based on oilfield data*. SPE Reservoir Evaluation & Engineering, 2014. **17**(01): p. 15-25.
26. Sheng, J.J., B. Leonhardt, and N. Azri, *Status of polymer-flooding technology*. Journal of Canadian petroleum technology, 2015. **54**(02): p. 116-126.
27. Standnes, D.C. and I. Skjevraak, *Literature review of implemented polymer field projects*. Journal of Petroleum Science and Engineering, 2014. **122**: p. 761-775.
28. Campbell, T. and R. Bachman, *Polymer-Augmented Waterflood In The Rapdan Upper Shaunavon Unit*. Journal of Canadian Petroleum Technology, 1987. **26**(04).
29. DeHekker, T., J. Bowzer, R. Coleman, and W. Bartos. *A Progress Report on Polymer-Augmented Waterflooding in Wyoming's North Oregon Basin and Byron Fields*. in *SPE Enhanced Oil Recovery Symposium*. 1986. Society of Petroleum Engineers.
30. Weiss, W. and R. Baldwin, *Planning and implementing a large-scale polymer flood*. Journal of petroleum technology, 1985. **37**(04): p. 720-730.
31. Moore, J.K., *Reservoir Barrier and Polymer Waterflood, Northeast Hallsville Crane Unit*. Journal of Petroleum Technology, 1969. **21**(09): p. 1,130-1,136.
32. Olajire, A.A., *Review of ASP EOR (alkaline surfactant polymer enhanced oil recovery) technology in the petroleum industry: Prospects and challenges*. Energy, 2014. **77**: p. 963-982.
33. Sorbie, K., *Polymer-Improved Oil Recovery, 115 Glasgow*. Scotland: Blackie & Son, 1991: p. 126-163.
34. Borthakur, A., M. Rahman, A. Sarmah, and B. Subrahmanyam, *PARTIALLY HYDROLYZED POLYACRYLAMIDE FOR ENHANCED OIL-RECOVERY*. RESEARCH AND INDUSTRY, 1995. **40**(2): p. 90-94.
35. Morgan, S.E. and C.L. McCormick, *Water-soluble polymers in enhanced oil recovery*. Progress in polymer science, 1990. **15**(1): p. 103-145.
36. Sun, Y., L. Saleh, and B. Bai, *Measurement and impact factors of polymer rheology in porous media*. INTECH Open Science/Open Mind, 2012: p. 187-188.

37. Wever, D., F. Picchioni, and A. Broekhuis, *Polymers for enhanced oil recovery: a paradigm for structure–property relationship in aqueous solution*. Progress in Polymer Science, 2011. **36**(11): p. 1558-1628.
38. Liu, J.-F., J.-Y. Feng, S.-Z. Yang, H.-Z. Gang, and B.-Z. Mu, *The recovery of viscosity of HPAM solution in presence of high concentration sulfide ions*. Journal of Petroleum Science and Engineering, 2020: p. 107605.
39. Thomas, A., *Polymer Flooding, Chemical Enhanced Oil Recovery (cEOR)-a Practical Overview*, Dr. Laura Romero-Zerón. InTech, DOI, 2016. **10**: p. 64623.
40. Saboorian-Jooybari, H., M. Dejam, and Z. Chen, *Heavy oil polymer flooding from laboratory core floods to pilot tests and field applications: Half-century studies*. Journal of Petroleum Science and Engineering, 2016. **142**: p. 85-100.
41. Kaminsky, R.D., R.C. Wattenbarger, R.C. Szafranski, and A. Coutee. *Guidelines for polymer flooding evaluation and development*. in *International petroleum technology conference*. 2007. International Petroleum Technology Conference.
42. Zhao, F.-l., Y.-f. Wang, C.-L. Dai, S. Ren, and C. Jiao, *Techniques of enhanced oil recovery after polymer flooding*. Zhongguo Shi You Daxue Xuebao(Journal of China University of Petroleum: Edition of Natural Science), 2006. **30**(1): p. 86-89.
43. Sheng, J.J., *Modern chemical enhanced oil recovery: theory and practice*. 2010: Gulf Professional Publishing.
44. Wang, D., P. Han, Z. Shao, and R.S. Seright. *Sweep improvement options for the Daqing oil field*. in *SPE/DOE symposium on improved oil recovery*. 2006. Society of Petroleum Engineers.
45. Hirasaki, G. and G. Pope, *Analysis of factors influencing mobility and adsorption in the flow of polymer solution through porous media*. Society of Petroleum Engineers Journal, 1974. **14**(04): p. 337-346.
46. Delshad, M., D.H. Kim, O.A. Magbagbeola, C. Huh, G.A. Pope, and F. Tarahhom. *Mechanistic interpretation and utilization of viscoelastic behavior of polymer solutions for improved polymer-flood efficiency*. in *SPE Symposium on Improved Oil Recovery*. 2008. Society of Petroleum Engineers.
47. Zamani, N., I. Bondino, R. Kaufmann, and A. Skauge, *Effect of porous media properties on the onset of polymer extensional viscosity*. Journal of Petroleum Science and Engineering, 2015. **133**: p. 483-495.
48. Müller, A., J. Odell, and A. Keller, *Elongational flow and rheology of monodisperse polymers in solution*. Journal of non-newtonian fluid mechanics, 1988. **30**(2-3): p. 99-118.
49. Rodriguez, S., C. Romero, M. Sargenti, A. Müller, A.E. Saez, and J. Odell, *Flow of polymer solutions through porous media*. Journal of non-newtonian fluid mechanics, 1993. **49**(1): p. 63-85.
50. Chauveteau, G., *Fundamental Criteria in Polymer Flow Through Porous Media: And Their Importance in the Performance Differences of Mobility-Control Buffers*. 1986.
51. Azad, M.S. and J.J. Trivedi, *Quantification of the viscoelastic effects during polymer flooding: a critical review*. SPE Journal, 2019. **24**(06): p. 2,731-2,757.
52. Xia, H., D. Wang, W. Wu, and H. Jiang. *Effect of the visco-elasticity of displacing fluids on the relationship of capillary number and displacement efficiency in weak oil-wet cores*. in *Asia Pacific Oil and Gas Conference and Exhibition*. 2007. Society of Petroleum Engineers.

53. Han, X.-Q., W.-Y. Wang, and Y. Xu. *The viscoelastic behavior of HPAM solutions in porous media and it's effects on displacement efficiency*. in *International Meeting on Petroleum Engineering*. 1995. Society of Petroleum Engineers.
54. Qi, P., D.H. Ehrenfried, H. Koh, and M.T. Balhoff, *Reduction of residual oil saturation in sandstone cores by use of viscoelastic polymers*. *SPE Journal*, 2017. **22**(02): p. 447-458.
55. Wei, B., L. Romero-Zerón, and D. Rodrigue, *Oil displacement mechanisms of viscoelastic polymers in enhanced oil recovery (EOR): a review*. *Journal of Petroleum Exploration and Production Technology*, 2014. **4**(2): p. 113-121.
56. Vik, B., A. Kadir, V. Kippe, K. Sandengen, T. Skauge, J. Solbakken, and D. Zhu. *Viscous oil recovery by polymer injection; impact of in-situ polymer rheology on water front stabilization*. in *SPE Europec featured at 80th EAGE Conference and Exhibition*. 2018. Society of Petroleum Engineers.
57. Huh, C. and G.A. Pope. *Residual oil saturation from polymer floods: laboratory measurements and theoretical interpretation*. in *SPE Symposium on Improved Oil Recovery*. 2008. Society of Petroleum Engineers.
58. Sandengen, K., K. Melhuus, and A. Kristoffersen, *Polymer "viscoelastic effect"; does it reduce residual oil saturation*. *Journal of Petroleum Science and Engineering*, 2017. **153**: p. 355-363.
59. Jung, J.C., K. Zhang, B.H. Chon, and H.J. Choi, *Rheology and polymer flooding characteristics of partially hydrolyzed polyacrylamide for enhanced heavy oil recovery*. *Journal of Applied Polymer Science*, 2013. **127**(6): p. 4833-4839.
60. Kamal, M.S., A.S. Sultan, U.A. Al-Mubaiyedh, and I.A. Hussein, *Review on Polymer Flooding: Rheology, Adsorption, Stability, and Field Applications of Various Polymer Systems*. *Polymer Reviews*, 2015. **55**(3): p. 491-530.
61. Swiecinski, F., P. Reed, and W. Andrews. *The thermal stability of polyacrylamides in EOR applications*. in *SPE Improved Oil Recovery Conference*. 2016. Society of Petroleum Engineers.
62. Moradi-Araghi, A. and P.H. Doe, *Hydrolysis and precipitation of polyacrylamides in hard brines at elevated temperatures*. *SPE Reservoir Engineering*, 1987. **2**(02): p. 189-198.
63. Zaitoun, A. and B. Potie. *Limiting conditions for the use of hydrolyzed polyacrylamides in brines containing divalent ions*. in *SPE Oilfield and Geothermal Chemistry Symposium*. 1983. Society of Petroleum Engineers.
64. Du, Y. and L. Guan. *Field-scale polymer flooding: lessons learnt and experiences gained during past 40 years*. in *SPE International Petroleum Conference in Mexico*. 2004. Society of Petroleum Engineers.
65. Li, M., J. Guo, B. Peng, M. Lin, Z. Dong, and Z. Wu, *Formation of crude oil emulsions in chemical flooding*, in *Emulsions and emulsion stability*. 2005, CRC Press. p. 537-568.
66. Nguyen, D.T. and N. Sadeghi. *Stable emulsion and demulsification in chemical EOR flooding: Challenges and best practices*. in *SPE EOR Conference at Oil and Gas West Asia*. 2012. Society of Petroleum Engineers.
67. Chen, D., F. Li, Y. Gao, and M. Yang, *Pilot performance of chemical demulsifier on the demulsification of produced water from polymer/surfactant flooding in the Xinjiang oilfield*. *Water*, 2018. **10**(12): p. 1874.
68. Thomas, S., *Enhanced oil recovery-an overview*. *Oil & Gas Science and Technology-Revue de l'IFP*, 2008. **63**(1): p. 9-19.

69. Morel, D.C., S. Jouenne, M. Vert, and E. Nahas. *Polymer injection in deep offshore field: the Dalia Angola case*. in *SPE annual technical conference and exhibition*. 2008. Society of Petroleum Engineers.
70. Hirasaki, G.J., C.A. Miller, and M. Puerto, *Recent advances in surfactant EOR*. *SPE journal*, 2011. **16**(04): p. 889-907.
71. Farrell, H., M. Gregory, and M. Borah. *Progress report: big muddy field low-tension flood demonstration project with emphasis on injectivity and mobility*. in *SPE Enhanced Oil Recovery Symposium*. 1984. Society of Petroleum Engineers.
72. Reppert, T., J. Bragg, J. Wilkinson, T. Snow, N. Maer Jr, and W. Gale. *Second Ripley surfactant flood pilot test*. in *SPE/DOE Enhanced Oil Recovery Symposium*. 1990. Society of Petroleum Engineers.
73. Maerker, J. and W. Gale, *Surfactant flood process design for Loudon*. *SPE reservoir engineering*, 1992. **7**(01): p. 36-44.
74. Iglauer, S., Y. Wu, P. Shuler, Y. Tang, and W.A. Goddard III, *New surfactant classes for enhanced oil recovery and their tertiary oil recovery potential*. *Journal of Petroleum science and Engineering*, 2010. **71**(1-2): p. 23-29.
75. Sheng, J.J., *Status of surfactant EOR technology*. *Petroleum*, 2015. **1**(2): p. 97-105.
76. Larson, R., H. Davis, and L. Scriven, *Elementary mechanisms of oil recovery by chemical methods*. *Journal of Petroleum Technology*, 1982. **34**(02): p. 243-258.
77. Pashley, R. and M. Karaman, *Surfactants and self-assembly*. *Applied colloid and surface chemistry*. New York: Wiley, 2004: p. 61-7.
78. Negin, C., S. Ali, and Q. Xie, *Most common surfactants employed in chemical enhanced oil recovery*. *Petroleum*, 2017. **3**(2): p. 197-211.
79. Kamal, M.S., I.A. Hussein, and A.S. Sultan, *Review on surfactant flooding: phase behavior, retention, IFT, and field applications*. *Energy & Fuels*, 2017. **31**(8): p. 7701-7720.
80. Sandersen, S.B., *Enhanced oil recovery with surfactant flooding*. 2012.
81. Jia, H., et al., *Mechanism studies on the application of the mixed cationic/anionic surfactant systems to enhance oil recovery*. *Fuel*, 2019. **258**: p. 116156.
82. Adibhatla, B. and K. Mohanty, *Parametric analysis of surfactant-aided imbibition in fractured carbonates*. *Journal of colloid and interface science*, 2008. **317**(2): p. 513-522.
83. Jada, A. and M. Salou, *Effects of the asphaltene and resin contents of the bitumens on the water-bitumen interface properties*. *Journal of Petroleum Science and Engineering*, 2002. **33**(1-3): p. 185-193.
84. Jennings Jr, H.Y., C. Johnson Jr, and C. McAuliffe, *A caustic waterflooding process for heavy oils*. *Journal of Petroleum Technology*, 1974. **26**(12): p. 1,344-1,352.
85. Cooke Jr, C., R. Williams, and P. Kolodzie, *Oil recovery by alkaline waterflooding*. *Journal of petroleum technology*, 1974. **26**(12): p. 1,365-1,374.
86. Johnson Jr, C., *Status of caustic and emulsion methods*. *Journal of Petroleum Technology*, 1976. **28**(01): p. 85-92.
87. Bahadori, A., *Fundamentals of enhanced oil and gas recovery from conventional and unconventional reservoirs*. 2018: Gulf Professional Publishing.
88. Mayer, E., R. Berg, J. Carmichael, and R. Weinbrandt, *Alkaline injection for enhanced oil recovery-A status report*. *Journal of Petroleum Technology*, 1983. **35**(01): p. 209-221.

89. Andersen, P.Ø., S. Evje, H. Kleppe, and S.M. Skjaeveland, *A model for wettability alteration in fractured reservoirs*. SPE Journal, 2015. **20**(06): p. 1,261-1,275.
90. AlGeer, M., A. Gmira, S. Al-Enezi, and A. Yousef. *Impact of individual ions on oil/brine/rock interface: A macroscopic insight on wettability alteration*. in *Abu Dhabi International Petroleum Exhibition & Conference*. 2016. Society of Petroleum Engineers.
91. Lashkarbolooki, M., M. Riazi, F. Hajibagheri, and S. Ayatollahi, *Low salinity injection into asphaltenic-carbonate oil reservoir, mechanistical study*. Journal of Molecular Liquids, 2016. **216**: p. 377-386.
92. Al-Shalabi, E.W. and K. Sepehrnoori, *A comprehensive review of low salinity/engineered water injections and their applications in sandstone and carbonate rocks*. Journal of Petroleum Science and Engineering, 2016. **139**: p. 137-161.
93. Elakneswaran, Y., M. Takeya, A. Ubaidah, M. Shimokawara, H. Okano, and T. Nawa. *Integrated Geochemical Modelling of Low Salinity Waterflooding for Enhanced Oil Recovery in Carbonate Reservoir*. in *International Petroleum Technology Conference*. 2020. International Petroleum Technology Conference.
94. Zahid, A., A. Shapiro, and A. Skauge, *Experimental Studies of Low Salinity Water Flooding in Carbonate Reservoirs: A Mew Promising Approach*. Paper SPE, 2012. **155625**.
95. Fathi, S.J., T. Austad, and S. Strand, *Water-based enhanced oil recovery (EOR) by "smart water": Optimal ionic composition for EOR in carbonates*. Energy & fuels, 2011. **25**(11): p. 5173-5179.
96. Chandrasekhar, S. and K. Mohanty. *Wettability Alteration with Brine Composition in High Temperature Carbonate*. Paper SPE 166280. in *SPE Annual Technical Conference and Exhibition, New Orleans, Louisiana, USA*. 2013.
97. Al-Attar, H.H., M.Y. Mahmoud, A.Y. Zekri, R. Almehaideb, and M. Ghannam, *Low-salinity flooding in a selected carbonate reservoir: experimental approach*. Journal of Petroleum Exploration and Production Technology, 2013. **3**(2): p. 139-149.
98. Altahir, M., M. Yu, and F. Hussain. *Low salinity water flooding in carbonate rocks–dissolution effect*. in *International Symposium of the Society of Core Analysts held in Vienna, Austria SCA2017-070*. 2017.
99. Hiorth, A., L. Cathles, and M. Madland, *The impact of pore water chemistry on carbonate surface charge and oil wettability*. Transport in porous media, 2010. **85**(1): p. 1-21.
100. Mahani, H., R. Menezes, S. Berg, A. Fadili, R. Nasralla, D. Voskov, and V. Joekar-Niasar, *Insights into the impact of temperature on the wettability alteration by low salinity in carbonate rocks*. Energy & Fuels, 2017. **31**(8): p. 7839-7853.
101. Mahani, H., A.L. Keya, S. Berg, W.-B. Bartels, R. Nasralla, and W.R. Rossen, *Insights into the mechanism of wettability alteration by low-salinity flooding (LSF) in carbonates*. Energy & Fuels, 2015. **29**(3): p. 1352-1367.
102. Ligthelm, D.J., J. Gronsveld, J. Hofman, N. Brussee, F. Marcelis, and H. van der Linde. *Novel Waterflooding Strategy By Manipulation Of Injection Brine Composition*. in *EUROPEC/EAGE conference and exhibition*. 2009. Society of Petroleum Engineers.
103. Lager, A., K.J. Webb, C. Black, M. Singleton, and K.S. Sorbie, *Low salinity oil recovery-an experimental investigation1*. Petrophysics, 2008. **49**(01).
104. RezaeiDoust, A., T. Puntervold, S. Strand, and T. Austad, *Smart water as wettability modifier in carbonate and sandstone: A discussion of similarities/differences in the chemical mechanisms*. Energy & fuels, 2009. **23**(9): p. 4479-4485.

105. Tang, G.-Q. and N.R. Morrow, *Influence of brine composition and fines migration on crude oil/brine/rock interactions and oil recovery*. Journal of Petroleum Science and Engineering, 1999. **24**(2-4): p. 99-111.
106. Strand, S., E.J. Høgnesen, and T. Austad, *Wettability alteration of carbonates—Effects of potential determining ions (Ca²⁺ and SO₄²⁻) and temperature*. Colloids and Surfaces A: Physicochemical and Engineering Aspects, 2006. **275**(1-3): p. 1-10.
107. Thomas, M.M., J.A. Clouse, and J.M. Longo, *Adsorption of organic compounds on carbonate minerals: 1. Model compounds and their influence on mineral wettability*. Chemical geology, 1993. **109**(1-4): p. 201-213.
108. Standnes, D.C. and T. Austad, *Wettability alteration in carbonates: Interaction between cationic surfactant and carboxylates as a key factor in wettability alteration from oil-wet to water-wet conditions*. Colloids and Surfaces A: Physicochemical and Engineering Aspects, 2003. **216**(1-3): p. 243-259.
109. Karoussi, O. and A.A. Hamouda, *Imbibition of sulfate and magnesium ions into carbonate rocks at elevated temperatures and their influence on wettability alteration and oil recovery*. Energy & fuels, 2007. **21**(4): p. 2138-2146.
110. Brady, P.V. and G. Thyne, *Functional wettability in carbonate reservoirs*. Energy & Fuels, 2016. **30**(11): p. 9217-9225.
111. Bagci, S., M.V. Kok, and U. Turksoy, *Effect of brine composition on oil recovery by waterflooding*. Petroleum science and technology, 2001. **19**(3-4): p. 359-372.
112. Gupta, R., P. Smith, L. Hu, T. Willingham, M. Cascio, J. Shyeh, and C. Harris, *Enhanced waterflood for Middle East carbonate cores—Impact of injection water composition Paper SPE 142668 presented at SPE Middle East oil and gas show and conference*. Manama, Bahrain, 2011.
113. Yousef, A.A., S.H. Al-Saleh, A. Al-Kaabi, and M.S. Al-Jawfi, *Laboratory investigation of the impact of injection-water salinity and ionic content on oil recovery from carbonate reservoirs*. SPE Reservoir Evaluation & Engineering, 2011. **14**(05): p. 578-593.
114. Awolayo, A., H. Sarma, and A.M. AlSumaiti. *A laboratory study of ionic effect of smart water for enhancing oil recovery in carbonate reservoirs*. in *SPE EOR conference at oil and gas West Asia*. 2014. Society of Petroleum Engineers.
115. Alameri, W., T.W. Teklu, R.M. Graves, H. Kazemi, and A.M. AlSumaiti. *Experimental and numerical modeling of low-salinity waterflood in a low permeability carbonate reservoir*. in *SPE Western Regional Meeting*. 2015. Society of Petroleum Engineers.
116. Puntervold, T., S. Strand, R. Ellouz, and T. Austad, *Modified seawater as a smart EOR fluid in chalk*. Journal of Petroleum Science and Engineering, 2015. **133**: p. 440-443.
117. Qiao, C., L. Li, R.T. Johns, and J. Xu, *A mechanistic model for wettability alteration by chemically tuned waterflooding in carbonate reservoirs*. SPE Journal, 2015. **20**(04): p. 767-783.
118. Fathi, S.J., T. Austad, and S. Strand, *“Smart water” as a wettability modifier in chalk: the effect of salinity and ionic composition*. Energy & fuels, 2010. **24**(4): p. 2514-2519.
119. Mohsenzadeh, A., P. Pourafshary, and Y. Al-Wahaibi. *Oil recovery enhancement in carbonate reservoirs via low saline water flooding in presence of low concentration active ions; A case study*. in *SPE EOR Conference at Oil and Gas West Asia*. 2016. Society of Petroleum Engineers.
120. Fani, M., H. Al-Hadrami, P. Pourafshary, G. Vakili-Nezhaad, and N. Mosavat. *Optimization of smart water flooding in carbonate reservoir*. in *Abu Dhabi International Petroleum Exhibition & Conference*. 2018. Society of Petroleum Engineers.

121. Nasralla, R.A., et al., *Low salinity waterflooding for a carbonate reservoir: Experimental evaluation and numerical interpretation*. Journal of Petroleum Science and Engineering, 2018. **164**: p. 640-654.
122. Sarvestani, A.D., S. Ayatollahi, and M.B. Moghaddam, *Smart water flooding performance in carbonate reservoirs: an experimental approach for tertiary oil recovery*. Journal of Petroleum Exploration and Production Technology, 2019. **9**(4): p. 2643-2657.
123. Masalmeh, S., M. Al-Hammadi, A. Farzaneh, and M. Sohrabi. *Low Salinity Water Flooding in Carbonate: Screening, Laboratory Quantification and Field Implementation*. in *Abu Dhabi International Petroleum Exhibition & Conference*. 2019. Society of Petroleum Engineers.
124. Xie, Q., S. He, and W. Pu, *The effects of temperature and acid number of crude oil on the wettability of acid volcanic reservoir rock from the Hailar Oilfield*. Petroleum Science, 2010. **7**(1): p. 93-99.
125. Mahani, H., A.L. Keya, S. Berg, W.-B. Bartels, R. Nasralla, and W. Rossen. *Driving mechanism of low salinity flooding in carbonate rocks*. in *EUROPEC 2015*. 2015. Society of Petroleum Engineers.
126. Derkani, M.H., A.J. Fletcher, W. Abdallah, B. Sauerer, J. Anderson, and Z.J. Zhang, *Low salinity waterflooding in carbonate reservoirs: review of interfacial mechanisms*. Colloids and Interfaces, 2018. **2**(2): p. 20.
127. Awolayo, A.N., H.K. Sarma, and L.X. Nghiem, *Brine-dependent recovery processes in carbonate and sandstone petroleum reservoirs: review of laboratory-field studies, interfacial mechanisms and modeling attempts*. Energies, 2018. **11**(11): p. 3020.
128. Romanuka, J., et al. *Low salinity EOR in carbonates*. in *SPE Improved Oil Recovery Symposium*. 2012. Society of Petroleum Engineers.
129. Katende, A. and F. Sagala, *A critical review of low salinity water flooding: Mechanism, laboratory and field application*. Journal of Molecular Liquids, 2019. **278**: p. 627-649.
130. AlQuraishi, A.A., S.N. AlHussin, and H.Q. AlYami. *Efficiency and recovery mechanisms of low salinity water flooding in sandstone and carbonate reservoirs*. in *Offshore Mediterranean Conference and Exhibition*. 2015. Offshore Mediterranean Conference.
131. Khisamov, V., V. Akhmetgareev, and T. Shilova. *Core Tests and Field Case Studies of Successful and Unsuccessful Low-Salinity Waterfloods from Four Oil Fields*. in *79th EAGE Conference and Exhibition 2017-Workshops*. 2017. European Association of Geoscientists & Engineers.
132. Mahani, H., T. Sorop, D.J. Ligthelm, D. Brooks, P. Vledder, F. Mozahem, and Y. Ali. *Analysis of field responses to low-salinity waterflooding in secondary and tertiary mode in Syria*. in *SPE Europec/EAGE Annual Conference and Exhibition*. 2011. Society of Petroleum Engineers.
133. Yousef, A.A., S. Al-Saleh, A.U. Al-Kaabi, and M.S. Al-Jawfi. *Laboratory investigation of novel oil recovery method for carbonate reservoirs*. in *Canadian Unconventional Resources and International Petroleum Conference*. 2010. Society of Petroleum Engineers.
134. Hadi, Y., F. Hussain, and F. Othman. *Low salinity water flooding in carbonate reservoirs—dissolution effect*. in *IOP Conference Series: Materials Science and Engineering*. 2019. IOP Publishing.
135. Den Ouden, L., R. Nasralla, H. Guo, H. Bruining, and C. Van Kruijsdijk. *Calcite dissolution behaviour during low salinity water flooding in carbonate rock*. in *IOR 2015-18th European Symposium on Improved Oil Recovery*. 2015. European Association of Geoscientists & Engineers.

136. Okasha, T.M. and A. Alshwaish. *Effect of brine salinity on interfacial tension in Arab-D carbonate reservoir, Saudi Arabia*. in *SPE Middle East Oil and Gas Show and Conference*. 2009. Society of Petroleum Engineers.
137. Mokhtari, R., S. Ayatollahi, and M. Fatemi, *Experimental investigation of the influence of fluid-fluid interactions on oil recovery during low salinity water flooding*. *Journal of Petroleum Science and Engineering*, 2019. **182**: p. 106194.
138. Zahid, A., E.H. Stenby, and A.A. Shapiro. *Smart waterflooding (high sal/low sal) in carbonate reservoirs*. in *SPE Europec/EAGE Annual Conference*. 2012. Society of Petroleum Engineers.
139. Ayirala, S.C., S.H. Al-Saleh, and A.A. Al-Yousef, *Microscopic scale interactions of water ions at crude oil/water interface and their impact on oil mobilization in advanced water flooding*. *Journal of Petroleum Science and Engineering*, 2018. **163**: p. 640-649.
140. Tetteh, J.T., E. Rankey, and R. Barati. *Low salinity waterflooding effect: crude oil/brine interactions as a recovery mechanism in carbonate rocks*. in *OTC Brasil*. 2017. Offshore Technology Conference.
141. Yi, Z. and H.K. Sarma. *Improving waterflood recovery efficiency in carbonate reservoirs through salinity variations and ionic exchanges: A promising low-cost "Smart-Waterflood" approach*. in *Abu Dhabi International Petroleum Conference and Exhibition*. 2012. Society of Petroleum Engineers.
142. Strand, S., T. Austad, T. Puntervold, E.J. Høgnesen, M. Olsen, and S.M.F. Barstad, "Smart water" for oil recovery from fractured limestone: a preliminary study. *Energy & fuels*, 2008. **22**(5): p. 3126-3133.
143. Ravari, R., S. Strand, and T. Austad. *Care must be taken to use outcrop limestone cores to mimic reservoir core material in SCAL linked to wettability alteration*. in *Proceedings of the 11th International Symposium on Reservoir Wettability, Calgary, CA, USA*. 2010.
144. Yousef, A.A., S. Al-Saleh, and M.S. Al-Jawfi. *Improved/enhanced oil recovery from carbonate reservoirs by tuning injection water salinity and ionic content*. in *SPE improved oil recovery symposium*. 2012. Society of Petroleum Engineers.
145. Skrettingland, K., T. Holt, M.T. Tweheyo, and I. Skjevraak, *Snorre Low-Salinity-Water Injection--Coreflooding Experiments and Single-Well Field Pilot*. *SPE Reservoir Evaluation & Engineering*, 2011. **14**(02): p. 182-192.
146. Ahmetgareev, V., A. Zeinijahromi, A. Badalyan, R. Khisamov, and P. Bedrikovetsky, *Analysis of low salinity waterflooding in Bastrykskoye field*. *Petroleum Science and Technology*, 2015. **33**(5): p. 561-570.
147. Bedrikovetsky, P., A. Zeinijahromi, A. Badalyan, V. Ahmetgareev, and R. Khisamov. *Fines-Migration-Assisted Low-Salinity Waterflooding: Field Case Analysis (Russian)*. in *SPE Russian petroleum technology conference*. 2015. Society of Petroleum Engineers.
148. Reinholdtsen, A.J., A. RezaeiDoust, S. Strand, and T. Austad. *Why Such a Small Low Salinity EOR--Potential from the Snorre Formation?* in *IOR 2011-16th European Symposium on Improved Oil Recovery*. 2011. European Association of Geoscientists & Engineers.
149. Al-Ibadi, H., K. Stephen, and E. Mackay. *Heterogeneity Effects on Low Salinity Water Flooding*. in *SPE Europec featured at 82nd EAGE Conference and Exhibition*. 2020. Society of Petroleum Engineers.
150. Chang, H., et al., *Advances in polymer flooding and alkaline/surfactant/polymer processes as developed and applied in the People's Republic of China*. *Journal of petroleum technology*, 2006. **58**(02): p. 84-89.

151. Feng, R.-S., Y.-J. Guo, X.-M. Zhang, J. Hu, and H.-B. Li, *Alkali/surfactant/polymer flooding in the daqing oilfield class II reservoirs using associating polymer*. Journal of Chemistry, 2013. **2013**.
152. Vermolen, E.C., M. Pingo-Almada, B.M. Wassing, D.J. Ligthelm, and S.K. Masalmeh. *Low-salinity polymer flooding: improving polymer flooding technical feasibility and economics by using low-salinity make-up brine*. in *IPTC 2014: International Petroleum Technology Conference*. 2014. European Association of Geoscientists & Engineers.
153. Mohammadi, H. and G. Jerauld. *Mechanistic modeling of the benefit of combining polymer with low salinity water for enhanced oil recovery*. in *SPE Improved Oil Recovery Symposium*. 2012. Society of Petroleum Engineers.
154. Alzayer, H. and M. Sohrabi. *Numerical simulation of improved heavy oil recovery by low-salinity water injection and polymer flooding*. in *SPE Saudi Arabia section technical symposium and exhibition*. 2013. Society of Petroleum Engineers.
155. Borazjani, S., P. Bedrikovetsky, and R. Farajzadeh, *Analytical solutions of oil displacement by a polymer slug with varying salinity*. Journal of Petroleum Science and Engineering, 2016. **140**: p. 28-40.
156. Santo, A. and A. Muggeridge. *An Investigation into the Benefits of Combined Polymer-Low Salinity Waterflooding*. in *SPE Asia Pacific Oil and Gas Conference and Exhibition*. 2018. Society of Petroleum Engineers.
157. Alfazazi, U., W. AlAmeri, and M.R. Hashmet, *Experimental investigation of polymer flooding with low-salinity preconditioning of high temperature–high-salinity carbonate reservoir*. Journal of Petroleum Exploration and Production Technology, 2019. **9**(2): p. 1517-1530.
158. AlSofi, A.M., J. Wang, A.M. AlBoqmi, M.B. AlOtaibi, S.C. Ayirala, and A.A. AlYousef, *Smartwater synergy with chemical enhanced oil recovery: Polymer effects on smartwater*. SPE Reservoir Evaluation & Engineering, 2019. **22**(01): p. 61-77.
159. Shakeel, M., P. Pourafshary, and M. Rehan Hashmet, *Hybrid Engineered Water–Polymer Flooding in Carbonates: A Review of Mechanisms and Case Studies*. Applied Sciences, 2020. **10**(17): p. 6087.
160. Seright, R.S., A. Campbell, P. Mozley, and P. Han, *Stability of partially hydrolyzed polyacrylamides at elevated temperatures in the absence of divalent cations*. Spe Journal, 2010. **15**(02): p. 341-348.
161. Ayirala, S.C., E. Uehara-Nagamine, A.N. Matzakos, R.W. Chin, P.H. Doe, and P.J. van den Hoek. *A designer water process for offshore low salinity and polymer flooding applications*. in *SPE Improved Oil Recovery Symposium*. 2010. Society of Petroleum Engineers.
162. Pourafshary, P. and N. Moradpour, *Hybrid EOR Methods Utilizing Low-Salinity Water*, in *Enhanced Oil Recovery Processes-New Technologies*. 2019, IntechOpen.
163. AlSofi, A.M., J. Wang, A.M. AlBoqmi, M.B. AlOtaibi, S.C. Ayirala, and A.A. AlYousef. *SmartWater Synergy with Chemical EOR for a Slightly Viscous Arabian Heavy Reservoir*. in *SPE Heavy Oil Conference and Exhibition*. 2016. Society of Petroleum Engineers.
164. Zhang, P., M.T. Tweheyo, and T. Austad, *Wettability alteration and improved oil recovery in chalk: The effect of calcium in the presence of sulfate*. Energy & fuels, 2006. **20**(5): p. 2056-2062.
165. Bartels, W.-B., H. Mahani, S. Berg, and S. Hassanizadeh, *Literature review of low salinity waterflooding from a length and time scale perspective*. Fuel, 2019. **236**: p. 338-353.
166. Al Shalabi, E.W., K. Sepehrnoori, and M. Delshad, *Mechanisms behind low salinity water injection in carbonate reservoirs*. Fuel, 2014. **121**: p. 11-19.

167. Fathi, S.J., T. Austad, and S. Strand. *Water-based enhanced oil recovery (EOR) by "smart water" in carbonate reservoirs*. in *SPE EOR Conference at Oil and Gas West Asia*. 2012. Society of Petroleum Engineers.
168. Chandrasekhar, S., H. Sharma, and K.K. Mohanty, *Dependence of wettability on brine composition in high temperature carbonate rocks*. *Fuel*, 2018. **225**: p. 573-587.
169. Jabbar, M.Y., H.S. Al-Hashim, and W. Abdallah. *Effect of brine composition on wettability alteration of carbonate rocks in the presence of polar compounds*. in *SPE Saudi Arabia Section Technical Symposium and Exhibition*. 2013. Society of Petroleum Engineers.
170. Levitt, D. and G.A. Pope. *Selection and screening of polymers for enhanced-oil recovery*. in *SPE symposium on improved oil recovery*. 2008. Society of Petroleum Engineers.
171. Zaitoun, A., P. Makakou, N. Blin, R.S. Al-Maamari, A.-A.R. Al-Hashmi, and M. Abdel-Goad, *Shear stability of EOR polymers*. *Spe Journal*, 2012. **17**(02): p. 335-339.
172. Wang, D., J. Cheng, Q. Yang, G. Wenchao, L. Qun, and F. Chen. *Viscous-elastic polymer can increase microscale displacement efficiency in cores*. in *SPE annual technical conference and exhibition*. 2000. Society of Petroleum Engineers.
173. Silveira, B., L. Lopes, and R. Moreno, *Rheological approach of HPAM solutions under harsh conditions for EOR applications*. *Int J Eng Technol IJET-IJENS*, 2016. **16**(3): p. 1-8.
174. Moghadasi, L., et al. *Laboratory Investigation on Synergy Effect of Low Salinity-Polymer Water Injection on Sandstone Porous Media*. in *Offshore Mediterranean Conference and Exhibition*. 2019. Offshore Mediterranean Conference.
175. Lee, S., D.H. Kim, C. Huh, and G.A. Pope. *Development of a comprehensive rheological property database for EOR polymers*. in *SPE Annual Technical Conference and Exhibition*. 2009. Society of Petroleum Engineers.
176. AlSofi, A.M., J. Wang, and Z.F. Kaidar, *SmartWater synergy with chemical EOR: Effects on polymer injectivity, retention and acceleration*. *Journal of Petroleum Science and Engineering*, 2018. **166**: p. 274-282.
177. Unsal, E., A. Ten Berge, and D. Wever, *Low salinity polymer flooding: Lower polymer retention and improved injectivity*. *Journal of Petroleum Science and Engineering*, 2018. **163**: p. 671-682.
178. Aluhwal, H. and O. Kalifa, *Simulation study of improving oil recovery by polymer flooding in a Malaysian reservoir*. Department of Petroleum Engineering, Universiti Teknologi Malaysia, 2008: p. 212.
179. Guetni, I., C. Marlière, D. Rousseau, I. Bihannic, M. Pelletier, and F. Villieras. *Transport of HPAM Solutions in low Permeability Porous Media: Impacts of Salinity and Clay Content*. in *SPE Europec featured at 81st EAGE Conference and Exhibition*. 2019. Society of Petroleum Engineers.
180. Bennetzen, M.V., S.F.H. Gilani, K. Mogensen, M. Ghozali, and N. Bounoua. *Successful polymer flooding of low-permeability, oil-wet, carbonate reservoir cores*. in *Abu Dhabi International Petroleum Exhibition and Conference*. 2014. Society of Petroleum Engineers.
181. El-Khatib, M.F., *Investigation of Low Salinity Polymer and Surfactant Flooding in Carbonate Reservoir at Reservoir Conditions*. 2018, The University of Bergen.
182. Wang, J., S.C. Ayirala, A.M. AlSofi, A.A. Al-Yousef, and S. Aramco. *SmartWater Synergy with Surfactant Polymer Flooding for Efficient Oil Mobilization in Carbonates*. in *SPE EOR Conference at Oil and Gas West Asia*. 2018. Society of Petroleum Engineers.

183. Karimov, D., M.R. Hashmet, and P. Pourafshary. *A Laboratory Study to Optimize Ion Composition for the Hybrid Low Salinity Water/Polymer Flooding*. in *Offshore Technology Conference Asia*. 2020. Offshore Technology Conference.
184. Pires, A.P., P.G. Bedrikovetsky, and A.A. Shapiro, *A splitting technique for analytical modelling of two-phase multicomponent flow in porous media*. *Journal of Petroleum Science and Engineering*, 2006. **51**(1-2): p. 54-67.
185. Webb, K., A. Lager, and C. Black. *Comparison of high/low salinity water/oil relative permeability*. in *International symposium of the society of core analysts, Abu Dhabi, UAE*. 2008.
186. Han, B. and J. Lee. *Sensitivity analysis on the design parameters of enhanced oil recovery by polymer flooding with low salinity waterflooding*. in *The Twenty-fourth International Ocean and Polar Engineering Conference*. 2014. International Society of Offshore and Polar Engineers.
187. Khamees, T. and R.E. Flori. *Modeling the Combined Effects of Water Salinity and Polymer Rheology on the Performance of Polymer Flooding and In-Depth Gel Treatment*. in *SPE Western Regional Meeting*. 2018. Society of Petroleum Engineers.
188. Xin, X., G. Yu, Z. Chen, K. Wu, X. Dong, and Z. Zhu, *Effect of polymer degradation on polymer flooding in heterogeneous reservoirs*. *Polymers*, 2018. **10**(8): p. 857.
189. Dang, T., Z. Chen, T. Nguyen, and W. Bae, *Rheological modeling and numerical simulation of HPAM polymer viscosity in porous media*. *Energy Sources, Part A: Recovery, Utilization, and Environmental Effects*, 2015. **37**(20): p. 2189-2197.
190. Gu, X., H. Sang, C. Pu, L. Zhang, and Q. Zhao. *Effect of pH on Gelling Performance and stability of HPAM/Cr3+ Weak Gel*. in *2015 International Forum on Energy, Environment Science and Materials*. 2015. Atlantis Press.
191. Austad, T., S. Strand, E. Høghnesen, and P. Zhang. *Seawater as IOR fluid in fractured chalk*. in *SPE international symposium on oilfield chemistry*. 2005. Society of Petroleum Engineers.
192. Alotaibi, M.B., R. Azmy, and H.A. Nasr-El-Din. *Wettability challenges in carbonate reservoirs*. in *SPE Improved Oil Recovery Symposium*. 2010. Society of Petroleum Engineers.
193. Zhang, P. and T. Austad, *Wettability and oil recovery from carbonates: Effects of temperature and potential determining ions*. *Colloids and Surfaces A: Physicochemical and Engineering Aspects*, 2006. **279**(1-3): p. 179-187.
194. Gomari, K.R., A. Hamouda, and R. Denoyel, *Influence of sulfate ions on the interaction between fatty acids and calcite surface*. *Colloids and Surfaces A: Physicochemical and Engineering Aspects*, 2006. **287**(1-3): p. 29-35.
195. Al-Nofli, K., P. Pourafshary, N. Mosavat, and A. Shafiei, *Effect of initial wettability on performance of smart water flooding in carbonate reservoirs—an experimental investigation with ior implications*. *Energies*, 2018. **11**(6): p. 1394.
196. Tavassoli, S., A.K. Korrani, G.A. Pope, and K. Sepehrnoori, *Low-salinity surfactant flooding—a multimechanistic enhanced-oil-recovery method*. *SPE Journal*, 2016. **21**(03): p. 0744-0760.
197. Sekerbayeva, A., P. Pourafshary, and M.R. Hashmet, *Application of anionic Surfactant\Engineered water hybrid EOR in carbonate formations: An experimental analysis*. *Petroleum*, 2020.
198. Paul, G. and H. Froning, *Salinity effects of micellar flooding*. *Journal of Petroleum Technology*, 1973. **25**(08): p. 957-958.
199. Trushenski, S.P., D.L. Dauben, and D.R. Parrish, *Micellar flooding-fluid propagation, interaction, and mobility*. *Society of Petroleum Engineers Journal*, 1974. **14**(06): p. 633-645.

200. Glover, C., M. Puerto, J. Maerker, and E. Sandvik, *Surfactant phase behavior and retention in porous media*. Society of Petroleum Engineers Journal, 1979. **19**(03): p. 183-193.
201. Johannessen, A.M. and K. Spildo, *Enhanced oil recovery (EOR) by combining surfactant with low salinity injection*. Energy & Fuels, 2013. **27**(10): p. 5738-5749.
202. Alagic, E. and A. Skauge, *Combined low salinity brine injection and surfactant flooding in mixed-wet sandstone cores*. Energy & fuels, 2010. **24**(6): p. 3551-3559.
203. Zivar, D., P. Pourafshary, and N. Moradpour, *Capillary desaturation curve: does low salinity surfactant flooding significantly reduce the residual oil saturation?* Journal of Petroleum Exploration and Production Technology, 2021: p. 1-12.
204. Al-Ajmi, A.I.A., *Low Salinity Waterflood in Combination with Surfactant/Polymer; Effect of Surfactant Slug Size*. 2014, The University of Bergen.
205. Fortenberry, R.P., *Experimental demonstration and improvement of chemical EOR techniques in heavy oils*. 2013.
206. Bataweel, M.A. and H.A. Nasr-El-Din. *ASP vs. SP flooding in high salinity/hardness and temperature in sandstone cores*. in *SPE EOR Conference at Oil and Gas West Asia*. 2012. Society of Petroleum Engineers.
207. Dang, C., L. Nghiem, N. Nguyen, C. Yang, Z. Chen, and W. Bae, *Modeling and optimization of alkaline-surfactant-polymer flooding and hybrid enhanced oil recovery processes*. Journal of Petroleum Science and Engineering, 2018. **169**: p. 578-601.
208. Shariatpanahi, S.F., S. Strand, and T. Austad, *Initial wetting properties of carbonate oil reservoirs: effect of the temperature and presence of sulfate in formation water*. Energy & fuels, 2011. **25**(7): p. 3021-3028.
209. Chen, P. and K.K. Mohanty, *Surfactant-mediated spontaneous imbibition in carbonate rocks at harsh reservoir conditions*. SPE Journal, 2013. **18**(01): p. 124-133.
210. Hirasaki, G. and D.L. Zhang. *Surface chemistry of oil recovery from fractured, oil-wet, carbonate formation*. in *International Symposium on Oilfield Chemistry*. 2003. Society of Petroleum Engineers.
211. Kon, W., M.J. Pitts, and H. Surkalo. *Mature waterfloods renew oil production by alkaline-surfactant-polymer flooding*. in *SPE Eastern regional meeting*. 2002. Society of Petroleum Engineers.
212. Ibrahim, Z.B., A.A.A. Manap, P.A. Hamid, V.Y. Hon, P.H. Lim, and K. Wyatt. *Laboratory aspect of chemical EOR processes evaluation for Malaysian oilfields*. in *SPE Asia Pacific Oil & Gas Conference and Exhibition*. 2006. Society of Petroleum Engineers.
213. Ehrlich, R., H. Hasiba, and P. Raimondi, *Alkaline waterflooding for wettability alteration-evaluating a potential field application*. Journal of Petroleum Technology, 1974. **26**(12): p. 1,335-1,343.
214. Samanova, A., *Surfactant/LSW Flooding in Carbonates: An Investigation of Hybrid EOR Design to Improve Oil Displacement*. 2021, Nazarbayev University: Kazakhstan.
215. Ge, J., A. Feng, G. Zhang, P. Jiang, H. Pei, R. Li, and X. Fu, *Study of the factors influencing alkaline flooding in heavy-oil reservoirs*. Energy & fuels, 2012. **26**(5): p. 2875-2882.
216. Gu, X., H. Sang, C. Pu, L. Zhang, and Q. Zhao. *Effect of pH on Gelling Performance and stability of HPAM/Cr³⁺ Weak Gel*. in *2015 International Forum on Energy, Environment Science and Materials*. 2015. Atlantis Press.
217. Metzger, T.G., *The Rheology Handbook*. 3rd ed. ed. 2011, Hannover: Vincentz Network.

218. Tang, G.-Q. and A. Kovscek, *An experimental investigation of the effect of temperature on recovery of heavy oil from diatomite*. SPE Journal, 2004. **9**(02): p. 163-179.
219. Fu, W., *Modeling of temperature effect on low salinity waterflooding*. 2016.
220. Agi, A., R. Junin, J. Gbonhinbor, and M. Onyekonwu, *Natural polymer flow behaviour in porous media for enhanced oil recovery applications: a review*. Journal of Petroleum Exploration and Production Technology, 2018. **8**(4): p. 1349-1362.
221. Seright, R.S., T. Fan, K. Wavrik, and R. de Carvalho Balaban, *New insights into polymer rheology in porous media*. SPE Journal, 2011. **16**(01): p. 35-42.
222. AlSofi, A.M., J. Wang, Z. Leng, M. Abbad, and Z.F. Kaidar. *Assessment of polymer interactions with carbonate rocks and implications for EOR applications*. in *SPE Kingdom of Saudi Arabia Annual Technical Symposium and Exhibition*. 2017. Society of Petroleum Engineers.
223. Donaldson, E.C., R.D. Thomas, and P.B. Lorenz, *Wettability determination and its effect on recovery efficiency*. Society of Petroleum Engineers Journal, 1969. **9**(01): p. 13-20.
224. Kulynych, V., *The influence of wettability on oil recovery*. AGH Drilling, Oil, Gas, 2015. **32**.
225. Morrow, N., I. Chatzis, and J. Taber, *Entrapment and mobilization of residual oil in bead packs*. SPE Reservoir Engineering, 1988. **3**(03): p. 927-934.
226. Tang, J.S., *Interwell Tracer Tests To Determine Residual Oil Saturation To Waterflood At Judy Creek Bhl'a'pool*. Journal of Canadian Petroleum Technology, 1992. **31**(08).
227. Abrams, A., *The influence of fluid viscosity, interfacial tension, and flow velocity on residual oil saturation left by waterflood*. Society of Petroleum Engineers Journal, 1975. **15**(05): p. 437-447.
228. Chatzis, I. and N.R. Morrow, *Correlation of capillary number relationships for sandstone*. Society of Petroleum Engineers Journal, 1984. **24**(05): p. 555-562.
229. Fulcher Jr, R., T. Ertekin, and C. Stahl, *Effect of capillary number and its constituents on two-phase relative permeability curves*. Journal of petroleum technology, 1985. **37**(02): p. 249-260.
230. Guo, H., et al., *Proper use of capillary number in chemical flooding*. Journal of Chemistry, 2017. **2017**.
231. Hilfer, R., R. Armstrong, S. Berg, A. Georgiadis, and H. Ott, *Capillary saturation and desaturation*. Physical Review E, 2015. **92**(6): p. 063023.
232. Morrow, N.R., *Interplay of capillary, viscous and buoyancy forces in the mobilization of residual oil*. Journal of Canadian Petroleum Technology, 1979. **18**(03).
233. Garnes, J., A. Mathisen, A. Scheie, and A. Skauge. *Capillary number relations for some North, Sea reservoir sandstones*. in *SPE/DOE Enhanced Oil Recovery Symposium*. 1990. Society of Petroleum Engineers.
234. Moore, T. and R. Slobod, *The effect of viscosity and capillarity on the displacement of oil by water*. Producers Monthly, 1956. **20**(10): p. 20-30.
235. Donaldson, E.C., G.V. Chilingarian, and T.F. Yen, *Enhanced oil recovery, II: Processes and operations*. 1989: Elsevier.
236. Lake, L.W., *Enhanced oil recovery*. 1989.
237. Taber, J., *Dynamic and static forces required to remove a discontinuous oil phase from porous media containing both oil and water*. Society of Petroleum Engineers Journal, 1969. **9**(01): p. 3-12.

238. Schneider, F. and W. Owens, *Steady-state measurements of relative permeability for polymer/oil systems*. Society of Petroleum Engineers Journal, 1982. **22**(01): p. 79-86.
239. Pusch, G., T. Lotsch, and T. Muller, *Investigation of the Oil Displacing Efficiency of Suitable Polymer Products in Porous Media, Aspects of Recovery Mechanisms During Polymer Flooding*. DGMK-Report, 295-6. German Soc. Petrol. Sci. Coal Chem, 1987.
240. Zhong, H., Q. Zang, H. Yin, and H. Xia, *Experimental study on medium viscosity oil displacement using viscoelastic polymer*. Geofluids, 2018. **2018**.
241. Clarke, A., A.M. Howe, J. Mitchell, J. Staniland, and L.A. Hawkes, *How viscoelastic-polymer flooding enhances displacement efficiency*. SPE Journal, 2016. **21**(03): p. 0675-0687.
242. Fathi, Z. and F.W. Ramirez, *Optimal injection policies for enhanced oil recovery: part 2-surfactant flooding*. Society of Petroleum Engineers Journal, 1984. **24**(03): p. 333-341.
243. Abeysinghe, K.P., I. Fjelde, and A. Lohne. *Displacement of Oil by surfactant flooding in mixed-wet condition*. in *International Symposium of the society of core analysts held in Aberdeen, Scotland, UK*. 2012.
244. Abeysinghe, K.P., I. Fjelde, and A. Lohne. *Dependency of remaining oil saturation on wettability and capillary number*. in *SPE Saudi Arabia Section Technical Symposium and Exhibition*. 2012. Society of Petroleum Engineers.
245. Ghorpade, T., S. Patil, A. Dandekar, and S. Khataniar. *Application of Alkali-Surfactant-Polymer ASP Flooding for Improving Viscous Oil Recovery From Alaskan North Slope Reservoir*. in *SPE Western Regional Meeting*. 2016. Society of Petroleum Engineers.
246. Qi, L., et al., *Supplement and optimization of classical capillary number experimental curve for enhanced oil recovery by combination flooding*. Science China Technological Sciences, 2014. **57**(11): p. 2190-2203.
247. Wenxiang, W., W. Demin, and J. Haifeng. *Effect of the visco-elasticity of displacing fluids on the relationship of capillary number and displacement efficiency in weak oil-wet cores*. in *Asia Pacific Oil and Gas Conference and Exhibition*. Jakarta, Indonesia. 2007.
248. Vermolen, E., M. Van Haasterecht, and S. Masalmeh. *A systematic study of the polymer visco-elastic effect on residual oil saturation by core flooding*. in *SPE EOR Conference at Oil and Gas West Asia*. 2014. Society of Petroleum Engineers.
249. El-Hoshoudy, A., S. Desouky, M. Elkady, A. Al-Sabagh, M. Betiha, and S. Mahmoud, *Hydrophobically associated polymers for wettability alteration and enhanced oil recovery—Article review*. Egyptian Journal of Petroleum, 2017. **26**(3): p. 757-762.
250. Janiga, D., R. Czarnota, J. Stopa, P. Wojnarowski, and P. Kosowski, *Performance of nature inspired optimization algorithms for polymer enhanced oil recovery process*. Journal of Petroleum Science and Engineering, 2017. **154**: p. 354-366.
251. Wang, D., H. Xia, Z. Liu, and Q. Yang. *Study of the mechanism of polymer solution with visco-elastic behavior increasing microscopic oil displacement efficiency and the forming of steady" Oil thread" flow channels*. in *SPE Asia Pacific oil and gas conference and exhibition*. 2001. Society of Petroleum Engineers.
252. Wang, J. and M. Dong. *A laboratory study of polymer flooding for improving heavy oil recovery*. in *Canadian International Petroleum Conference*. 2007. Petroleum Society of Canada.
253. Xia, H., D. Wang, G. Wang, W.-g. Ma, H.W. Deng, and J. Liu. *Mechanism of the effect of micro-forces on residual oil in chemical flooding*. in *SPE symposium on improved oil recovery*. 2008. Society of Petroleum Engineers.

254. Urbissinova, T., J.J. Trivedi, and E. Kuru. *Effect of elasticity during viscoelastic polymer flooding- a possible mechanism of increasing the sweep efficiency.* in *SPE western regional meeting.* 2010. Society of Petroleum Engineers.